Title
Dynamics of Redox Reactions Structure Decomposition and Greenhouse Gas Fluxes in Humid Tropical Forest Soils

Author
Hall, Steven James

Publication Date
2013

Peer reviewed|Thesis/dissertation

Dynamics of Redox Reactions Structure Decomposition and Greenhouse Gas Fluxes in Humid Tropical Forest Soils

By

Steven James Hall

A dissertation submitted in partial satisfaction of the

requirements for the degree of

Doctor of Philosophy

in

Environmental Science, Policy, and Management

in the

Graduate Division

of the

University of California, Berkeley

Committee in charge:

Professor Whendee L. Silver, chair

Professor Mary Firestone

Professor Robert Rhew

Fall 2013

Abstract

Dynamics of Redox Reactions Structure Decomposition and Greenhouse Gas Fluxes in Humid Tropical Forest Soils

by

Steven James Hall

Doctor of Philosophy in Environmental Science, Policy, and Management

University of California, Berkeley

Professor Whendee L. Silver, Chair

Upland humid tropical forest soils experience fluctuations in oxygen (O_2) availability and redox potential as a consequence of high rainfall, clay content, and respiration rates. Research in wetland ecosystems suggests that spatial and temporal variation in redox reactions strongly affect the biogeochemical cycling of carbon (C) and nitrogen (N). Here, I explored the impact of soil redox dynamics on decomposition and soil-atmosphere greenhouse gas fluxes in humid tropical ecosystems of the Luquillo Experimental Forest (LEF), Puerto Rico. Traditional theory and ecosystem models predict that elevated soil moisture leads to O_2 limitation, constraining the enzymatic processes that mediate organic matter decomposition, and promoting the accumulation of soil C. Testing these hypotheses in upland humid tropical soils revealed the need for a more nuanced conceptual framework. In short: variation in moisture alone did not determine redox dynamics, hydrolytic enzymes activities persisted under reducing conditions, and redox fluctuations *promoted* decomposition on short (days) and long-term (decades) timescales.

In Chapter One, I showed a relative decoupling between the temporal dynamics of soil moisture, soil redox reactions, and greenhouse gas fluxes over scales of days to weeks, using a field moisture manipulation experiment. Anaerobic biogeochemical processes such as iron (Fe) reduction and methanogenesis co-occurred in proximity to a well-aerated soil atmosphere and were little affected by fluctuations in soil moisture. Instead, redox reactions and gas fluxes appeared to vary constitutively according to differences in microtopography. In Chapter Two, I further explored relationships between reducing conditions and organic matter decomposition, by analyzing extracellular hydrolytic enzyme activities within and among sites differing in topography and rainfall. The enzymatic latch hypothesis proposes that reducing conditions inhibit hydrolytic enzymes via an accumulation of phenolic substances. I found little evidence for an enzymatic latch, and instead documented a strong positive relationship between reducing conditions, using reduced Fe (Fe(II)) as a proxy, and hydrolytic enzyme activities in a subset of sites. Furthermore, enzyme activities generally did not decline in an anaerobic incubation relative to aerobic controls. The assumption that reducing conditions constrain the decomposition activities of hydrolytic enzymes does not appear generally applicable in humid tropical forests.

Next, in Chapter Three I examined the influence of temporal redox fluctuations on decomposition. Anaerobic conditions by definition limit the activity of oxidative enzymes, which

require O_2. The redox cycling of Fe, however, can potentially generate reactive oxygen species that mimic the function of oxidative enzymes. We demonstrated that concentrations of Fe(II) explained most of the variation in phenol oxidative activity within and among several sites in the LEF. Furthermore, Fe(II) oxidation stimulated short-term respiration, likely via a pH-mediated increase in dissolved organic C. Thus, stimulatory effects of redox fluctuations on oxidative decomposition processes might partially counteract short-term effects of O_2 limitation.

Finally, in Chapter Four I examined the overall impact of reducing conditions in comparison with other variables as they related to spatial patterns in soil C concentrations and turnover across the LEF. Soil C increased with Fe(II), an index of reducing conditions, but C tended to decline with increasing concentrations of reducible Fe oxides. Furthermore, the residence time of mineral-associated C (modeled using measurements of bomb radiocarbon) declined with Fe(II) concentrations. Together, the findings from these studies suggest a complex relationship between moisture, redox dynamics, and decomposition. First, short-term fluctuations in rainfall may have little overall impact on redox dynamics and the overall decomposition process, but longer-term differences in moisture among sites are associated with characteristic differences in redox reactions and greenhouse gas fluxes. Second, portions of the decomposition process mediated by hydrolytic enzymes appear resistant to periodic O_2 deprivation and chronic reducing conditions, as well as the accumulation of phenolic substances. Third, redox cycling may give rise to important emergent mechanisms not evident under static aerobic conditions, mediated by coupled biotic and abiotic reactions with Fe oxides. Fourth, reducing conditions are associated with elevated soil C concentrations at the landscape scale, although the presence of reducible Fe oxides constrains C accumulation, and redox cycling might accelerate the turnover of mineral C over decadal scales. Together, these findings have implications for understanding the biogeochemical function of humid tropical soils, and their response to altered precipitation regimes and feedbacks to climate change. Two mechanisms thought to underlie the persistence of C in soils—reducing conditions induced by high soil moisture and the presence of reactive Fe minerals—may actually play unexpected roles in the decomposition of soil organic matter, a finding with potentially broad application across terrestrial and aquatic ecosystems.

Table of Contents

Acknowledgements

I give whole-hearted thanks to all who made this endeavor possible. Whendee Silver provided exceptional guidance, resources, and the freedom to tackle risky questions. I benefitted tremendously from her dynamic and creative approach to science, and exposure to the wide-ranging projects and fabulous colleagues in her lab. Interaction with Mary Firestone and Rob Rhew was another highlight of my Berkeley experience, as they provided highly useful comments, context, and critique on my ideas and research from start to finish. Attending the Firestone lab meetings over the years was an education in microbial ecology in and of itself. Interactions with Gary Sposito in the halls of Hilgard yielded key insights, as I continued to ponder his questions for years after the fact. Todd Dawson gave me a fantastic introduction to stable isotopes and the preparation to dive into that discipline for my postdoc research. Discussions with Ken Hammel stimulated my thinking about iron that ultimately led to Chapter Three. Conversations and fieldwork with Aaron Thompson inspired deeper thinking about the dynamics of iron in soils. Bill McDowell lent valuable wisdom about the workings of the Luquillo forests.

My colleagues in the Silver lab provided crucial help in many ways. Wendy Yang, Becca Ryals, and especially Dan Lipzin helped me dive into the methods and concepts of biogeochemistry. Andrew McDowell and Don Herman kept the whole operation afloat and exposed me to a wealth of knowledge surrounding analytical chemistry. I thank Paul Brooks for all of his help with running the ICP and interpreting isotope data, and for all of the side discussions on transportation policy. Heather Dang, Jonathan Treffkorn, Julia Cosgrove, Taichi Natake, Devin Kirschner, Omar Gutierrez, and Katherine Lam (in no particular order), devoted hundreds of hours to sample processing and analysis and saved me from many more grey hairs. I enjoyed stimulating discussions with Gavin McNicol, who also facilitated the radiocarbon measurements and contributed to Chapter Four.

And finally, thanks to Casey and Silly the dog for constant love, support, and for tolerating all of the long field campaigns, late nights, and working weekends. And, to my parents, Joan and George, for teaching me diligence, scholarship and writing, and the encouragement to pursue the strange adventure that is academia.

Introduction

The biogeochemical dynamics of humid tropical forest ecosystems have important implications for Earth's climate system as a consequence of their large pools of carbon (C) and nitrogen (N), which cycle rapidly between vegetation, soils, and the atmosphere. Humid tropical forests support the highest gross primary productivity of any terrestrial biome, and their soils produce the highest fluxes of the greenhouse gases carbon dioxide (CO_2) and nitrous oxide (N_2O), also yielding a significant net flux of methane (CH_4) (Matson and Vitousek, 1990; Raich and Schlesinger, 1992; Carmo et al., 2006; Beer et al., 2010; Bloom et al., 2010). Understanding the biogeochemical mechanisms controlling soil C cycling and associated greenhouse gas fluxes in the humid tropics is especially important given that this biome contains almost as much organic C in soils as does the atmosphere (Jobbagy and Jackson, 2000). Substantial research has focused on the impact of increased temperatures on organic matter decomposition and trace gas production (Davidson and Janssens, 2006; Kirschbaum, 2006), yet comparatively less work has focused on the impacts of variation in soil moisture and redox dynamics on these processes. Climate change is generally expected to alter precipitation patterns in humid tropical ecosystems with regionally-specific effects, which are likely characterized by an overall increase in temporal variability and extreme events (Karl et al., 1995; Meehl et al., 2006; Romps, 2011). One important nexus between precipitation dynamics and soil biogeochemical cycling concerns the impact of oxygen (O_2) availability and anaerobic redox reactions on decomposition and trace gas fluxes.

Research over the past 15 years has demonstrated that oxygen (O_2) availability and anaerobic metabolic processes vary spatially and temporally in upland humid tropical soils, with potentially important implications for biogeochemical cycling (Silver et al., 1999; Schuur et al., 2001; Teh et al., 2005; Cleveland et al., 2010; Liptzin et al., 2011). A combination of high rainfall and high clay content can maintain soil moisture at or above field capacity for extended periods in these ecosystems. High rates of primary productivity and soil C inputs coupled with high soil moisture can lead to O_2 consumption in excess of diffusive supply, despite the fact that these upland soils are rarely flooded. In wetland ecosystems, effects of O_2 availability on respiration and concomitant rates of anaerobic redox reactions have long been identified as critical variables regulating organic matter decomposition and greenhouse gas production (Ponnamperuma, 1972; Freeman et al., 2001; Yu et al., 2007), but relatively little research has examined their influence on the biogeochemical dynamics of upland humid tropical forest soils. The presence of anaerobic microsites inside soil aggregates that persist even in well-aerated upland soils has long been noted (Sexstone et al., 1985), although the broader implications for decomposition have not been well explored. Here, I used a combination of field and laboratory experiments and field measurements spanning ecological gradients in the Luquillo Experimental Forest, Puerto Rico, to examine linkages between redox reactions, decomposition, and greenhouse gas emissions. Understanding these linkages could have important implications for understanding the response of humid tropical soils to the altered precipitation regimes predicted to accompany climate change.

In Chapter One, I tested the impact of spatial and temporal variation in precipitation, moisture and redox reactions on fluxes of CO_2, N_2O, and CH_4 across a small catchment, using a short-term (24-day) field precipitation manipulation experiment. In particular, I asked whether prolonged precipitation inputs resulted in the stepwise depletion of O_2 and anaerobic terminal

electron acceptors, as often observed in wetlands and aquifers (Achtnich et al., 1995; Chapelle et al., 1995). I assessed the utility of spatial and temporal variation in soil moisture, O_2, and indices of other redox reactions to predict these trace gas fluxes in accordance with thermodynamic theory.

In Chapter Two, I tested the effects of spatial and temporal variation in O_2 availability and reducing conditions on the potential activities of microbial extracellular enzymes over larger spatial scales, spanning site gradients of topography and rainfall. Extracellular enzymes are thought to represent the proximate agents of organic matter decomposition, but their activities have seldom been measured in humid tropical forest soils. The "enzymatic latch" hypothesis predicts a decline in the activity of hydrolytic enzymes under reducing conditions due to the accumulation of phenolic compounds, which are thought to directly inhibit enzyme activity. The presence of O_2, in turn, allows phenol oxidase enzymes to degrade the inhibitory phenolic compounds (Freeman et al., 2001). Energetic considerations have also been invoked to explain declining soil enzyme activities under anaerobic conditions (McLatchey and Reddy, 1998), but these hypotheses have not been tested in humid tropical forest soils, where relationships between extracellular enzymes and reducing conditions remain unknown.

Redox reactions in humid tropical forests have been shown to vary spatially as a consequence of variation in precipitation and site hydrology, and recent work also highlights their temporal dynamics (Liptzin et al., 2011). In Chapter Three, I examined some possible impacts of temporal redox fluctuations on soil organic matter decomposition. Dissimilatory reduction of iron (Fe) oxides constitutes a dominant terminal electron accepting process under anaerobic conditions in humid tropical soils (Dubinsky et al., 2010). Conversely, under aerobic conditions, reduced iron (Fe(II)) rapidly oxidizes to Fe(III). Theory suggests that Fe(II) oxidation could affect organic matter decomposition via at least two mechanisms that have yet to be considered in natural soils. Reactions between Fe(II) and O_2 generate reactive oxygen species including hydrogen peroxide (H_2O_2), which reacts with Fe(II) to produce hydroxyl radical, a strong and non-selective oxidant of organic compounds. Thus, Fe(II) oxidation could provide an alternative mechanism for oxidizing phenolics and biochemically recalcitrant compounds such as lignin. Reduction and oxidation of Fe in soils drives proton consumption and production, respectively, and thus results in significant temporal variation in pH. Previous work showed that increased pH following Fe reduction resulted in increased in soluble organic C (Thompson et al., 2006), which could potentially stimulate microbial respiration. In theory, decreased pH could also solubilize C given the characteristic surface charge properties of tropical soils (Chorover and Sposito, 1995). Thus, we also examined linkages between pH fluctuations and short-term CO_2 production following Fe(II) oxidation. These emergent properties of redox fluctuations could have important implications for understanding the impact of rainfall fluctuations on decomposition in humid tropical forest soils.

Finally, in Chapter Four, I examined the impact of reducing conditions on spatial variation in soil C storage and turnover at the ecosystem scale, in relationship to other geochemical and biological factors thought to influence C stabilization. Concentrations of reactive "poorly-crystalline" minerals often correlate strongly with soil organic C concentrations (Torn et al., 1997; Kleber et al., 2005), but reactive Fe can become depleted over pedogenic timescales as a consequence of reductive dissolution. Reducing conditions are typically thought to slow overall rates of decomposition, but the presence of reactive Fe oxide minerals to drive

anaerobic respiration might ameliorate this effect. Thus, the net impact on soil C from reducing conditions, reactive minerals, and their interactions is difficult to predict, but assessing these mechanisms together could provide insight into patterns of soil C concentrations and turnover.

References

Achtnich, C., Bak, F., Conrad, R., 1995. Competition for electron donors among nitrate reducers, ferric iron reducers, sulfate reducers, and methanogens in anoxic paddy soil. Biology and Fertility of Soils 19, 65–72.

Beer, C., Reichstein, M., Tomelleri, E., Ciais, P., Jung, M., Carvalhais, N., Rödenbeck, C., Arain, M.A., Baldocchi, D., Bonan, G.B., Bondeau, A., Cescatti, A., Lasslop, G., Lindroth, A., Lomas, M., Luyssaert, S., Margolis, H., Oleson, K.W., Roupsard, O., Veenendaal, E., Viovy, N., Williams, C., Woodward, F.I., Papale, D., 2010. Terrestrial Gross Carbon Dioxide Uptake: Global Distribution and Covariation with Climate. Science 329, 834 – 838.

Bloom, A.A., Palmer, P.I., Fraser, A., Reay, D.S., Frankenberg, C., 2010. Large-scale controls of methanogenesis inferred from methane and gravity spaceborne data. Science 327, 322–325.

Carmo, J.B. do, Keller, M., Dias, J.D., Camargo, P.B. de, Crill, P., 2006. A source of methane from upland forests in the Brazilian Amazon. Geophysical Research Letters 33, L04809.

Chapelle, F.H., McMahon, P.B., Dubrovsky, N.M., Fujii, R.F., Oaksford, E.T., Vroblesky, D.A., 1995. Deducing the distribution of terminal electron-accepting processes in hydrologically diverse groundwater systems. Water Resources Research 31, 359–371.

Chorover, J., Sposito, G., 1995. Dissolution behavior of kaolinitic tropical soils. Geochimica et Cosmochimica Acta 59, 3109–3121.

Cleveland, C.C., Wieder, W.R., Reed, S.C., Townsend, A.R., 2010. Experimental drought in a tropical rain forest increases soil carbon dioxide losses to the atmosphere. Ecology 91, 2313–2323.

Davidson, E., Janssens, I., 2006. Temperature sensitivity of soil carbon decomposition and feedbacks to climate change. Nature 440, 165–173.

Dubinsky, E.A., Silver, W.L., Firestone, M.K., 2010. Tropical forest soil microbial communities couple iron and carbon biogeochemistry. Ecology 91, 2604–2612.

Freeman, C., Ostle, N., Kang, H., 2001. An enzymatic "latch" on a global carbon store -- a shortage of oxygen locks up carbon in peatlands by restraining a single enzyme. Nature 409, 149.

Jobbagy, E.G., Jackson, R.B., 2000. The vertical distribution of soil organic carbon and its relation to climate and vegetation. Ecological Applications 10, 423–436.

Karl, T.R., Knight, R.W., Plummer, N., 1995. Trends in high-frequency climate variability in the twentieth century. Nature 377, 217–220.

Keller, M., Weitz, A.M., Bryan, B., Rivera, M.M., Silver, W.L., 2000. Soil-atmosphere nitrogen oxide fluxes: Effects of root disturbance. Journal of Geophysical Research-Atmospheres 105, 17693–17698.

Kirschbaum, M.U.F., 2006. The temperature dependence of organic-matter decomposition—still a topic of debate. Soil Biology and Biochemistry 38, 2510–2518.

Kleber, M., Mikutta, R., Torn, M.S., Jahn, R., 2005. Poorly crystalline mineral phases protect organic matter in acid subsoil horizons. European Journal of Soil Science 56, 717–725.
Liptzin, D., Silver, W.L., Detto, M., 2011. Temporal dynamics in soil oxygen and greenhouse gases in two humid tropical forests. Ecosystems 14, 171–182.
Matson, P., Vitousek, P., 1990. Ecosystem approach to a global nitrous oxide budget. BioScience 40, 667–672.
McLatchey, G.P., Reddy, K.R., 1998. Regulation of organic matter decomposition and nutrient release in a wetland soil. Journal of Environmental Quality 27, 1268–1274.
Meehl, G.A., Washington, W.M., Santer, B.D., Collins, W.D., Arblaster, J.M., Hu, A., Lawrence, D.M., Teng, H., Buja, L.E., Strand, W.G., 2006. Climate Change Projections for the Twenty-First Century and Climate Change Commitment in the CCSM3. Journal of Climate 19, 2597–2616.
Ponnamperuma, F.N., 1972. The chemistry of submerged soils. Advances in Agronomy 24, 29–96.
Raich, J.W., Schlesinger, W.H., 1992. The global carbon dioxide flux in soil respiration and its relationship to vegetation and climate. Tellus B 44, 81–99.
Romps, D.M., 2011. Response of tropical precipitation to global warming. Journal of the Atmospheric Sciences 68, 123–138.
Schuur, E.A.G., Chadwick, O.A., Matson, P.A., 2001. Carbon cycling and soil carbon storage in mesic to wet Hawaiian montane forests. Ecology 82, 3182–3196.
Sexstone, A., Revsbech, N., Parkin, T., Tiedje, J., 1985. Direct measurement of oxygen profiles and denitrification rates in soil aggregates. Soil Science Society of America Journal 49, 645–651.
Silver, W.L., Lugo, A.E., Keller, M., 1999. Soil oxygen availability and biogeochemistry along rainfall and topographic gradients in upland wet tropical forest soils. Biogeochemistry 44, 301–328.
Teh, Y., Silver, W., Conrad, M., 2005. Oxygen effects on methane production and oxidation in humid tropical forest soils. Global Change Biology 11, 1283–1297.
Thompson, A., Chadwick, O.A., Boman, S., Chorover, J., 2006. Colloid mobilization during soil iron redox oscillations. Environmental Science & Technology 40, 5743–5749.
Torn, M., Trumbore, S., Chadwick, O., Vitousek, P., Hendricks, D., 1997. Mineral control of soil organic carbon storage and turnover. Nature 389, 170–173.
Yu, K.W., Bohme, F., Rinklebe, J., Neue, H.U., DeLaune, R.D., 2007. Major biogeochemical processes in soils - A microcosm incubation from reducing to oxidizing conditions. Soil Science Society of America Journal 71, 1406–1417.

Chapter 1

When wet gets wetter: decoupling of moisture, redox biogeochemistry, and greenhouse gas fluxes in a humid tropical forest soil

Abstract

Upland humid tropical forest soils are often characterized by fluctuating redox dynamics that vary temporally and spatially across the landscape. An increase in the frequency and intensity of rainfall events with climate change is likely to affect soil redox reactions that control the production and emissions of greenhouse gases. We used a 24-day rainfall manipulation experiment to evaluate temporal and spatial trends of surface soil (0 – 20 cm) redox-active chemical species and greenhouse gas fluxes in the Luquillo Experimental Forest, Puerto Rico. Treatments consisted of a high rainfall simulation (60 mm d^{-1}), a fluctuating rainfall regime, and a control. Water addition generated high temporal and spatial variation in soil moisture (0.3 – 0.6 $m^3 m^{-3}$), but had no significant effect on soil oxygen (O_2) concentrations. Extractable nitrate (NO_3^-) concentrations decreased with daily water additions and reduced iron (Fe(II)) concentrations increased towards the end of the experiment. Overall, redox indicators displayed a weak, non-deterministic, nonlinear relationship with soil moisture. High concentrations of Fe(II) and manganese (Mn) were present even where moisture was relatively low, and net Mn reduction occurred in all plots including controls. Mean CO_2 fluxes were best explained by soil C concentrations and a composite redox indicator, and not water addition. Several plots were CH_4 sources irrespective of water addition, while other plots oscillated between weak CH_4 sources and sinks. Fluxes of N_2O were highest in control plots and were consistently low in water addition plots. Together, these data suggest 1) a relative decoupling between soil moisture and redox processes at our spatial and temporal scales of measurement, 2) the co-occurrence of aerobic and anaerobic biogeochemical processes in well-drained surface soils, and 3) an absence of threshold effects from sustained precipitation on redox reactions over the scale of weeks. Our data suggests a need to re-evaluate representations of moisture in biogeochemical models.

Introduction

Humid tropical forests exert substantial influence on the atmospheric concentrations of the greenhouse gases carbon dioxide (CO_2), nitrous oxide (N_2O), and methane (CH_4). These ecosystems generate the highest soil-atmosphere CO_2 fluxes of any biome, provide the largest natural source of N_2O, and are increasingly thought to provide a substantial net source of CH_4 (Matson & Vitousek 1990; Raich & Schlesinger 1992; Carmo and others 2006; Bloom and others 2010). While the net C balance of humid tropical forest soils remains uncertain, they contain a significant portion (approximately 500 Pg) of the terrestrial organic carbon (C) pool (Jobbagy & Jackson 2000). Global climate change is likely to affect soil C storage and greenhouse gas fluxes from humid tropical forest soils, yet the relative impact of different environmental drivers remains poorly understood. The stimulation of organic matter decomposition rates under increasing temperatures has been widely acknowledged (Davidson & Janssens 2006), but the biogeochemical impacts of altered precipitation regimes have received

less attention. Drought can potentially increase or decrease soil respiration in humid tropical forests (Wood & Silver 2012; Cleveland and others 2010), but potential consequences of short-term variability in precipitation (days to weeks) have not yet been closely examined. Theoretical and empirical evidence points to an increase in the frequency and magnitude of extreme precipitation events with global climate change (Karl and others 1995; Romps 2011). Variability in soil moisture has long been known to impact soil oxygen (O_2) concentrations, especially in the humid tropics where increased rainfall often correlates with declines in O_2, presumably due to decreased gas-phase diffusion (Vine and others 1942; Silver and others 1999). Rainfall-induced variability in O_2 concentrations could generate important feedbacks on the redox-sensitive biogeochemical reactions controlling soil greenhouse gas production. Oxygen provides the most energetically-favorable electron acceptor for microbial respiration, and directly inhibits production of N_2O and CH_4 due to lower energy yields from denitrification and methanogenesis (Megonigal and others 2003). While the importance of anaerobic biogeochemical cycling of C, nitrogen (N), manganese (Mn), iron (Fe), and sulfur (S) has long been documented in wetland ecosystems (Ponnamperuma 1972), the significance of anaerobic processes such as Fe reduction and methanogenesis has only recently been recognized in upland humid tropical forest soils (Peretyazhko & Sposito 2005; Teh and others 2005; Chacon and others 2006). Understanding the environmental drivers of aerobic and anaerobic biogeochemical reactions in upland humid tropical forests could provide insight into dynamics of soil greenhouse gas fluxes from these ecosystems.

The presence of soil moisture concentrations above field capacity or flooded conditions are typically accepted as critical constraints for inducing soil O_2 depletion. Water table depth and time since flooding have provided effective proxies for redox conditions and CO_2 and CH_4 fluxes across a range of wetland ecosystems (Ponnamperuma 1972; Jungkunst & Fiedler 2007). Studies in upland soils have also shown suppression of soil respiration by high soil moisture, presumably due to O_2 depletion (Linn & Doran 1984). Since soil moisture is a relatively tractable variable, relationships between moisture and redox processes have been incorporated into mechanistic models used to describe soil redox dynamics, organic matter decomposition, and trace gas fluxes (Li and others 1992; Parton and others 1993). Building on research in temperate ecosystems, work in the humid tropics has suggested that soil moisture dominantly influences the redox reactions that control greenhouse gas fluxes. Several studies suggested that suppression of microbial organic matter decomposition under anaerobic conditions could explain observations of declining CO_2 fluxes under high soil moisture, in addition to the impact of decreased diffusivity (Schuur & Matson 2001; Chambers and others 2004; Cleveland and others 2010). Fluxes of N_2O from humid tropical forest soils often exhibit positive relationships with soil moisture indicative of stimulated denitrification rates (Keller & Reiners 1994; Erickson and others 2001; Koehler and others 2009; Rowlings and others 2012). And, while humid tropical soils have previously been thought to provide a net CH_4 sink in the absence of disturbance (Keller & Reiners 1994; Steudler and others 1996; Rowlings and others 2012), recent data suggests the presence of a cryptic CH_4 source in these ecosystems likely related to moisture variability (Teh and others 2005; Carmo and others 2006). Other studies demonstrated that rainfall can shift soils from CH_4 sinks to sources (Vasconcelos and others 2004; Yu and others 2008; Itoh and others 2009), and it is unknown whether this relationship is widespread. In particular, we ask whether variation in the magnitude and duration of rainfall and soil moisture is

sufficient to explain dynamics of redox reactions and greenhouse gas fluxes in upland humid tropical forests.

The relationships between moisture and greenhouse gas fluxes discussed above are underpinned by theoretical differences in the thermodynamic energy yield of soil microbe-catalyzed redox reactions. Theory suggests that electron acceptors should be reduced in a predictable sequence, provided that microbes compete for electron donors (e.g. labile C) in a spatially homogeneous environment. Oxygen should be respired first, followed by nitrate (NO_3), manganese oxides (Mn(IV)), iron oxides (Fe(III)), sulfate (SO_4), and finally CO_2 (Megonigal and others 2003). The terminal electron accepting process (TEAP) model posits that dominant redox processes can be identified by evaluating spatial or temporal trends in the concentrations of electron acceptors and reduced products (Chapelle and others 1995). This framework provided insight into understanding the dynamics of redox reactions and greenhouse gas production across diverse wetland, sediment, and aquifer ecosystems (Achtnich and others 1995; Chapelle and others 1995; Hedin and others 1998; Yu and others 2007). As O_2 and other terminal electron acceptors are successively depleted, the production of CO_2, N_2O, and CH_4 often varies characteristically over time. Carbon dioxide production typically decreases monotonically, N_2O production peaks and then declines, and CH_4 production exhibits a threshold increase after other terminal electron acceptors have been depleted (Achtnich and others 1995; Yu and others 2007). The utility of this model to predict temporal and spatial patterns of redox reactions and greenhouse gas fluxes remains largely untested in upland humid tropical soils.

Well-drained upland humid tropical forest soils can experience sub-atmospheric O_2 concentrations due to a combination of high moisture and respiration rates. Soil O_2 concentrations in Puerto Rican forests correlated with differences in total rainfall at a landscape scale and with temporal variability in rainfall within sites over days to weeks (Silver and others 1999; Liptzin and others 2011). However, the relative influence of soil moisture on redox reactions and greenhouse gas fluxes has not been tested in these ecosystems, especially as compared with other soil characteristics such as C concentration. Given the rapid infiltration rates characteristic of these soils (McDowell and others 1992) and the potential for infiltrating water to supply dissolved O_2 to microbes, we expect a more nuanced relationship between rainfall, soil moisture, and redox processes in this ecosystem. Here, we tested the influence of soil moisture on redox reactions and greenhouse gas fluxes using a 24-day water addition experiment to amplify differences in soil moisture among plots. This timescale is relevant to the underlying periodicity of rainfall and O_2 fluctuations in this ecosystem, given that sustained periods of high precipitation and bulk soil O_2 depletion occur on scales of days to weeks (Heartsill-Scalley and others 2007; Liptzin and others 2011). Our 24-day water addition treatment represents an extreme but plausible end-member of potential rainfall scenarios. Dominant redox processes can shift over scales of days to weeks in wetland ecosystems (Achtnich and others 1995; Ratering & Conrad 1998), and we predicted similarly rapid responses in our tropical forest ecosystem given the facultative anaerobic capacity of the endemic microbial community (Pett-Ridge & Firestone 2005). We compared patterns in the concentrations of electron acceptors (O_2, NO_3, SO_4) and reduced products (Mn(II), Fe(II), and soil CH_4) as relative indicators of redox reactions. We predicted that sustained high soil moisture would deplete electron acceptors, correlating with a decline in CO_2 fluxes, a brief period of elevated N_2O fluxes, and an eventual increase in CH_4 fluxes. We also predicted that shorter

periods (days) of high soil moisture would suppress CO_2 fluxes, but would be insufficient to deplete electron acceptors and stimulate net positive CH_4 fluxes.

Methods

Study area

We conducted our experiment in the Bisley Watershed of the Luquillo Experimental Forest, Puerto Rico (18.3° N, -65.8° W), an NSF-funded Long Term Ecological Research and Critical Zone Observatory site. This subtropical wet forest ecosystem experiences a long-term mean precipitation of 3500 mm yr^{-1} and mean annual temperature of 23° C (Scatena 1989). Seasonal variation in rainfall is relatively low, with a minimum in March (5.6 ± 0.7 mm day^{-1}) and maximum in May (11.7 ± 1.3 mm day^{-1}) from 1988 to 2003 (Heartsill-Scalley and others 2007). Extreme precipitation events exceeding 100 mm day^{-1} can occur during any month, and most years experience several weeks of precipitation > 30 mm day^{-1}. Inter-annual precipitation is highly variable, ranging from 2600 – 5800 mm yr^{-1} between 1989 and 2011 (F. Scatena, unpublished data). Bisley watershed soils are ultisols supporting mature closed-canopy forest dominated by tabonuco (*Dacryodes excelsa*) and sierra palms (*Prestoea montana*) (Huffaker 2002). Overland flow of water is rare in these upland soils given that infiltration rates (0.07 – 1.5 cm min^{-1}) typically exceed rainfall (0.1 cm min^{-1}; McDowell and others 1992). Soil depth varies with topographic position in the Bisley watersheds and measures approximately 40 cm to saprolite in our experimental site. Surface soils (0 – 20 cm) have mean clay, silt and sand contents of 39, 51, and 11 %, respectively (T. Natake, unpublished data), with a mean bulk density of 0.7 g cm^{-3}.

Experimental Design

We established 18 plots measuring 1.25 x 1.25 m within a 20 x 30-m area in an upland valley (Scatena 1989). Plots were assigned to one of three treatments: daily water additions for 24 days ("continuous" treatment); a regime consisting of eight days of water addition followed by eight days of throughfall exclusion and a final eight days of water addition ("fluctuating" treatment); an un-manipulated control. Plot size was chosen to allow high replication within a relatively homogeneous landscape position while minimizing soil variability within a plot, and we positioned plots to avoid effects of downslope water movement. Throughfall was excluded for eight days in the fluctuating treatment using transparent plastic shelters suspended 1 m above the plot surface. Each simulated rainfall event amounted to the addition of approximately 60 mm day^{-1} of water collected from a nearby first-order stream. This water addition regime represents a high but realistic amount of precipitation that normally occurs for at least one week per year (Heartsill-Scalley and others 2007). Water was added via perforated transparent plastic trays suspended approximately 10 cm above the plot surface, from which water slowly percolated onto the soil. Trays were removed from plots between watering events. Our 24-day continuous watering treatment provided an end member of realistic precipitation patterns to test the response of redox reactions to sustained precipitation inputs. We conducted the experiment during October 2010.

Data collection

Soil moisture and O_2 concentrations were measured quasi-continuously in each plot (n = 18) at 30-minute intervals for two months prior to and during the experiment using time-domain reflectometry (Campbell Scientific, Logan, Utah) and galvanic cell sensors (Apogee Instruments, Logan, Utah) connected to a datalogger. Oxygen sensors were calibrated to local pressure and mean soil temperature at 100 % relative humidity, and were installed inside equilibration chambers consisting of 10-cm long polyvinyl-chloride tubes (5 cm diameter) with an open bottom and sealed top with a sampling port (three-way stopcock). These chambers were installed to a depth of 10 cm after removing an equivalent volume of soil, and 30 ml of headspace gas was sampled with a syringe at four-day intervals throughout the experiment to measure concentrations of CO_2, N_2O, and CH_4 (see below). Temperature sensors were installed at a depth of 10 cm in a subset of plots (n = 2 per treatment). Moisture sensors provided an integrated measurement of the 0 – 20 cm depth, the predominant location of roots and organic matter in this ecosystem (Odum and others 1970).

Soil-atmosphere fluxes of CO_2, CH_4, and N_2O were measured in each plot immediately prior to the experiment and at two-day intervals thereafter using a vented static flux chamber technique (total n = 234), with chamber collars removed between measurements. Chamber collars (26 cm diameter) were installed to 3 cm depth and removed two months prior to the experiment. Collars were subsequently installed in the same positions during measurements to minimize artifacts due to root mortality and decay (Keller et al., 2000). Mean height of the collar + chamber assembly was 18 cm. Gas concentrations were measured using a gas chromatograph (Shimadzu, Columbia, MD) equipped with a flame ionization detector, thermal conductivity detector, and electron capture detector for CH_4, CO_2, and N_2O, respectively. Fluxes were calculated by fitting gas concentration data from five samples collected over 40 min to a model derived from Fick's first law (Matthias and others 1978). This non-linear model accounts for inhibitory effects from increasing gas concentrations on fluxes throughout the measurement period.

Soils were sampled for chemical extraction prior to the experiment and at eight-day intervals thereafter. We composited three replicate 1.6-cm diameter soil cores (20 cm depth) for each plot. Separate replicate subsamples of each soil were extracted for 60 min in 1:10 slurries of 0.5 M hydrochloric acid (HCl) and filtered to 0.22 μm for Fe(II) and Mn analysis, and 1:5 slurries of potassium chloride and ammonium acetate were extracted and filtered to 10 μm and 0.22 μm for analysis of nitrate (NO_3^-) and sulfate (SO_4^{2-}), respectively. Potassium chloride extractions were subsequently combined with a phosphate solution and filtered to 0.45 μm to eliminate analytical interference from Fe (Yang and others 2012). We assumed that HCl-extractable Mn predominantly represents divalent reduced Mn (Mn(II)). We measured Fe(II) using a ferrozine assay accounting for interference from Fe(III) (Viollier and others 2000), Mn using inductively coupled plasma atomic emission spectroscopy, NO_3^- using cadmium reduction and colorimetry, and SO_4^{2-} using ion chromatography. Soil solutions were sampled from tension lysimeters (Prenart Super Quartz, Denmark) installed within 20 cm of the center of each plot at a depth of 10 cm. We sampled lysimeters at four-day intervals when yield was sufficient, filtered (pre-combusted Whatman GF-F), and frozen prior to analysis at University of New Hampshire by ion chromatography and combusted for measurement of dissolved organic C (DOC) on a

Shimadzu TOC-V. We acidified a subset of soil solution samples with HCl to pH < 2 in the field for Fe(II) analysis (as above) when sufficient volume was available. Soil C was measured in pre-treatment samples (air-dried and ground) from all plots by combustion on a CE Elantech elemental analyzer (Lakewood, NJ).

We modeled soil diffusivity for CO_2 using the Millington and Shearer (1971) model for aggregated porous media, incorporating diffusion through inter-aggregate and intra-aggregate pores. We estimated intra-aggregate porosity using volumetric soil moisture content at field capacity determined two days after a saturating rainfall event (Davidson & Trumbore 1995). Replicate measurements of field capacity among plots agreed closely (slope = 0.95, $R^2 = 0.96$).

Data Analysis

Response variables were analyzed using mixed-effects models that incorporated random effects for plots and temporal autocorrelation implemented using the nlme library in R (Pinheiro and others 2011). The optimal random effect structure was selected using likelihood ratio tests after saturating the model with fixed effects. Fluxes of CO_2 and N_2O were log-transformed and fourth-root transformed, respectively, to satisfy model assumptions. Non-linear trends were analyzed using additive mixed models implemented in the mgcv package in R (Wood 2006). Briefly, additive models fit a non-parametric smooth function to data with an optimum complexity chosen by an information criteria approach. For these models we describe the significance, approximate variance explained, and approximate degrees of freedom (d. f.) of the smooth function, which provides a measure of the curvature of the function. For example, a smooth function with three d. f. would have three inflection points. In addition, we summarized the co-variation among redox species sampled within a given plot using principal components analysis.

Results

Moisture dynamics

The continuous water addition treatment maintained soils above field capacity for the duration of the experiment, while the fluctuating and control treatments exhibited a pronounced decline in soil moisture (0.2 $m^3\ m^{-3}$) during the middle eight days of the experiment coinciding with a period of low rainfall, and a subsequent increase in moisture to initial levels (Figure 1). Water addition to the fluctuating treatment did not increase soil moisture relative to the controls, likely due to several substantial (> 20 mm) rain events at the beginning and end of the experiment. The continuously watered plots had slightly but significantly greater soil moisture than the other treatments before the experiment. Mean daily soil temperature averaged 24.3° C and varied by < 1° C over the experiment, and did not differ among treatments.

Variation among redox species

Oxygen concentrations were not significantly affected by either water supplementation treatment and showed relatively little temporal variation as compared with the other redox species (Figure 2). To account for spatial variation among plots, we report all redox species and gas flux data normalized to pre-treatment levels. Our additive model of O_2 concentrations showed a significant non-linear increase over time that was similar across all treatments ($p < 0.05$, smooth function with approximately 1.4 d.f.). Soil NO_3^- concentrations were initially similar among treatments and approximately doubled in the control and fluctuating treatments over the experiment, while NO_3^- in continuously watered treatments measured only 44% of the other treatments in the final samples (treatment contrast $p < 0.05$, Figure 2B). Lysimeter NO_3^- concentrations were initially low but increased significantly during the middle of the experiment in control and fluctuating treatments, coinciding with a decline in soil moisture (Figure 2F). Lysimeter NO_3^- remained consistently low in the continuously watered treatment, and lysimeter NH_4^+ concentrations declined significantly in all treatments over the experiment (Figure 2G).

Net Mn reduction occurred in all treatments, with final extractable Mn(II) concentrations reaching 182, 159, and 150 % of initial concentrations in the control, fluctuating, and continuous treatments, respectively (time effect $p < 0.001$, Figure 2C). Soil Fe(II) concentrations were largely static in control and fluctuating plots, but Fe(II) concentrations increased by 98 % in continuously-watered plots from day 18 to 25, reflecting considerable net Fe reduction (treatment by time interaction, $p < 0.05$, Figure 2D). In contrast, lysimeter Fe(II) concentrations showed considerable temporal variability across all treatments with large increases on days 17 and 21 (Figure 2h). Both soil and lysimeter SO_4^{2-} concentrations showed the least temporal variation of all the redox species (Figure 2E and Figure 2I). Lysimeter DOC concentrations generally showed similar trends among treatments, but showed a secondary peak in the fluctuating treatment on days 21 and 25 (Figure 2J). Control and continuously-watered plots had similar DOC concentrations over most of the experiment.

Oxygen concentrations displayed a significant non-linear pairwise negative relationship with soil moisture ($R^2 = 0.33$, $p < 0.0001$, smooth function with 3.7 d.f., Fig 3A). Oxygen concentrations below detection limit were occasionally recorded above 55 % soil moisture (Fig 3A). Continuous water addition was not sufficient to deplete soil O_2, however, and O_2 frequently approached atmospheric concentrations even at high soil moisture ($> 0.55\ m^3\ m^{-3}$). Redox-active chemical species measured in the soil atmosphere and soil extractions (O_2, NO_3^-, Mn(II), Fe(II), and CH_4) correlated according to thermodynamic predictions when analyzed together using principal component analysis; the first principal component explained 48 % of their combined co-variation (Table 1). That is, lower concentrations of O_2 and NO_3^- were associated with increased Mn(II), Fe(II), and CH_4, but not in a step-wise manner. Sulfate was not significantly correlated with the other redox species. The first principal component of redox species displayed a negative non-linear relationship with soil moisture similar to the relationship between O_2 and soil moisture ($R^2 = 0.38$, $p < 0.001$, smooth function with 2 d.f., Figure 3B).

Greenhouse gas fluxes

Fluxes of CO_2 varied significantly over time but showed similar temporal trends across all treatments (one smooth function with 7.8 d.f. $p < 0.0001$). Moisture and O_2 concentrations were significantly correlated with CO_2 fluxes (moisture: negative correlation, $p < 0.001$ and O_2:

positive correlation, $p < 0.04$), but explained comparatively little variation (8% of the sum of squares). Instead, constitutive spatial variation in CO_2 fluxes (plot random effects) accounted for 81% of the model sum of squares. Modeled diffusivity correlated only weakly with CO_2 fluxes ($R^2 = 0.07$, $p < 0.01$). Soil CO_2 concentrations at 10 cm were more variable than CO_2 surface fluxes, especially in the control plots where CO_2 declined to 33 % of initial concentrations between days 1 and 17 (Figure 4B). Changes in soil CO_2 concentrations did not significantly correlate with surface fluxes. When we averaged CO_2 fluxes over time by plot they correlated significantly with soil C concentrations ($p < 0.01$, Figure 5a) and with the first principal component of redox species ($p < 0.05$, Figure 5B), which together explained 62 % of the variation in mean CO_2 fluxes among plots.

Nitrous oxide fluxes were lowest in continuously watered plots and were highest and most variable in the control plots (Figure 4C). Fluxes of N_2O were significantly related to moisture, O_2, and their interaction ($p = 0.01$ for all three terms), with the highest N_2O fluxes occurring at intermediate O_2 and moisture (18 % and 0.5 $m^3 m^{-3}$, respectively, Figure 5C,D). Dynamics of soil N_2O concentrations did not follow those of surface fluxes. Soil N_2O concentrations were typically highest in the continuously watered plots, while surface fluxes were lowest in this treatment (Figure 4D).

Fluxes of CH_4 were not significantly related to O_2 or moisture. Although net positive CH_4 fluxes typically occurred at high soil moisture (Figure 5E), positive fluxes were also observed in plots with near-atmospheric soil O_2 concentrations (Figure 5F). Mean CH_4 fluxes averaged over the experiment showed a significant correlation with the redox principal component ($p = 0.02$, $R^2 = 0.30$). Soil CH_4 concentrations (10 cm depth) typically exceeded atmospheric levels in all plots.

Discussion

Redox species

Research over the last decade has highlighted the importance of anaerobic metabolic processes such as Fe reduction and methanogenesis in upland forest soils (Silver and others 1999; Peretyazhko & Sposito 2005; Teh and others 2005; Chacon and others 2006; Thompson and others 2006; Fimmen and others 2008; Liptzin & Silver 2009; Dubinsky and others 2010). The spatial and temporal dynamics of redox reactions in these soils are generally assumed to vary with soil moisture. In this study, volumetric soil moisture ranged between 0.3 and 0.6 $m^3 m^{-3}$ among plots, yet contrary to our first prediction moisture explained comparatively little temporal variability in indicators of redox reactions, including O_2, NO_3, Mn(II), Fe(II), and CH_4 concentrations. The temporal variation in soil moisture that we observed over the scale of days was equivalent to seasonal variation in moisture measured in other humid tropical forests (Kursar and others 1995; Koehler and others 2009; Wieder and others 2011). The relative decoupling between moisture and redox processes in this upland humid tropical forest contrasts with data from wetlands emphasizing the predominant role of moisture in controlling the spatial and temporal segregation of redox reactions (Patrick & Jugsujinda 1992; Achtnich and others 1995;

Ratering & Conrad 1998; Yao and others 1999). In our study, we found that concentrations of redox species co-varied according to thermodynamic predictions within plots, but we observed little segregation of distinct redox reactions within plots over time. That is, aerobic respiration, denitrification, Mn reduction, Fe reduction, and methanogenesis all apparently occurred in close spatial proximity (within a given plot). Furthermore, extended periods of elevated soil moisture did not drive temporal patterns in redox chemical species, with the possible exception of Fe(II) concentrations which ultimately increased, and NO_3^- which decreased in continuously-watered plots. The co-occurrence of multiple aerobic and anaerobic metabolic processes suggests the importance of aggregate-scale spatial variation in moisture, O_2, and electron acceptor availability, which facilitate the co-occurrence of multiple redox reactions that would not likely persist in a spatially homogenous environment.

While denitrification has long been known to occur within anaerobic soil aggregates in an otherwise aerobic environment (Sexstone and others 1985), we also measured considerable extractable Mn, Fe(II), and CH_4 at soil moisture below field capacity concomitant with abundant soil O_2 (a mean of 16 % over the experiment). Net Mn reduction occurred in all treatments, including plots where moisture declined well below field capacity, and soil Fe(II) concentrations were relatively high even in these drier plots. The high affinity of these clay-rich soils for moisture and their well-developed aggregate structure could explain the persistence of anaerobic microsites even under relatively drier conditions. Fimmen and others (2008) suggested that labile C supply stimulates Fe reduction in rhizosphere soil, providing an additional mechanism for generating anaerobic microsites even when macropores contain O_2. Net positive Mn and Fe reduction in a dominantly aerobic soil environment likely masks even greater rates of gross Mn and Fe reduction, given that Mn(II) and Fe(II) should oxidize in the presence of O_2. Indeed, increases in soil lysimeter solution Fe(II) concentrations suggest gross Fe reduction (Fe reduction followed by oxidation) even in control plots.

Concentrations of O_2 and a principal component summarizing variation among measured redox species exhibited nonlinear threshold responses to moisture, but sustained high moisture did not usually deplete O_2, and many plots showed near-atmospheric O_2 concentrations despite sustained periods with moisture exceeding field capacity. These data suggest that high soil moisture is necessary but not sufficient to deplete macropore O_2 in upland humid tropical forests. Additionally, infiltrating water could provide a significant source of O_2. Our water addition treatment could have supplied up to 2.5 g O_2 m^{-2} d^{-1} if added water had completely equilibrated with soil porewater, which is theoretically sufficient to account for the majority of C oxidation to CO_2 that we observed. It is likely, however, that water addition did not greatly contribute to O_2 supply given the importance of rapid preferential flow in this ecosystem, which precludes substantial O_2 exchange (McDowell and others 1992). In agreement with our results, water supplementation to soils in Panama caused only a small (1.4 %) decrease in bulk soil O_2 concentrations (Kursar and others 1995). During this experiment we also observed soil oligochaeta (earthworm) burrowing activity that increased within minutes of applying water to plots, leaving soil casts > 1 cm diameter on the soil surface. Worms were documented to mitigate hypoxia in marine sediments by burrowing (Norkko and others 2011). We suggest that an increase of faunal burrowing activity following precipitation events and O_2 supply from rainwater could help explain the observed decoupling between moisture and O_2 in soils with moisture contents above field capacity.

Combining our present data with previous research provides a more nuanced understanding of relationships between precipitation and soil O_2 concentrations. Previous O_2 measurements near our study site correlated negatively with cumulative rainfall measured over 28-day periods, and with trends in hourly rainfall over periods of 10 – 16 days (Silver and others 1999; Liptzin and others 2011). Rainfall frequency rather than magnitude had a greater influence on O_2 concentrations in these studies. We hypothesize that the minimal temporal response of O_2 concentrations to water addition that we documented in the present study may have been partly constrained by underlying long-term rainfall dynamics: rainfall events were frequent before the study began. Consequently, constitutive spatial variation may be responsible for the highly significant pairwise relationship between moisture and O_2 that we observed. The relative unresponsiveness of O_2 to large short-term variation in moisture documented here suggests caution in extrapolating long-term relationships between moisture and O_2 to shorter-term dynamics.

Controls on greenhouse gas fluxes

Fluxes of CO_2 and CH_4 exhibited relatively little temporal variability in response to high variation in soil moisture throughout our experiment. Contrary to our prediction, sustained high moisture neither suppressed CO_2 fluxes nor stimulated CH_4 fluxes, suggesting the resistance of microbial C cycling processes and/or root respiration. Modeled diffusivity showed little correlation with gas fluxes, suggesting that differences in biological rates as opposed to physical constraints governed variation among plots. These results contrast with data from temperate soils with comparable C concentrations that show an inhibition of organic matter decomposition as soil moisture exceeds field capacity (Linn & Doran 1984), an assumption incorporated in prominent ecosystem biogeochemical models (Li and others 1992; Parton and others 1993). The response of humid tropical forest soil microbial communities to variation in moisture and O_2 availability could be distinct from that of temperate ecosystems. In soil from our site, microbial biomass and taxonomic richness were greatest under conditions of fluctuating O_2 availability relative to static aerobic conditions (Pett-Ridge & Firestone 2005). From a microbial perspective, consistently high soil moisture could represent an appropriate reference condition in this ecosystem, whereas declines in moisture might impose greater stress. Indeed, Wood and Silver (2012) recently documented a suppressive effect of experimental drought on soil CO_2 fluxes from this ecosystem.

Mean soil CO_2 fluxes were best predicted by soil C concentrations and a principal component integrating the relative abundance of five redox-active chemical species. This model suggests that C substrate availability provides a first-order predictor of respiration that is further impacted by plot-specific differences in anaerobiosis. The principal component summarizing variation in five different redox reactions provided better explanatory power for CO_2 fluxes than O_2 concentrations alone, suggesting the importance of accounting for multiple co-occurring anaerobic processes in addition to aerobic respiration. Cleveland et al. (2010) found a significant negative relationship between O_2 concentrations and CO_2 fluxes in a lowland tropical forest over the scale of months, and suggested that a combination of anaerobiosis and dilution of DOC could explain declines in CO_2 fluxes under wet conditions. In our experiment, lysimeter DOC concentrations did not decline in rainfall addition treatments relative to controls, suggesting that

C substrate limitation due to water addition was not likely an overriding factor over the timescale of our study.

We documented significant interactive effects of moisture and O_2 availability on N_2O fluxes consistent with the "hole in the pipe" model, which predicts that rates of N cycling and diffusion will control N_2O fluxes (Davidson and others 2000). In our study, extractable and lysimeter NO_3 concentrations increased in control and fluctuating water-addition plots during periods of low soil moisture, likely fueling subsequent N_2O production. High moisture and low O_2 concentrations likely suppressed N_2O fluxes due to decreased NO_3 supply from nitrification and increased denitrification to N_2. In other humid tropical forest soils, moisture correlated positively with N_2O fluxes (Keller & Reiners 1994; Erickson and others 2001; Kiese & Butterbach-Bahl 2002; Koehler and others 2009; Rowlings and others 2012), but N_2O fluxes often display a Gaussian distribution across the entire range of potential soil moisture characterized by declines under very wet conditions (Kiese & Butterbach-Bahl 2002; Castellano and others 2010). Our data support the results of Wieder et al. (2011) and suggest that inhibitory effects of moisture on N_2O fluxes may dominate in high rainfall environments. We found that sustained high soil moisture was consistently associated with high soil N_2O concentrations, but low N_2O fluxes suggestive of reduction to N_2. The highest N_2O fluxes occurred in control plots where moisture declined and subsequently increased due to rainfall events, resulting in lower soil moisture than the fluctuating plots and potentially creating an optimum combination of substrate availability, moisture, and O_2 for nitrification/denitrification.

Several plots showed consistently positive net CH_4 fluxes over the experiment and were unaffected by water addition treatments, while others fluctuated between small net CH_4 sources or sinks. Surprisingly, almost all positive CH_4 fluxes occurred in the presence of measurable bulk soil O_2 concentrations. Liptzin et al. (2011) found an inverse correlation between O_2 and soil CH_4 concentrations over the scale of months in nearby sites, but our present data suggest caution in extrapolating from soil CH_4 concentrations to surface fluxes, as concentrations of CH_4 typically exceeded atmospheric levels even in the absence of net surface efflux. Variation in CH_4 oxidation may control the direction of fluxes in these soils (Teh and others 2005; Rowlings and others 2012), where several plots fluctuated between CH_4 sources and sinks. Notably, however, soil CH_4 fluxes did not increase in response to continuous water addition in our study. In wetland ecosystems, CH_4 production is typically suppressed until alternative electron acceptors are depleted during periods of sustained flooding (Ratering & Conrad 1998; Megonigal and others 2003; Yu and others 2007). In upland humid tropical forests, spatial heterogeneity of redox processes or high electron donor concentrations could allow gross CH_4 production despite the presence of alternative electron acceptors. The lack of correlation among CH_4 fluxes, moisture, and bulk soil O_2 concentrations further supports the importance of anaerobic microsites in controlling CH_4 fluxes. We cannot rule out that CH_4 is produced from soil below our measurement zone, but surface soils showed high potential methanogenesis (Chacon and others 2006) and soils are shallow (30 – 40 cm to saprolite) at our particular study site. In sum, our data suggests that sustained high soil moisture will not necessarily induce a spike in CH_4 production in upland humid tropical soils, in contrast to wetland soils where duration of flooding appears critical for predicting electron acceptor depletion and CH_4 fluxes (Ratering & Conrad 1998; Knorr & Blodau 2009), and in contrast to a seasonally-dry tropical forest where irrigation treatments sometimes stimulated net positive CH_4 fluxes (Vasconcelos and others 2004). While

CH_4 fluxes tended to increase with our integrated measure of anaerobiosis, concentrations of labile Fe oxides measured in a separate study (S. Hall, data not shown) typically exceeded Fe(II) pools by at least one order of magnitude in all soils measured, indicating substantial potential for Fe reduction. Our data point to the importance of localized CH_4 production "hot-spots" that persist despite the widespread presence of alternative electron acceptors.

Implications for climate change

The impact of climate change on precipitation regimes in humid tropical ecosystems remains highly uncertain, yet empirical and theoretical evidence points to an increase in the magnitude, variability, and importance of extreme events in some regions (Karl and others 1995; Romps 2011). Our data suggest that short-term increases in precipitation over the scale of weeks may have little additional impact on CO_2 and CH_4 fluxes from upland humid tropical forests. Such precipitation variability appears increasingly common at our site, reflected in highly variable inter-annual rainfall between 1989 and 2011 (2600 – 5800 mm yr^{-1}, F. Scatena unpublished data). Our results contrast with temperate wetland ecosystems, where variation in precipitation and water levels appear to play a defining role in constraining O_2 availability, terminal electron accepting processes, and greenhouse gas fluxes (Ponnamperuma 1972; Ratering & Conrad 1998; Jungkunst & Fiedler 2007; Knorr & Blodau 2009). The TEAP model, which posits that terminal electron acceptors will be reduced according to thermodynamic favorability during periods of high moisture, may be less useful for understanding plot-scale dynamics in upland humid tropical forests given their high spatial heterogeneity. Spatial segregation of redox processes within soil aggregates likely allows Mn and Fe reduction and methanogenesis to occur despite the close proximity of O_2. Given adequate baseline moisture availability, increased precipitation may have relatively little impact on microbial processes occurring at the aggregate scale. Droughts that cross a moisture threshold where anaerobic microsites disappear, however, may provoke a stronger biogeochemical response.

Conclusions

We found that sustained high and variable soil moisture regimes had relatively little impact on soil redox biogeochemical processes and greenhouse gas fluxes from a humid tropical forest soil over a 25-day field experiment. Pairwise relationships between moisture and redox indicators that reflect constitutive spatial soil heterogeneity, however, did show significant relationships in spite of relatively weak effects from water addition treatments themselves. These results suggest that moisture provides an adequate proxy for spatial variation in redox reactions, but less utility for predicting temporal variation over the timescale of our study. While spatial variability in bulk soil O_2 concentrations and trace gas fluxes generally exceeded temporal variability, we documented relatively large temporal variation in NO_3, Mn(II), and Fe(II) pools. Anaerobic redox processes co-occurred with relatively high O_2 concentrations in close proximity, showing a relative decoupling between moisture and O_2 at the plot scale. Overall, our data suggest that the TEAP model of sequential electron acceptor depletion over timescales of days to weeks is not a useful conceptual model of redox-sensitive biogeochemistry in this ecosystem. We observed net Fe reduction and a non-significant increase in CH_4 flux in the continuous water addition treatment at the end of the experiment, suggesting that long-term periods (> 24 days) of sustained soil moisture exceeding field capacity might ultimately

stimulate anaerobic processes beyond background rates. Such sustained rainfall, however, is difficult to envision given the present stochasticity of precipitation at this site.

Mean soil CO_2 fluxes displayed a negative relationship with reducing conditions, as predicted by thermodynamic theory, but surprisingly, water additions did not suppress CO_2 fluxes over the timescale of our study. Biogeochemical models typically incorporate inhibitory effects of moisture on soil respiration. Our results suggest that soil respiration in humid tropical forests may be resistant to short-term (days – weeks) increases in moisture, and suggest caution in applying models developed for temperate soils in humid tropical ecosystems. Furthermore, water supplementation consistently suppressed N_2O fluxes, contrasting with results from relatively drier ecosystems. Longer experiments encompassing a broader range of moisture conditions and humid tropical ecosystems are necessary to confirm these findings. A relatively wide range of soil moisture may have little short-term impact on CO_2 and CH_4 fluxes from humid tropical forests, questioning the representation of these processes in current biogeochemical models.

Acknowledgements

This article was published in the journal Ecosystems, with contributions from my co-authors William H. McDowell and Whendee L. Silver. We thank the editors and Springer for copyright permissions. We thank D. Kirschner for herculean field assistance, M. Almaraz, A. McDowell, J. Potter, C. Torrens, and S. van Bloem for logistics, and R. Rhew, M. Firestone, and two anonymous reviewers for comments. SJH was supported by the Department of Energy Office of Science Graduate Fellowship Program (DOE SCGF), made possible in part by the American Recovery and Reinvestment Act of 2009, administered by ORISE-ORAU under contract no. DE-AC05-06OR23100. Funding was provided by NSF grant EAR-08199072 to WLS, and the NSF Luquillo Critical Zone Observatory (EAR-0722476) with additional support provided by the USGS Luquillo WEBB program. This research was also supported by grant DEB 0620910 from NSF to the Institute for Tropical Ecosystem Studies, University of Puerto Rico, and to the International Institute of Tropical Forestry USDA Forest Service, as part of the Luquillo Long-Term Ecological Research Program.

References

Achtnich C, Bak F, Conrad R. 1995. Competition for electron donors among nitrate reducers, ferric iron reducers, sulfate reducers, and methanogens in anoxic paddy soil. Biol Fert Soils. 19:65–72.

Bloom AA, Palmer PI, Fraser A, Reay DS, Frankenberg C. 2010. Large-scale controls of methanogenesis inferred from methane and gravity spaceborne data. Science. 327:322–325.

Carmo JB do, Keller M, Dias JD, Camargo PB de, Crill P. 2006. A source of methane from upland forests in the Brazilian Amazon. Geophys Res Lett. 33:L04809.

Castellano MJ, Schmidt JP, Kaye JP, Walker C, Graham CB, Lin H, Dell CJ. 2010. Hydrological and biogeochemical controls on the timing and magnitude of nitrous oxide flux across an agricultural landscape. Global Change Biol. 16:2711–2720.

Chacon N, Silver WL, Dubinsky EA, Cusack DF. 2006. Iron reduction and soil phosphorus solubilization in humid tropical forests soils: The roles of labile carbon pools and an electron shuttle compound. Biogeochemistry. 78:67–84.

Chambers JQ, Tribuzy ES, Toledo LC, Crispim BF, Higuchi N, Santos J dos, Araújo AC, Kruijt B, Nobre AD, Trumbore SE. 2004. Respiration from a tropical forest ecosystem: partitioning of sources and low carbon use efficiency. Ecol Appl. 14:72–88.

Chapelle FH, McMahon PB, Dubrovsky NM, Fujii RF, Oaksford ET, Vroblesky DA. 1995. Deducing the distribution of terminal electron-accepting processes in hydrologically diverse groundwater systems. Water Resour Res. 31:359–371.

Cleveland CC, Wieder WR, Reed SC, Townsend AR. 2010. Experimental drought in a tropical rain forest increases soil carbon dioxide losses to the atmosphere. Ecology. 91:2313–2323.

Davidson EA, Janssens IA. 2006. Temperature sensitivity of soil carbon decomposition and feedbacks to climate change. Nature. 440:165–173.

Davidson EA, Keller M, Erickson HE, Verchot LV, Veldkamp E. 2000. Testing a conceptual model of soil emissions of nitrous and nitric oxides. BioScience. 50:667–680.

Davidson EA, Trumbore SE. 1995. Gas diffusivity and production of CO2 in deep soils of the eastern Amazon. Tellus B. 47:550–565.

Dubinsky EA, Silver WL, Firestone MK. 2010. Tropical forest soil microbial communities couple iron and carbon biogeochemistry. Ecology. 91:2604–2612.

Erickson HE, Keller M, Davidson EA. 2001. Nitrogen Oxide Fluxes and Nitrogen Cycling during Postagricultural Succession and Forest Fertilization in the Humid Tropics. Ecosystems. 4:67–84.

Fimmen RL, Richter D deB, Vasudevan D, Williams MA, West LT. 2008. Rhizogenic Fe–C redox cycling: a hypothetical biogeochemical mechanism that drives crustal weathering in upland soils. Biogeochemistry. 87:127–141.

Heartsill-Scalley T, Scatena FN, Estrada C, McDowell WH, Lugo AE. 2007. Disturbance and long-term patterns of rainfall and throughfall nutrient fluxes in a subtropical wet forest in Puerto Rico. J Hydrol. 333:472–485.

Hedin LO, von Fischer JC, Ostrom NE, Kennedy BP, Brown MG, Robertson GP. 1998. Thermodynamic constraints on nitrogen transformations and other biogeochemical processes at soil-stream interfaces. Ecology. 79:684–703.

Huffaker L. 2002. Soil survey of Caribbean National Forest and Luquillo Experimental Forest, Commonwealth of Puerto Rico.

Itoh M, Ohte N, Koba K. 2009. Methane flux characteristics in forest soils under an East Asian monsoon climate. Soil Biol Biochem. 41:388–395.

Jobbagy EG, Jackson RB. 2000. The Vertical Distribution of Soil Organic Carbon and Its Relation to Climate and Vegetation. Ecol Appl. 10:423–436.

Jungkunst HF, Fiedler S. 2007. Latitudinal differentiated water table control of carbon dioxide, methane and nitrous oxide fluxes from hydromorphic soils: feedbacks to climate change. Global Change Biol. 13:2668–2683.

Karl TR, Knight RW, Plummer N. 1995. Trends in high-frequency climate variability in the twentieth century. Nature. 377:217–220.

Keller M, Reiners WA. 1994. Soil-atmosphere exchange of nitrous oxide, nitric oxide, and methane under secondary succession of pasture to forest in the Atlantic lowlands of Costa Rica. Global Biogeochem Cycles. 8:399–409.

Kiese R, Butterbach-Bahl K. 2002. N_2O and CO_2 emissions from three different tropical forest sites in the wet tropics of Queensland, Australia. Soil Biology and Biochemistry. 34:975–987.
Knorr K, Blodau C. 2009. Impact of experimental drought and rewetting on redox transformations and methanogenesis in mesocosms of a northern fen soil. Soil Biol Biochem. 41:1187–1198.
Koehler B, Corre MD, Veldkamp E, Wullaert H, Wright SJ. 2009. Immediate and long□term nitrogen oxide emissions from tropical forest soils exposed to elevated nitrogen input. Global Change Biol. 15:2049–2066.
Kursar TA, Wright SJ, Radulovich R. 1995. The effects of the rainy season and irrigation on soil water and oxygen in a seasonal forest in Panama. Journal of Tropical Ecology. 11:497–515.
Li C, Frolking S, Frolking TA. 1992. A model of nitrous oxide evolution from soil driven by rainfall events: 1. Model structure and sensitivity. J Geophys Res 97:9759–9776.
Linn DM, Doran JW. 1984. Effect of water-filled pore space on carbon dioxide and nitrous oxide production in tilled and non-tilled soils. Soil Sci Soc Am J. 48:1267–1272.
Liptzin D, Silver WL, Detto M. 2011. Temporal Dynamics in Soil Oxygen and Greenhouse Gases in Two Humid Tropical Forests. Ecosystems. 14:171–182.
Liptzin D, Silver WL. 2009. Effects of carbon additions on iron reduction and phosphorus availability in a humid tropical forest soil. Soil Biol Biochem. 41:1696–1702.
Matson PA, Vitousek PM. 1990. Ecosystem approach to a global nitrous oxide budget. BioScience. 40:667–672.
Matthias AD, Yarger DN, Weinbeck RS. 1978. A numerical evaluation of chamber methods for determining gas fluxes. Geophys Res Lett. 5:765–768.
McDowell WH, Bowden WB, Asbury CE. 1992. Riparian nitrogen dynamics in two geomorphologically distinct tropical rain forest watersheds: subsurface solute patterns. Biogeochemistry. 18:53–75.
Megonigal JP, Hines ME, Visscher PT. 8.08 - Anaerobic Metabolism: Linkages to Trace Gases and Aerobic Processes. In: Treatise on Geochemistry. Oxford: Pergamon; 2003. pp. 317–424.
Millington RJ, Shearer RC. 1971. Diffusion in aggregated porous media. Soil Sci. 111:372–378.
Norkko J, Reed DC, Timmermann K, Norkko A, Gustafsson BG, Bonsdorff E, Slomp CP, Carstensen J, Conley DJ. 2011. A welcome can of worms? Hypoxia mitigation by an invasive species. Global Change Biol. 18:422–434.
Odum HT, Pigeon RF, Commission USAE. Rain forest structure and mineral-cycling homeostasis. In: A Tropical rain forest: a study of irradiation and ecology at El Verde, Puerto Rico. Division of Technical Information, U.S. Atomic Energy Commission; 1970.
Parton WJ, Scurlock JMO, Ojima DS, Gilmanov TG, Scholes RJ, Schimel DS, Kirchner T, Menaut J-C, Seastedt T, Moya EG, and others. 1993. Observations and modeling of biomass and soil organic matter dynamics for the grassland biome worldwide. Global Biogeochem Cycles. 7:785–809.
Patrick WH, Jugsujinda A. 1992. Sequential Reduction and Oxidation of Inorganic Nitrogen, Manganese, and Iron in Flooded Soil. Soil Sci Soc Am J. 56:1071–1073.
Peretyazhko T, Sposito G. 2005. Iron(III) reduction and phosphorous solubilization in humid tropical forest soils. Geochim Cosmochim Ac. 69:3643–3652.

Pett-Ridge J, Firestone MK. 2005. Redox fluctuation structures microbial communities in a wet tropical soil. Applied and Environmental Microbiology. 71:6998–7007.
Pinheiro J, Bates D, DebRoy S, Sarkar D, R Core Development Team. 2011. nlme: Linear and Nonlinear Mixed Effects Models.
Ponnamperuma FN. 1972. The chemistry of submerged soils. Adv Agron. 24:29–96.
Raich JW, Schlesinger WH. 1992. The global carbon dioxide flux in soil respiration and its relationship to vegetation and climate. Tellus B. 44:81–99.
Ratering S, Conrad R. 1998. Effects of short-term drainage and aeration on the production of methane in submerged rice soil. Global Change Biol. 4:397–407.
Romps DM. 2011. Response of Tropical Precipitation to Global Warming. J Atmos Sci. 68:123–138.
Rowlings DW, Grace PR, Kiese R, Weier KL. 2012. Environmental factors controlling temporal and spatial variability in the soil□atmosphere exchange of CO2, CH4 and N2O from an Australian subtropical rainforest. Global Change Biol. 18:726–738.
Scatena FN. 1989. An introduction to the physiography and history of the Bisley experimental watersheds in the Luquillo Mountains of Puerto Rico. USDA Forest Service General Technical Report. SO-72:1–22.
Schuur EAG, Matson PA. 2001. Net primary productivity and nutrient cycling across a mesic to wet precipitation gradient in Hawaiian montane forest. Oecologia. 128:431–442.
Sexstone AJ, Revsbech NP, Parkin TB, Tiedje JM. 1985. Direct measurement of oxygen profiles and denitrification rates in soil aggregates. Soil Sci Soc Am J. 49:645–651.
Silver WL, Lugo AE, Keller M. 1999. Soil oxygen availability and biogeochemistry along rainfall and topographic gradients in upland wet tropical forest soils. Biogeochemistry. 44:301–328.
Steudler PA, Melillo JM, Feigl BJ, Neill C, Piccolo MC, Cerri CC. 1996. Consequence of forest-to-pasture conversion on CH4 fluxes in the Brazilian Amazon Basin. J Geophys Res. 101:18547–18554.
Teh YA, Silver WL, Conrad ME. 2005. Oxygen effects on methane production and oxidation in humid tropical forest soils. Global Change Biology. 11:1283–1297.
Thompson A, Chadwick OA, Rancourt DG, Chorover J. 2006. Iron-oxide crystallinity increases during soil redox oscillations. Geochimica et Cosmochimica Acta. 70:1710–1727.
Vasconcelos SS, Zarin DJ, Capanu M, Littell R, Davidson EA, Ishida FY, Santos EB, Araújo MM, Aragão DV, Rangel-Vasconcelos LGT, and others. 2004. Moisture and substrate availability constrain soil trace gas fluxes in an eastern Amazonian regrowth forest. Global Biogeochem Cycles. 18:GB2009.
Vine H, Thompson H, Hardy F. 1942. Studies on aeration of cacao soils in Trinidad (II). Tropical Agriculture. 19:215–223.
Viollier E, Inglett PW, Hunter K, Roychoudhury AN, van Cappellen P. 2000. The ferrozine method revisited: Fe(II)/Fe(III) determination in natural waters. Appl Geochem. 15:785–790.
Wieder WR, Cleveland CC, Townsend AR. 2011. Throughfall exclusion and leaf litter addition drive higher rates of soil nitrous oxide emissions from a lowland wet tropical forest. Global Change Biol. 17:3195–3207.
Wood SN. 2006. Generalized Additive Models: An Introduction with R. Boca Raton (FL): CRC Press. 422p.

Wood T, Silver WL. 2012. Strong spatial variability in trace gas dynamics following experimental drought in a humid tropical forest. Global Biogeochem Cycles. 26:GB3005.
Yang WH, Herman D, Liptzin D, Silver WL. 2012. A new approach for removing iron interference from soil nitrate analysis. Soil Biology and Biochemistry. 46:123–128.
Yao H, Conrad R, Wassmann R, Neue HU. 1999. Effect of soil characteristics on sequential reduction and methane production in sixteen rice paddy soils from China, the Philippines, and Italy. Biogeochemistry. 47:269–295.
Yu KW, Bohme F, Rinklebe J, Neue HU, DeLaune RD. 2007. Major biogeochemical processes in soils - A microcosm incubation from reducing to oxidizing conditions. Soil Sci Soc Am J. 71:1406–1417.
Yu KW, Faulkner SP, Baldwin MJ. 2008. Effect of hydrological conditions on nitrous oxide, methane, and carbon dioxide dynamics in a bottomland hardwood forest and its implication for soil carbon sequestration. Global Change Biol. 14:798–812.

Tables

Table 1: Principal components analysis of co-variation among redox-active chemical species sampled at eight-day intervals over the experiment. PCA loading represents relationships between chemical species and the first principal component, which explained 48% of the variance among redox species.

Species	PCA loading	Redox state
O_2	-0.44	oxidized
NO_3	-0.28	oxidized
Mn(II)	0.51	reduced
Fe(II)	0.5	reduced
CH_4	0.47	reduced

Figure 1: Precipitation and soil moisture (m^3 m^{-3}) ± SE by treatment. The period of treatment application is shown in the shaded rectangle.

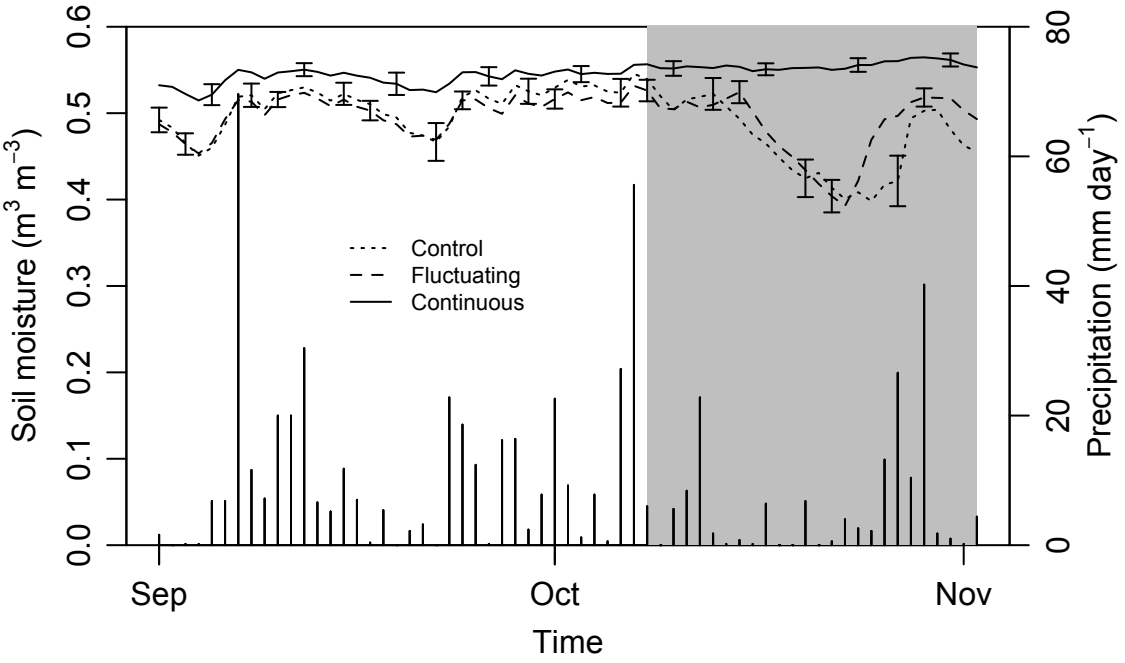

Figure 2: Soil atmosphere concentrations of O_2 at 10 cm (a), KCl-extractable soil NO_3 (b), HCl-extractable Mn(II) and Fe(II) (c,d), and ammonium acetate-extractable SO_4 (e). The right-hand column shows lysimeter concentrations of NO_3 (f), NH_4, (g) Fe(II) (h), SO_4 (i), and dissolved organic carbon (j). Data (± SE) are normalized to pre-treatment values.

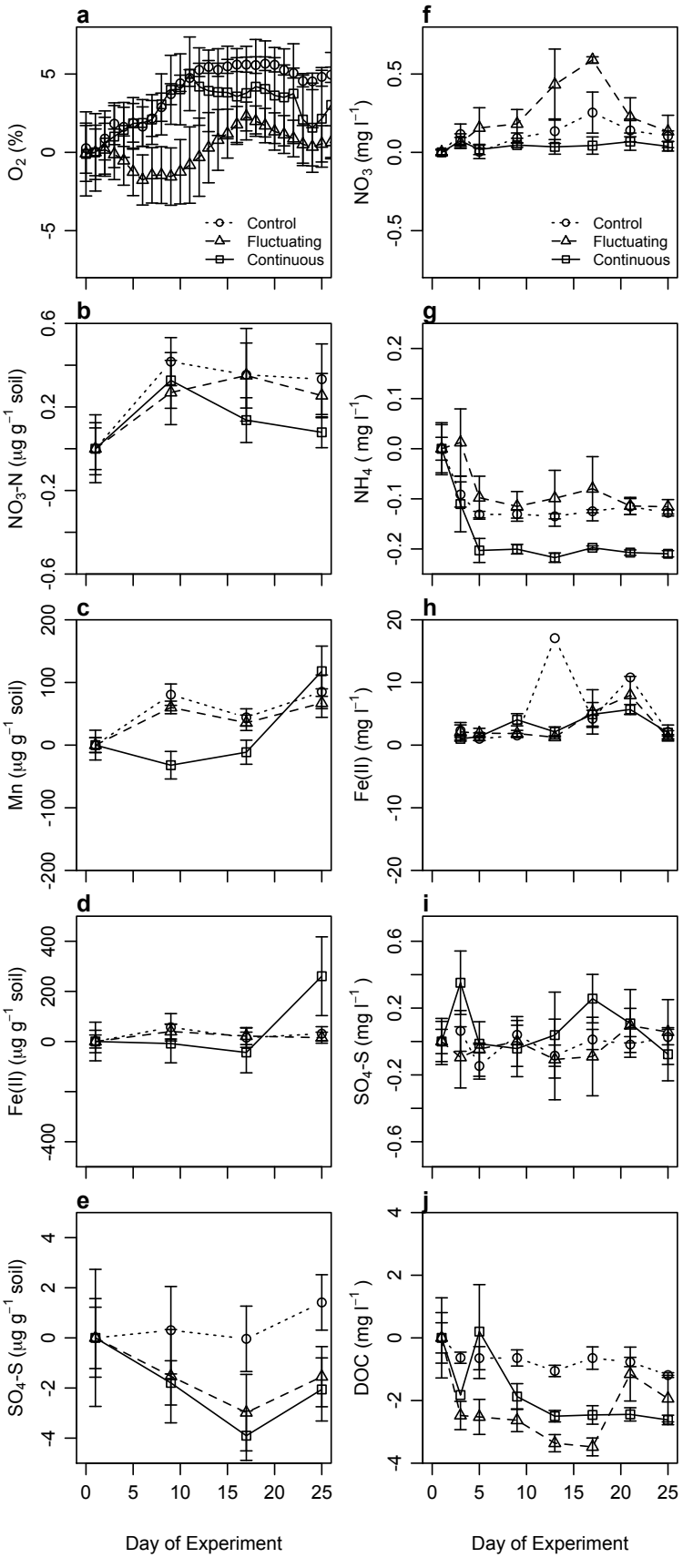

Figure 3: Relationships between daily mean volumetric soil moisture and O_2 concentrations measured at 10 cm depth (a), and the first principal component of redox species (O_2, NO_3, Mn(II), Fe(II), CH_4 concentrations) measured at eight-day intervals (b).

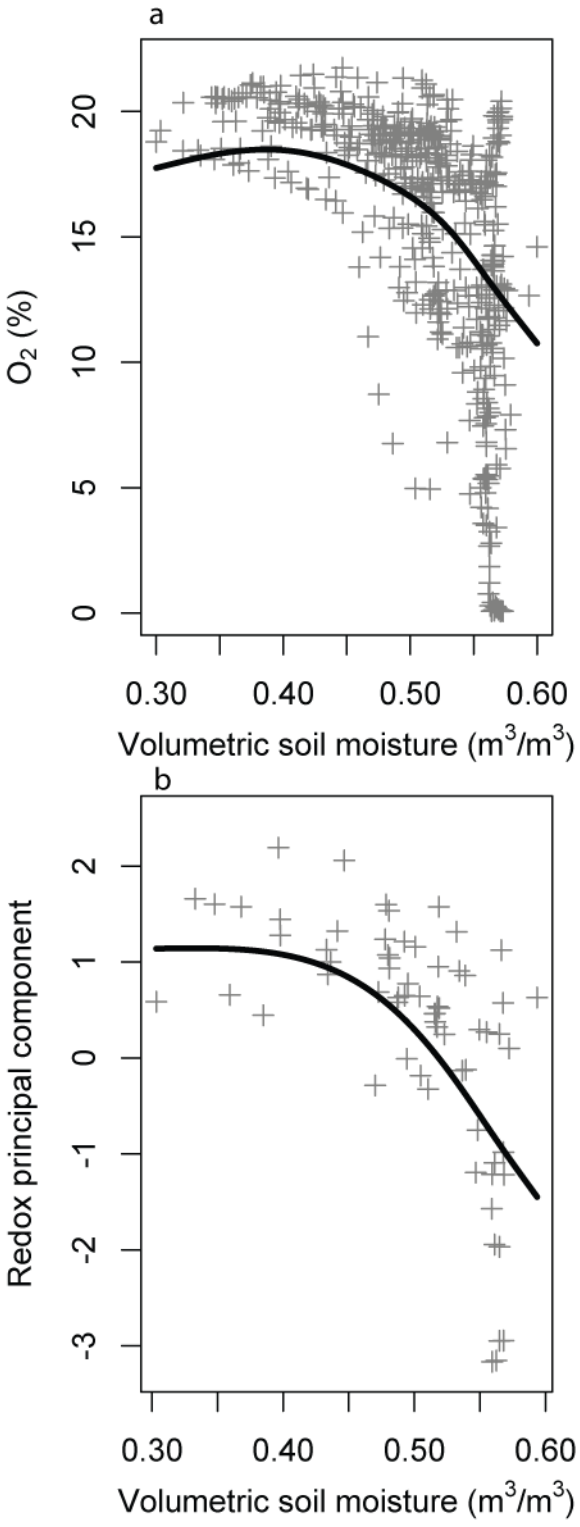

Figure 4: Normalized (± SE) soil-atmosphere fluxes and soil concentrations (10 cm depth) of CO_2, N_2O, and CH_4.

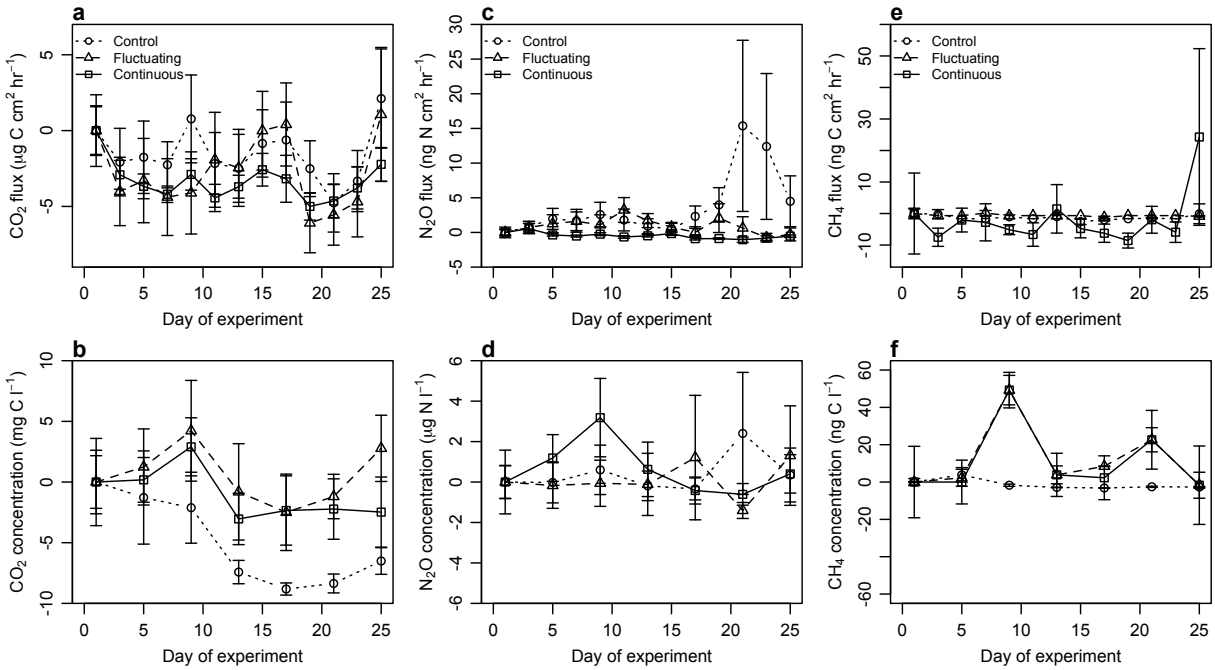

Figure 5: Pairwise relationships between greenhouse gas fluxes and covariates. Mean CO_2 fluxes plotted against soil C concentrations (a) and the composite redox indicator (b). Individual N_2O fluxes plotted against soil moisture (c) and O_2 (d), and CH_4 fluxes plotted against soil moisture (e) and O_2 (f).

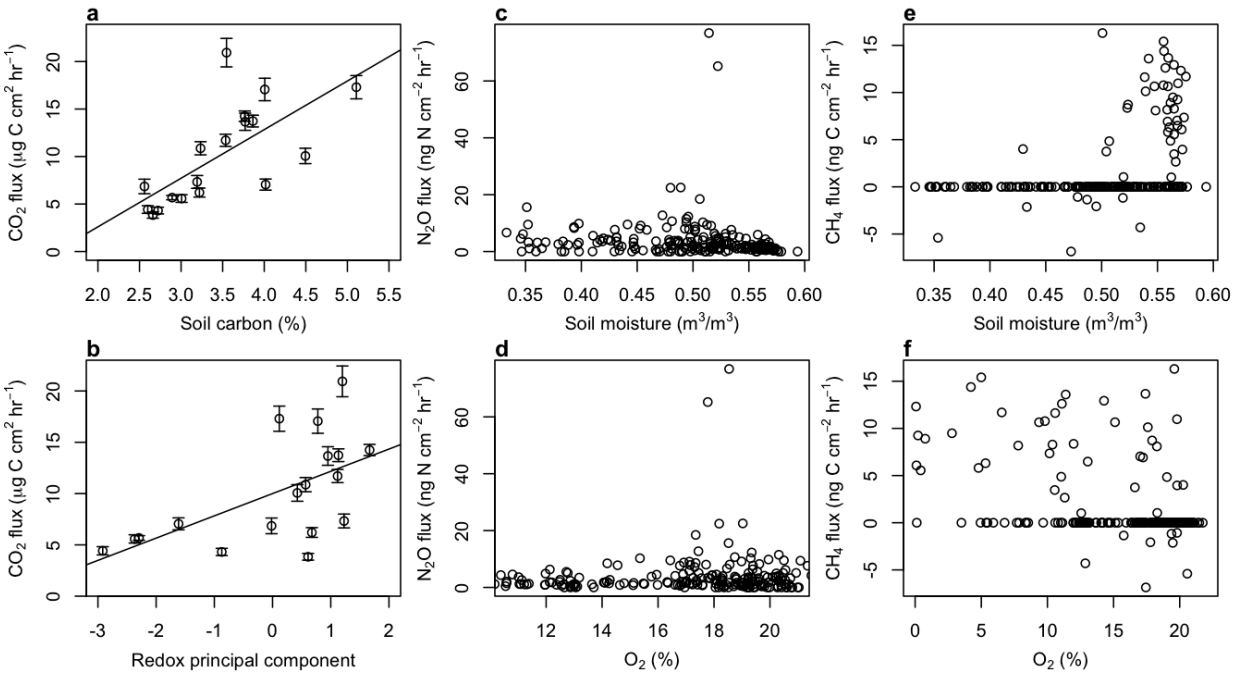

Chapter Two

Breaking the enzymatic latch:

Controls on hydrolytic enzyme activity in humid tropical forest soils

Abstract

The enzymatic latch hypothesis poses that oxygen (O_2) limitation promotes wetland carbon (C) storage by inhibiting hydrolytic enzymes that decompose organic matter. Upland humid tropical forest soils are typically characterized by low and fluctuating redox conditions yet have the fastest decomposition rates globally. We found that hydrolytic enzymes displayed neutral to strongly positive relationships with reducing conditions in several humid tropical forest soils; similar relationships were found with phenolic compounds, the proposed mechanism of the enzymatic latch. Enzyme activities did not systematically decline across a landscape O_2 gradient, as the hypothesis predicted. Activities in anaerobic laboratory incubations generally exceeded aerobic soils, and a four-fold increase in phenolics did not inhibit enzymes. Our data show that reducing conditions do not necessarily constrain soil hydrolytic enzyme activity and suggest these enzymes in turn can influence O_2 concentrations in upland soils. We suggest a critical re-examination of mechanisms by which O_2 influences decomposition.

Introduction

Humid tropical forest soils harbor a substantial portion (~ 500 Pg) of the global terrestrial C pool, yet simultaneously support the highest litter and root decomposition rates of any biome (Jobbagy and Jackson, 2000; Parton et al., 2007). Several mechanisms have been proposed to explain the apparent dichotomy of large soil C stocks and rapid decomposition rates. Humid tropical forests support high net primary productivity and litterfall that could exceed decomposition over short time periods and lead to transient accumulation of soil C from litter inputs. In many tropical forests, however, C is predominantly stored in mineral soil horizons (Jenny, 1950), which implies that factors that constrain microbial organic matter decomposition *in situ* are more important than a surfeit of litter. Recent work has implicated the importance of C protection in mineral complexes and environmental constraints on microbial activity as dominant factors regulating decomposition at the ecosystem scale (Schmidt et al., 2011). The availability of O_2, in particular, has been proposed as one critical integrator of these biophysical constraints on decomposition (Kleber, 2010; Davidson et al., 2012). Oxygen limitation and associated reducing conditions help protect soil C from decomposition in wetland ecosystems, and may affect decomposition in upland ecosystems as well (Ponnamperuma, 1972; Linn and Doran, 1984). In the humid tropics, a combination of finely textured soils, and high moisture, temperature, and respiration rates can lead to rapid O_2 depletion even in relatively well-drained surface soils (Silver et al., 1999; Schuur et al., 2001; Cleveland et al., 2010; Liptzin et al., 2011). Few studies have explicitly examined relationships between O_2 and C pools and fluxes in the humid tropics. Soil C concentrations increased monotonically as O_2 concentrations declined with increasing precipitation in Hawaii (Schuur et al., 2001), whereas topographic variation in O_2

among ridge, slope, and valley soils in a lower montane forest in Puerto Rico was not correlated with soil C concentrations (Silver et al., 1994, 1999). Although O_2 has long been known to influence overall rates of decomposition (Tenney and Waksman, 1930), the relative influence of spatial and temporal variability in O_2 and the specific mechanisms by which it affects soil organic matter decomposition remain unclear.

The catalytic activity of extracellular enzymes degrades macromolecular substrates into labile compounds and is thought to regulate organic matter decomposition (Sinsabaugh, 1994). The degradation of polyphenolic compounds such as lignin typically requires oxidative enzymes that catalyze reactions between organics and O_2 or H_2O_2 (Sinsabaugh, 2010), so anaerobic conditions by definition should promote the accumulation of these compounds (Kleber, 2010). The most abundant constituents in organic detritus, however, include compounds (e.g. cellulose and hemicellulose) that can be decomposed by hydrolytic enzymes after initial litter fragmentation, and thus do not directly require O_2 as a reactant. Hydrolytic enzymes are also responsible for liberating much of the organic nitrogen (N) and phosphorus (P) ultimately assimilated by plants and microbes, and thus play a critical role in decomposition and ecosystem productivity.

Even though hydrolytic enzymes do not require O_2, experimental work suggests that reducing conditions may inhibit hydrolytic enzyme activities indirectly (McLatchey and Reddy, 1998; Freeman et al., 2001, 2004). Oxygen availability could affect hydrolytic enzyme activity via at least two mechanisms. First, O_2 limitation may inhibit hydrolytic enzyme activity indirectly by promoting the accumulation of phenolic substances, a ubiquitous component of organic matter that interferes with enzyme catalysis (Wetzel, 1992; Freeman et al., 2001; Allison, 2006; Joanisse et al., 2007; Yao et al., 2009). The decomposition of phenolic compounds requires O_2, leading Freeman et al. (2001) to propose that anaerobiosis imposes an "enzymatic latch" on hydrolytic enzymes by promoting phenolic accumulation. Wetland soils exposed to O_2 exhibited increased phenol oxidase activity, resulting in decreased phenolic concentrations and increased hydrolytic enzyme activities (Freeman et al., 2001, 2004). In tropical montane forest soils, Bruijnzeel et al. (1993) also proposed (but did not test) that high concentrations of phenolic compounds could decrease organic matter decomposition. Secondly, the potential energy yield of C mineralization theoretically declines in the absence of O_2, because anaerobic C degradation depends on fermentation and respiratory processes such as dissimilatory iron (Fe) reduction that yield less energy per unit C substrate than aerobic respiration (Megonigal et al., 2003). Enzyme production under anaerobic conditions may decline accordingly due to energetic constraints on enzyme synthesis (McLatchey and Reddy, 1998). The net impact of anaerobiosis on enzyme activity, however, remains uncertain given that multiple factors influence enzyme activity *in situ*, including enzyme degradation and inhibition (Allison, 2006). In sum, reducing conditions have been thought to inhibit soil hydrolytic enzyme activity by at least two distinct mechanisms— kinetic constraints on enzyme catalysis, and energetic constraints on enzyme synthesis—but their importance has not been assessed in upland soils.

The enzymatic latch hypothesis and thermodynamic considerations predict a decline in enzyme activity under reducing conditions. We tested these hypotheses by evaluating the potential activities of a suite of hydrolytic enzymes involved with C, N, and P acquisition in six humid tropical forest sites that differed in long-term mean soil O_2 concentrations. These

ecosystems exhibit redox heterogeneity within and among sites (Silver et al., 1999; Liptzin et al., 2011), allowing us to assess the impact of reducing conditions on enzymes at multiple spatial scales. We compared enzyme activities with soil phenolics and with Fe(II) concentrations as an index of reducing conditions. Concentrations of alternative electron acceptors or their reduced equivalents have frequently been used to infer the relative importance of anaerobic processes in ecosystems (Chapelle et al., 1995; Hedin et al., 1998). Iron oxides represent the most abundant anaerobic terminal electron acceptor in highly weathered humid tropical soils, where microbes and humic substances reduce ferric iron (Fe(III)) to ferrous iron (Fe(II)) in the absence of O_2 (Chacón et al., 2006; Thompson et al., 2006; Dubinsky et al., 2010). Because Fe(II) rapidly oxidizes to Fe(III) in the presence of O_2 (Patrick and Henderson, 1980), Fe(II) concentrations provide an integrative metric of O_2 availability in soils where aerobic and anaerobic processes occur in close proximity (Hall et al., 2013).

Methods

We sampled soils across gradients of topography and elevation in the Luquillo Experimental Forest (LEF), Puerto Rico (18.3° N, -65.8° W), an NSF-funded Long Term Ecological Research and Critical Zone Observatory site (Table 1). These sites encompass a gradient of long-term mean soil O_2 availability. Previous work documented a trend of decreasing mean soil O_2 from ridges to slopes to riparian valleys within a lower montane forest in the Bisley watershed (19, 16, and 10 % O_2, respectively) and along a montane forest elevation gradient (10 – 8 % O_2) (Silver et al., 1999). It is important to note that average soil O_2 concentrations are indicative of the relative importance of anaerobic microsites at an ecosystem scale (Silver et al. 1999, Liptzin et al. 2011). Soil O_2 concentrations exhibit temporal variability associated with rainfall frequency over scales of weeks to months, and most sites (except the lower montane ridges and slopes) occasionally experience bulk soil O_2 concentrations < 3% (ibid). Annual precipitation varied between 2600 – 5800 (mean 3500) mm y^{-1} in the lower montane forest and increased with elevation, with significant contributions from fog at higher elevations (F. Scatena, unpublished data). Our field samples, therefore, provide a representative snapshot of spatial patterns in O_2 availability. In the laboratory, we conducted controlled experiments to directly examine the influence of soil O_2 on enzyme activities over timescales relevant to field conditions (Liptzin et al., 2011).

Plant communities and soils vary with elevation in the LEF concomitant with precipitation and soil O_2. Tabonuco (*Dacryodes excelsa*) forest dominates the lower montane sites, while the montane sites are characterized by sierra palm (*Prestoea montana*), palo colorado (*Cyrilla racemiflora*) and elfin (also previously described as "cloud") forest (*Tabebuia rigida*) communities (McDowell et al., 2012). Soils are classified as oxisols, ultisols, and inceptisols in the USDA taxonomy.

In June 2011, we sampled four replicate lower montane forest catenas, each containing ridge, slope, and riparian valley topographic zones. In each catena, we established five replicate 0.25-m^2 plots in each topographic zone that were randomly stratified within intervals of 5 – 10 m along a 50 m linear transect. We similarly sampled five replicate plots from each of the three montane forest sites on the elevation gradient in February 2012. In each plot, we collected two replicate 6-cm diameter soil cores at depths of 0 – 10 cm and 10 – 20 cm (total n = 150); these

depths contain the majority of roots and organic matter in these ecosystems (Silver et al., 1994). Replicate cores from each depth were composited, thoroughly mixed, and subsamples (3 g dry mass equivalent) immediately extracted in a 1:10 ratio with 0.5 M hydrochloric acid (HCl) to minimize oxidation of Fe(II) prior to analysis. These extractions were shaken for 1 hour, filtered to 0.22 μm, and assayed for Fe(II) and Fe(III) concentrations using a colorimetric ferrozine method (Viollier et al., 2000). Separate soil subsamples (3 g) were extracted with deionized water in a 1:5 ratio and filtered to 0.45 μm for soluble organic C analysis on a Shimadzu 5050A TOC analyzer, and phenolic substance analysis using the Folin-Ciocalteau method with a phenol standard (Box, 1983). This widely used method provides an index of phenolic compounds based on their capacity to chemically reduce the Folin reagent and does not necessarily correspond to the mass of total phenolics, which are biochemically diverse. The Folin assay, however, provides an index of phenolic compounds demonstrably related to soil enzyme activity in other studies (Freeman et al., 2004; Joanisse et al., 2007). Soil subsamples were stored at field temperature (25°C) and analyzed within one week of collection for hydrolytic enzymes (Turner and Romero, 2010). Gravimetric water content for each sample was determined by drying two replicate 10 g subsamples at 105° C to constant mass. Additional subsamples were air-dried and ground for organic C analysis by combustion on an elemental analyzer (CE Elantech, Lakewood, NJ).

Laboratory incubation

Approximately 6 kg of soil from 0 - 20 cm depth was collected from an upland valley site in the lower montane forest and shipped overnight to U.C. Berkeley. Soils from this site exhibit large O_2 fluctuations over scales of days to weeks (Liptzin et al., 2011). We removed recognizable litter and weighed 125 g (dry mass equivalent) of homogenized soil into each of 24 polystyrene filter flasks fitted with a pre-combusted Whatman GF/F filter. Flasks were randomly assigned to one of four treatment combinations in a factorial design of headspace (aerobic and anaerobic) and solution addition (water or water + labile C) with six replicates per treatment. The anaerobic treatment was imposed in a glovebox (Coy Laboratory Products, Grass Lake, MI) with a headspace composition of 85 % nitrogen, 10% carbon dioxide, and 5% hydrogen, with a palladium catalyst to remove O_2. All reagents used in the anaerobic treatment were purged with helium and prepared inside of the glovebox after overnight headspace equilibration. Soils received daily additions of 6 mL deionized water or an equimolar solution of glucose plus sodium acetate to add 0.05 mg C g $soil^{-1}$ day^{-1} in order to simulate field levels of labile C (Chacón et al., 2006; Liptzin and Silver, 2009). Enzyme assays were conducted immediately before treatments were imposed and after 6, 12, and 18 days. This timescale is representative of periodic anaerobiosis in the field, where soil O_2 fluctuates over scales of days to weeks (Liptzin et al., 2011).

Enzyme assays

We measured the potential activities of five hydrolytic enzymes related to C, N, and P acquisition using fluorescent methylumbelliferone (MUB)-linked substrates. Briefly, cellobiohydrolase and β-glucosidase respectively hydrolyze glucose dimers and monomers from cellulose, β-xylosidase hydrolyses xylose monomers from xylan (hemicellulose), N-acetyl β-D-glucosaminidase (NAGase) hydrolyses amino sugars from peptidoglycan and chitin, and acid phosphotase hydrolyzes phosphomonoesters to inorganic phosphate. Soils (1 g dry mass equivalent) were slurried in 125 ml of 62.5 mM sodium acetate buffer with a stainless steel

mixer and dispensed into black polystyrene 96-well plates with eight technical replicates per soil. We added MUB substrates dissolved in deionized water to soil slurries in a 1:5 ratio, yielding final substrate and buffer concentrations of 400 μM and 50 mM, respectively. We selected substrate concentrations based on pilot assays in order to maximize catalytic activity according to Michaelis-Menten kinetics (German et al., 2011). We measured fluorescence after 6 hours for all enzymes except for acid phosphatase (2 hours) to achieve linearity. We calculated enzyme activity on the basis of soil mass and soil C content after accounting for background fluorescence and quenching. Mass-based enzyme activities provide an absolute metric of potential catalytic activity in a given soil, whereas normalizing by C content can partially account for differences in organic substrates among soils, given that enzyme activities often scale with organic matter concentrations (Sinsabaugh et al., 2008). Enzyme assays for the anaerobic incubation treatment were conducted in the anaerobic chamber, with plates removed immediately prior (30 seconds) to the fluorescence measurements.

Statistical Analysis

We assessed differences in enzyme activity among sites using generalized linear models that incorporated a unique variance term for each site. Relationships between enzyme activities, phenolics, and Fe(II) were analyzed using mixed effects models that included transects, plots (within transects), and transect x depth interactions as potential random effects to account for spatial structure; soil depth was included as a fixed effect. Correlations between enzymes and Fe(II) differed categorically in direction between the lower montane ridge and slope soils, on one hand, and the lower montane valley, palm, colorado, and elfin forest soils, on the other. The former group of sites is characterized by higher mean bulk soil O_2 concentrations, whereas the latter sites experience a higher frequency of bulk soil $O_2 < 3\%$ (discussed above). We thus generated separate statistical models for these two groups of sites. Variables were normalized by mean and standard deviation to facilitate comparisons (a normalized model coefficient of 0.5 implies that varying a predictor variable by one standard deviation yields a change of 0.5 standard deviations in the response variable), and variables for the low-O_2 sites were log transformed to remove residual heteroskedasticity. We selected the optimal random effect structure for each model using Akaike's Information Criterion (AIC) on saturated models fit using restricted maximum likelihood (REML), and then selected fixed effects by comparing the AIC of models fit using maximum likelihood estimation. Insufficient soil remained to assay phenolics in 12 samples, so model selection was conducted on the reduced dataset (n = 138). Laboratory incubations were similarly analyzed with mixed models that included experimental units as random effects to account for repeated measurements; we report p-values for fixed effects based on the t statistic approximation. Labile C additions did not affect enzyme activities over the incubation, so we pooled the data and focused the present analysis on headspace treatment effects. Differences among treatments and days were assessed using Tukey's honestly significant difference test. We generated models in R using the lmer and lme functions in the lme4 and nlme packages for the field and laboratory data, respectively (Pinheiro et al., 2011; Bates et al., 2012).

Results

All soils contained measurable concentrations of Fe(II) indicative of reducing conditions in soil microsites, even in sites characterized by near-atmospheric soil O_2 concentrations in the bulk soil (Fig. 1a, Table 1). Concentrations of Fe(II) increased by more than an order of magnitude with increasing elevation and decreasing bulk soil O_2, but were similar among ridges, slopes, and valleys in the lower montane forest. Soil C concentrations did not scale linearly with Fe(II) or mean site O_2 (Fig. 1b). Phenolics did not show consistent trends with site elevation or topographic position (Table 1).

Landscape patterns in hydrolytic enzyme activity

Enzyme activities did not vary consistently with bulk soil O_2 among sites, and each enzyme showed largely distinct patterns of variation (Fig. 2, Table S1 in Supporting Information). Activities of cellobiohydrolase and β-glucosidase in 0 – 10 cm soil differed between the extremes of the O_2 gradient (ridge and elfin sites) but not among sites with intermediate bulk soil O_2 (the slope, valley and palm sites. When normalized by soil C, cellobiohydrolase showed greater variation among sites but remained similar among the ridge, slope, and valley sites. β-xylosidase activity consistently decreased as O_2 declined from ridges to slopes to valleys in the lower montane forest, and from the palm and colorado to the elfin forests. These trends were consistent when evaluated both on the basis of soil mass and soil C. Acid phosphatase activity was highest in the ridge and slope sites and low in the other four sites, when expressed on both a mass and soil C basis. Conversely, NAGase (mass basis) did not vary among ridges, slopes, or valleys, but increased in the palm, colorado, and cloud sites. The activity of NAGase showed a monotonic increasing relationship with soil C concentrations when we assessed pairwise relationships at the level of individual samples, and NAGase was the only enzyme that displayed a consistent relationship with soil C (Fig. S1). When normalized by soil C, however, no trends in NAGase were evident with mean O_2 concentrations among sites (Fig. 2).

Subsurface (10 – 20 cm) soils showed less significant variation in enzyme activities across the site O_2 gradient (Fig. 2, Table S1). In 10 – 20 cm soil, cellobiohydrolase activity on a mass basis was similar among five of the six sites assayed, whereas β-glucosidase activity was more variable among sites but was similar among the extremes of the O_2 gradient (ridge and elfin sites). When normalized by soil C, β-glucosidase activity was highest in the valley soils.

Relationships among enzymes, Fe(II), phenolics, and C

Enzyme activities typically varied by two orders of magnitude within a given site and often displayed significant relationships with Fe(II), but less so with phenolics. Patterns in enzyme activities fell into two main groupings: the ridge and slope sites, on one hand, and the valley, palm, colorado, and elfin forests, on the other. On a soil mass basis, ridge and slope soils exhibited strong positive relationships with Fe(II) for all enzymes assayed, with standardized coefficients between 0.36 – 0.61 (Table 2a, Fig. 3). Enzymes frequently displayed positive or neutral pairwise relationships with phenolics in these sites (Fig. S2), but the inclusion of phenolics seldom improved model AIC. The sites with lower mean O_2 concentrations (valley, palm, colorado, and elfin forest) also showed neutral or positive relationships between soil-mass based enzyme activity and phenolics, but displayed neutral or negative relationships with Fe(II) concentrations with smaller standardized coefficients than the high-O_2 sites (Table 2b, Fig. 3).

Phenolics and soluble organic C concentrations were strongly correlated ($R^2 = 0.72$) across both groups of sites (Fig. S3).

Normalizing enzyme activities by soil C concentrations suggested different relationships between enzymes and Fe(II). In the high-O_2 sites, acid phosphatase and NAGase activities normalized by C showed negative relationships with Fe(II), and enzymes involved in C acquisition showed neutral relationships (Table S2). In the low-O_2 sites, cellobiohydrolase, β-xylosidase, and acid phosphatase displayed a negative relationship with Fe(II) when normalized by soil C. Phenolics showed no relationship with C-normalized enzymes except for a negative coefficient with NAGase in the low-O_2 sites.

Effects of anaerobiosis on soil enzyme activity

Imposing anaerobiosis on soils in the laboratory did not suppress enzyme activity relative to aerobic controls for four out of the five enzymes assayed. Rather, enzyme activity in anaerobic soils significantly exceeded activity in aerobic soils at the end of the experiment for three out of five enzymes assayed, which measured 151, 154, and 132 % of the respective aerobic activities for NAGase ($p = 0.001$), β-cellobiohydrolase ($p < 0.01$) and β-xylosidase ($p < 0.001$, Fig. 4). In the case of β-xylosidase, activity increased under anaerobic conditions relative to the beginning of the experiment ($p < 0.05$), whereas NAGase and cellobiohydrolase showed consistent enzyme activity under anaerobic conditions accompanied by a decline under aerobic conditions ($p < 0.05$ and $p < 0.01$, respectively). β-glucosidase activity after 18 days did not significantly differ from initial measurements ($p = 0.08$), but activity in anaerobic soils significantly exceeded aerobic controls on day 12 ($p < 0.001$). Acid phosphatase showed highly variable trends over time; activity in anaerobic soils exceeded aerobic soils after 12 days ($p < 0.001$), but this pattern reversed after 18 days due to an increase in aerobic and a decrease in anaerobic activity ($p < 0.001$).

Phenolic compounds measured in soil leachate varied significantly by time, headspace, and C addition treatment. On day 6, phenolics did not differ by treatment and averaged 0.45 mg l^{-1}, whereas by day 18 soluble phenolics had significantly increased to 1.27, 1.70, and 2.01 mg l^{-1} in the anaerobic, anaerobic + C, and aerobic + C treatments, respectively, while the aerobic treatment decreased to 0.27 mg l^{-1} ($p < 0.001$).

Discussion

We found that reducing conditions and high concentrations of phenolic compounds were ubiquitous in surface soils across the humid tropical forest landscape in the Luquillo Mountains, Puerto Rico. Phenolics and reducing conditions have been proposed to impose kinetic and thermodynamic constraints on hydrolytic enzyme catalysis and production in soils (McLatchey and Reddy, 1998; Freeman et al., 2001). However, we found that enzyme activities did not consistently decline with reducing conditions, especially in sub-surface soils. Normalizing enzyme activities to account for differences in C among soils revealed lower relative activity of β-xylosidase in sites with lower mean O_2 availability, but the other enzymes showed inconsistent trends with O_2. In the laboratory, we found that anaerobiosis led to an increase in three enzymes relative to aerobic controls, despite high phenolic concentrations.

Enzyme activities and soil phenolic compounds

We found largely neutral or positive relationships between phenolic compounds and hydrolytic enzyme activities in the field. Furthermore, a four-fold increase in soluble phenolics in our anaerobic incubation did not suppress enzyme activity. This increase was likely driven by a combination of colloid dispersion under anaerobic conditions (Thompson et al., 2006) and the inhibition of O_2-dependent enzymes that degrade phenolics (Freeman et al., 2001). The phenolic concentrations we observed under anaerobic conditions (2.4 mg l^{-1}) were similar to those observed to inhibit enzymes in a peatland (Freeman et al., 2004), but presumably differed in their chemical composition. Together, our field and laboratory data suggest that the overall importance of phenolic substances in controlling ecosystem patterns of enzyme activity among soils may be lower than previously believed.

Our data provide a broader ecosystem context to the findings of Freeman et al. (2001, 2004) and Allison (2006), which suggested a negative effect of phenolic compounds on hydrolytic enzyme activity. In those studies enzyme activities were significantly affected by adding or removing phenolic compounds. The overall lack of response of enzyme activities to phenolics could be due in part to adaptation of their endemic microbial communities and selection for enzymes that function under high phenolic concentrations (Triebwasser et al., 2012). Furthermore, phenolics comprise a biochemically diverse suite of compounds with varying impacts on enzyme catalysis, and might also function as an index of C substrate availability. The addition of tannins, for example, has been observed to stimulate soil respiration (Kraus et al., 2004). Here, phenolics displayed a strong positive correlation with soluble organic C concentrations in our soils. Also, NAGase activity was positively related to phenolics on a mass basis and negatively related on a soil C basis, further implying a linkage between phenolics and C.

Scale-dependence of enzyme activities and reducing conditions

Relationships between mass-based enzyme activities and Fe(II) as an index of reducing conditions varied categorically among sites based on their mean soil O_2 availability. Sites characterized by lower mean soil O_2 concentrations (valley and upper elevation sites) displayed equivocal or weak negative relationships between enzymes and reduced Fe, while sites that typically experienced higher average O_2 conditions (ridge and slope sites) showed strong positive relationships among enzymes and reduced Fe. In the higher-O_2 sites, a positive relationship between carbohydrate-degrading enzymes and Fe(II) likely reflects the importance of biological O_2 demand, coupled with high soil moisture, in generating anaerobic microsites. Increased hydrolytic enzyme activity likely fueled respiration by supplying labile C monomers, leading to O_2 depletion and stimulating Fe reduction. The importance of C availability in driving dissimilatory Fe reduction in these soils was further suggested by the finding that enzymes from the high-O_2 sites displayed no relationship with reducing conditions when normalized by soil C concentrations. This is consistent with previous research that documented net Fe reduction in soils exposed to an aerobic atmosphere after the addition of labile C (Liptzin and Silver, 2009). We acknowledge the critical importance of soil moisture in restricting O_2 diffusion, although gravimetric soil moisture was equivalent among ridges, slopes, and valleys in the lower montane forest. Thus, for clay and organic-matter rich soils with high water holding capacity, variation in

moisture per se may not always provide the most important proximate driver of reducing conditions. This perspective contrasts with a traditional paradigm of wetland ecology, where spatial or temporal variation in moisture has been thought to determine patterns of Fe reduction by limiting O_2 supply (Kirk, 2004). In our study, the impact of soil moisture on generating reducing conditions may have been increasingly important in the higher-rainfall sites, which were characterized by higher gravimetric soil moisture, lower respiration rates (McGroddy and Silver, 2000), and higher Fe(II) concentrations than the lower montane forests.

Our results also highlight the importance of the metric of enzyme activity used to infer relationships of C and nutrient dynamics with environmental drivers. Several enzymes showed negative relationships with Fe(II) when their activities were normalized by soil C, as a consequence of the fact that most enzymes did not scale linearly with C concentrations. Expressing enzymes on a soil mass basis, however, provides the more relevant metric for assessing potential catalytic rates. Research in wetlands documented absolute declines in hydrolytic enzymes under reducing conditions (McLatchey and Reddy, 1998; Freeman et al., 2001). In contrast, reducing conditions only affected relative (C-normalized) rather than absolute enzyme activities in our terrestrial humid tropical soils. The assumption that reducing conditions suppress enzyme activity may not apply in the context of terrestrial ecosystems where enzyme activity in itself can be a driver of reducing conditions. Our findings suggest that ecosystem models could potentially incorporate reciprocal, instead of unidirectional, relationships between reducing conditions and enzymes.

The strong negative relationship between Fe(II) and acid phosphatase activity evident on both a mass and soil C basis in the lower-O_2 sites was an exception to the patterns described above. This may reflect the underlying importance of Fe-phosphorus (P) complexes in controlling P availability in these weathered, Fe oxide-rich soils (Sanchez, 1976). Iron reduction can significantly increase concentrations of P available for plant and microbial assimilation, presumably by solubilizing these Fe-P complexes (Chacón et al., 2006; Liptzin and Silver, 2009). Declines in acid phosphatase activity with increasing Fe(II), therefore, may actually reflect increased P availability as opposed to constraints on enzyme activity from reducing conditions.

Enzyme activity under anaerobic conditions

Our laboratory data shows that anaerobiosis does not constrain hydrolytic enzyme activity over timescales relevant to natural O_2 fluctuations in the lower montane forest sites (Liptzin et al., 2011). Our anaerobic incubation decreased the activity of only one enzyme, acid phosphatase, relative to the control; this may have resulted from increased P availability under anaerobic conditions as discussed above. Activities of the other four enzymes, in contrast, were significantly *greater* under anaerobic conditions. Potential soil enzyme activity reflects the net effects of enzyme production, storage, degradation, and inhibition (Allison, 2006). A shift in any or all of these factors could explain the patterns observed here, while leading to the preservation of potential enzyme activity in soils.

Conclusions

We tested the hypothesis that microbial enzyme activity declines under anaerobic conditions due to kinetic constraints on enzyme activity from phenolic substances and energetic constraints on enzyme production. Soluble phenolics did not explain patterns in enzyme activity in the field or laboratory, and indices of reducing conditions showed a variable relationship with enzyme activities depending on site characteristics. The activity of some enzymes decreased across a landscape-scale gradient of sites differing in average soil O_2 concentrations, partially supporting the coarse-scale utility of reducing conditions as an index of decomposition (Tenney and Waksman, 1930; Ponnamperuma, 1972; Schuur et al., 2001). Nevertheless, one enzyme consistently increased as O_2 declined at the landscape scale, and enzyme activity in subsurface soils varied little among sites despite their differences in mean O_2. We propose an alternative hypothesis that hydrolytic enzymes can contribute to localized hotspots of O_2 consumption in humid soils that generate reducing microsites. This leads to a reciprocal relationship between enzymes and O_2, as opposed to a simple one-way interaction between environmental conditions and enzyme activity. The overall resistance of hydrolytic enzyme activities to reducing conditions likely reflects the fact that these enzymes do not fundamentally require O_2 as a reactant. Furthermore, endemic soil microbial communities have likely adapted to a soil environment characterized by constitutive fine-scale spatial and temporal variation in O_2. Previous work in these ecosystems documented increasing microbial richness and abundance under conditions of fluctuating O_2 availability as compared with static aerobic conditions (Pett-Ridge and Firestone, 2005). Together, this suggests that variation in the frequency and extent of reducing conditions in surface soils (Liptzin et al., 2011) may have little immediate effect on hydrolytic enzyme activity, a proximate driver of organic matter decomposition. Finally, we suggest a re-evaluation of the common assumption, embedded in ecosystem models, that decomposition varies intrinsically with O_2 availability as controlled by soil moisture (Li et al., 1992; Parton et al., 1993). Oxygen availability demonstrably affects the catalysis of oxidase enzymes that require O_2 as a substrate, but declines in O_2 alone are insufficient to suppress the hydrolytic enzymes that play a critical role in the decomposition process.

Acknowledgements

I thank Jonathan Treffkorn and Whendee L. Silver for their contributions to this manuscript. We thank R. Ryals, H. Dang, A. McDowell, and C. Torrens for crucial help in the field and lab, and M. Firestone and R. Rhew for critical review. SJH was supported by the DOE Office of Science Graduate Fellowship Program, supported by the American Recovery and Reinvestment Act of 2009 and administered by ORISE-ORAU under contract no. DE-AC05-06OR23100. Funding was provided by NSF grant EAR-08199072 to WLS, the NSF Luquillo Critical Zone Observatory (EAR-0722476) with additional support provided by the USGS Luquillo WEBB program, and grant DEB 0620910 from NSF to the Institute for Tropical Ecosystem Studies, University of Puerto Rico, and to the International Institute of Tropical Forestry USDA Forest Service, as part of the Luquillo Long-Term Ecological Research Program.

Literature Cited

Allison, S.D., 2006. Soil minerals and humic acids alter enzyme stability: implications for ecosystem processes. Biogeochemistry 81, 361–373.

Bates, D., Maechler, M., Bolker, B., 2012. lme4: Linear mixed-effects models using S4 classes.

Box, J.D., 1983. Investigation of the Folin-Ciocalteau phenol reagent for the determination of polyphenolic substances in natural waters. Water Research 17, 511–525.

Bruijnzeel, L.A., Waterloo, M.J., Proctor, J., Kuiters, A.T., Kotterink, B., 1993. Hydrological observations in montane rain forests on Gunung Silam, Sabah, Malaysia, with special reference to the `Massenerhebung' effect. Journal of Ecology 81, 145–167.

Chacón, N., Silver, W.L., Dubinsky, E.A., Cusack, D.F., 2006. Iron reduction and soil phosphorus solubilization in humid tropical forests soils: The roles of labile carbon pools and an electron shuttle compound. Biogeochemistry 78, 67–84.

Chapelle, F.H., McMahon, P.B., Dubrovsky, N.M., Fujii, R.F., Oaksford, E.T., Vroblesky, D.A., 1995. Deducing the distribution of terminal electron-accepting processes in hydrologically diverse groundwater systems. Water Resources Research 31, 359–371.

Cleveland, C.C., Wieder, W.R., Reed, S.C., Townsend, A.R., 2010. Experimental drought in a tropical rain forest increases soil carbon dioxide losses to the atmosphere. Ecology 91, 2313–2323.

Davidson, E.A., Samanta, S., Caramori, S.S., Savage, K., 2012. The Dual Arrhenius and Michaelis–Menten kinetics model for decomposition of soil organic matter at hourly to seasonal time scales. Global Change Biology 18, 371–384.

Dubinsky, E.A., Silver, W.L., Firestone, M.K., 2010. Tropical forest soil microbial communities couple iron and carbon biogeochemistry. Ecology 91, 2604–2612.

Freeman, C., Ostle, N., Fenner, N., Kang, H., 2004. A regulatory role for phenol oxidase during decomposition in peatlands. Soil Biology & Biochemistry 36, 1663–1667.

Freeman, C., Ostle, N., Kang, H., 2001. An enzymatic "latch" on a global carbon store -- a shortage of oxygen locks up carbon in peatlands by restraining a single enzyme. Nature 409, 149.

German, D.P., Weintraub, M.N., Grandy, A.S., Lauber, C.L., Rinkes, Z.L., Allison, S.D., 2011. Optimization of hydrolytic and oxidative enzyme methods for ecosystem studies. Soil Biology and Biochemistry 43, 1387–1397.

Hall, S.J., McDowell, W.H., Silver, W.L., 2013. When wet gets wetter: Decoupling of moisture, redox biogeochemistry, and greenhouse gas fluxes in a humid tropical forest soil. Ecosystems 16, 576–589.

Hedin, L.O., von Fischer, J.C., Ostrom, N.E., Kennedy, B.P., Brown, M.G., Robertson, G.P., 1998. Thermodynamic constraints on nitrogen transformations and other biogeochemical processes at soil-stream interfaces. Ecology 79, 684–703.

Jenny, H., 1950. Causes of the high nitrogen and organic matter content of certain tropical forest soils. Soil Science 69, 63–70.

Joanisse, G.D., Bradley, R.L., Preston, C.M., Munson, A.D., 2007. Soil enzyme inhibition by condensed litter tannins may drive ecosystem structure and processes: the case of Kalmia angustifolia. New Phytologist 175, 535–546.

Jobbagy, E.G., Jackson, R.B., 2000. The vertical distribution of soil organic carbon and its relation to climate and vegetation. Ecological Applications 10, 423–436.

Kirk, G., 2004. The Biogeochemistry of Submerged Soils. Wiley, West Sussex.

Kleber, M., 2010. What is recalcitrant soil organic matter? Environmental Chemistry 7, 320–332.

Kraus, T.E.C., Zasoski, R.J., Dahlgren, R.A., Horwath, W.R., Preston, C.M., 2004. Carbon and nitrogen dynamics in a forest soil amended with purified tannins from different plant species. Soil Biology and Biochemistry 36, 309–321.

Li, C., Frolking, S., Frolking, T., 1992. A model of nitrous oxide evolution from soil driven by rainfall events: 1. Model structure and sensitivity. Journal of Geophysical Research 97, 9759–9776.

Linn, D.M., Doran, J.W., 1984. Effect of water-filled pore space on carbon dioxide and nitrous oxide production in tilled and non-tilled soils. Soil Science Society of America Journal 48, 1267–1272.
Liptzin, D., Silver, W.L., 2009. Effects of carbon additions on iron reduction and phosphorus availability in a humid tropical forest soil. Soil Biology & Biochemistry 41, 1696–1702.
Liptzin, D., Silver, W.L., Detto, M., 2011. Temporal dynamics in soil oxygen and greenhouse gases in two humid tropical forests. Ecosystems 14, 171–182.
McDowell, W.H., Scatena, F.N., Waide, R.B., Brokaw, N., Camilo, G., Covich, A., Crowl, T., Gonzalez, G., Greathouse, E., Klawinski, P., Lodge, D., Lugo, A., Pringle, C., Richardson, B., Richardson, M., Schaefer, D., Silver, W., Thompson, J., Vogt, D., Vogt, K., Willig, M., Woolbright, L., Zou, X., Zimmerman, J., 2012. Geographic and ecological setting of the Luquillo Mountains, in: Brokaw, N., Crowl, T., Lugo, A., McDowell, W.H., Scatena, F.N., Waide, R.B., Willig, M. (Eds.), A Caribbean Forest Tapestry: The Multidimensional Nature of Disturbance and Response. Oxford University Press, USA, pp. 72–163.
McGroddy, M., Silver, W.L., 2000. Variations in belowground carbon storage and soil CO2 flux rates along a wet tropical climate gradient. Biotropica 32, 614–624.
McLatchey, G.P., Reddy, K.R., 1998. Regulation of organic matter decomposition and nutrient release in a wetland soil. Journal of Environmental Quality 27, 1268–1274.
Megonigal, J.P., M.E. Hines, Visscher, P.T., 2003. Anaerobic metabolism: linkages to trace gases and aerobic processes, in: Schlesinger, W.H. (Ed.), Biogeochemistry. Elsevier-Pergamon, Oxford, pp. 317–424.
Parton, W., Silver, W.L., Burke, I.C., Grassens, L., Harmon, M.E., Currie, W.S., King, J., Adair, E.C., Brandt, L., Hart, S.C., Fasth, B., 2007. Global-scale similarities in nitrogen release patterns during long-term decomposition. Science 315, 361–364.
Parton, W.J., Scurlock, J.M.O., Ojima, D.S., Gilmanov, T.G., Scholes, R.J., Schimel, D.S., Kirchner, T., Menaut, J.-C., Seastedt, T., Moya, E.G., Kamnalrut, A., Kinyamario, J.I., 1993. Observations and modeling of biomass and soil organic matter dynamics for the grassland biome worldwide. Global Biogeochemical Cycles 7, 785–809.
Patrick, W.H., Henderson, R.E., 1980. Reduction and reoxidation cycles of manganese and iron in flooded soil and in water solution. Soil Science Society of America Journal 45, 855–859.
Pett-Ridge, J., Firestone, M.K., 2005. Redox fluctuation structures microbial communities in a wet tropical soil. Applied and Environmental Microbiology 71, 6998–7007.
Pinheiro, J., Bates, D., DebRoy, S., Sarkar, D., R Core Development Team, 2011. nlme: Linear and Nonlinear Mixed Effects Models.
Ponnamperuma, F.N., 1972. The chemistry of submerged soils. Advances in Agronomy 24, 29–96.
Sanchez, P.A., 1976. Properties and Management of Soils in the Tropics. John Wiley and Sons.
Schmidt, M.W.I., Torn, M.S., Abiven, S., Dittmar, T., Guggenberger, G., Janssens, I.A., Kleber, M., Kogel-Knabner, I., Lehmann, J., Manning, D.A.C., Nannipieri, P., Rasse, D.P., Weiner, S., Trumbore, S.E., 2011. Persistence of soil organic matter as an ecosystem property. Nature 478, 49–56.
Schuur, E.A.G., Chadwick, O.A., Matson, P.A., 2001. Carbon cycling and soil carbon storage in mesic to wet Hawaiian montane forests. Ecology 82, 3182–3196.

Silver, W.L., Lugo, A.E., Keller, M., 1999. Soil oxygen availability and biogeochemistry along rainfall and topographic gradients in upland wet tropical forest soils. Biogeochemistry 44, 301–328.
Silver, W.L., Scatena, F.N., Johnson, A.H., Siccama, T.G., Sanchez, M.J., 1994. Nutrient availability in a montane wet tropical forest - Spatial patterns and methodological considerations. Plant and Soil 164, 129–145.
Sinsabaugh, R.L., 1994. Enzymic analysis of microbial pattern and process. Biology and Fertility of Soils 17, 69–74.
Sinsabaugh, R.L., 2010. Phenol oxidase, peroxidase and organic matter dynamics of soil. Soil Biology & Biochemistry 42, 391–404.
Sinsabaugh, R.L., Lauber, C.L., Weintraub, M.N., Ahmed, B., Allison, S.D., Crenshaw, C., Contosta, A.R., Cusack, D., Frey, S., Gallo, M.E., Gartner, T., Hobbie, S., Holland, K., Keeler, B., Powers, J., Stursova, M., Takacs-Vesbach, C., Waldrop, M., Wallenstein, M., Zak, D., Zeglin, L., 2008. Stoichiometry of soil enzyme activity at global scale. Ecology Letters 11, 1–13.
Tenney, F.G., Waksman, S.A., 1930. Composition of natural organic materials and their decomposition in the soil: V. Decomposition of various constituents in plant materials, under anaerobic conditions. Soil Science 30, 143–160.
Thompson, A., Chadwick, O.A., Boman, S., Chorover, J., 2006. Colloid mobilization during soil iron redox oscillations. Environmental Science & Technology 40, 5743–5749.
Triebwasser, D.J., Tharayil, N., Preston, C.M., Gerard, P.D., 2012. The susceptibility of soil enzymes to inhibition by leaf litter tannins is dependent on the tannin chemistry, enzyme class and vegetation history. New Phytologist 196, 1122–1132.
Turner, B.L., Romero, T., 2010. Stability of hydrolytic enzyme activity and microbial phosphorus during storage of tropical rain forest soils. Soil Biology and Biochemistry 459–465.
Viollier, E., Inglett, P., Hunter, K., Roychoudhury, A., van Cappellen, P., 2000. The ferrozine method revisited: Fe(II)/Fe(III) determination in natural waters. Applied Geochemistry 15, 785–790.
Wetzel, R.G., 1992. Gradient-dominated ecosystems: sources and regulatory functions of dissolved organic matter in freshwater ecosystems. Hydrobiologia 229, 181–198.
Yao, H., Bowman, D., Rufty, T., Shi, W., 2009. Interactions between N fertilization, grass clipping addition and pH in turf ecosystems: Implications for soil enzyme activities and organic matter decomposition. Soil Biology and Biochemistry 41, 1425–1432.

Table 1: Soil characteristics (means and standard errors) by site and depth increment. See methods for details on soil analyses.

Site	Elevation (m)	N (°)	W (°)	Depth	Soil Moisture (g^{-1} H_2O g^{-1} soil)	Carbon (%)	Fe(II) (µg g^{-1} soil)	Soluble phenolics (µg g^{-1} soil)
Bisley ridge	240 - 300	18.3157	65.7487	0 - 10 cm	0.94 (0.04)	5.9 (0.3)	0.46 (0.04)	11 (2)
				10 - 20 cm	0.74 (0.03)	3.6 (0.2)	0.25 (0.02)	6.1 (1.2)
Bisley slope	220 - 280			0 - 10 cm	0.95 (0.05)	5.1 (0.4)	0.27 (0.04)	5 (0.9)
				10 - 20 cm	0.74 (0.04)	2.8 (0.2)	0.11 (0.02)	2.3 (0.7)
Bisley valley	210 - 240			0 - 10 cm	0.93 (0.03)	4.2 (0.2)	0.38 (0.11)	1.2 (0.2)
				10 - 20 cm	0.80 (0.03)	3.4 (0.2)	0.43 (0.19)	1 (0.2)
Palm	614	18.2988	65.7803	0 - 10 cm	1.82 (0.86)	12.4 (2.3)	1.22 (0.44)	10.7 (2.6)
				10 - 20 cm	0.86 (0.08)	4.9 (0.5)	0.7 (0.2)	0.4 (0.2)
Colorado	736	18.2942	65.7852	0 - 10 cm	1.06 (0.05)	7.1 (1.1)	1.35 (0.8)	2.5 (0.6)
				10 - 20 cm	0.88 (0.05)	7 (1.1)	2.69 (1.21)	2.2 (0.5)
Elfin	936	18.2702	65.761	0 - 10 cm	1.71 (0.17)	16.7 (2.0)	3.74 (0.77)	5 (1.8)
				10 - 20 cm	1.33 (0.12)	14.6 (2.0)	4.11 (0.79)	3.1 (0.6)

Table 2: Optimum mixed effects models for soil hydrolytic enzyme activity. (a) Models for the lower montane ridge and slope sites (high-O_2 sites), and (b) models for the valley, palm, colorado, and elfin forest sites (low-O_2 sites). Fixed effects represent REML model coefficients and standard errors using data normalized by mean and standard deviation.

a) High-O_2 sites

	Fixed effects			Random effects (variance)			
Enzyme	Fe(II)	Phenolics	Depth	Transect	Depth x transect interaction	Plot	Residual
Cellobiohydrolase	0.61 (0.08)	--	-0.27 (0.06)	0.06	--	0.11	0.15
β-xylosidase	0.42 (0.10)	0.17 (0.09)	-0.14 (0.07)	0.26	--	--	0.26
β-glucosidase	0.44 (0.08)	--	-0.34 (0.07)	0.21	--	--	0.28
Acid phosphatase	0.36 (0.08)	--	-0.22 (0.09)	0.32	0.08	0.15	0.08
N-acetyl β-D-glucosaminidase	0.49 (0.09)	--	-0.30 (0.07)	0.20	--	0.10	0.20

b) Low-O_2 sites

	Fixed effects			Random effects (variance)			
Enzyme	Fe(II)	Phenolics	Depth	Transect	Depth x transect interaction	Plot	Residual
Cellobiohydrolase	--	--	-0.54 (0.14)	0.06	0.17	0.10	0.40
β-xylosidase	-0.27 (0.12)	--	-0.43 (0.08)	0.23	0.05	0.25	0.21
β-glucosidase	--	--	-0.38 (0.14)	0.21	0.22	0.25	0.23
Acid phosphatase	-0.32 (0.13)	0.26 (0.14)	-0.33 (0.05)	0.40	--	0.29	0.17
N-acetyl β-D-glucosaminidase	--	0.31 (0.10)	-0.35 (0.12)	0.27	0.16	0.12	0.11

Figure Captions

Figure 1: Soil organic C (a) and Fe(II) concentrations (b) by site (mean ± SE). See methods for details regarding analyses.

Figure 2: Potential activity of five hydrolytic enzymes across sites with decreasing mean long-term soil O_2 concentrations from left to right. Enzyme activities are expressed as the MUB production rate in terms of soil mass in the left column and soil C in the right column. CBHase refers to β-cellobiohydrolase, XYLase to β-xylosidase, BGase to β-glucosidase, APase to acid phosphatase, and NAGase to N-acetyl β-D-glucosaminidase, respectively.

Figure 3: Hydrolytic enzyme activities (soil mass basis) and soil Fe(II) concentrations for the higher-O_2 sites (ridge and slope) and the lower-O_2 sites (valley, palm, colorado, and elfin). CBHase refers to β-cellobiohydrolase, XYLase to β-xylosidase, BGase to β-glucosidase, APase to acid phosphatase, and NAGase to N-acetyl β-D-glucosaminidase, respectively.

Figure 4: Hydrolytic enzyme activities in soils exposed to aerobic or anaerobic conditions over an 18-day laboratory incubation. Mixed effects models showed significant time by treatment interactions for cellobiohydrolase ($p < 0.01$), β-glucosidase ($p < 0.05$), acid phosphatase ($p < 0.0001$), and NAGase ($p < 0.01$). β-xylosidase showed significant time and treatment effects, respectively ($p < 0.001$ and $p < 0.0001$).

Figure 1

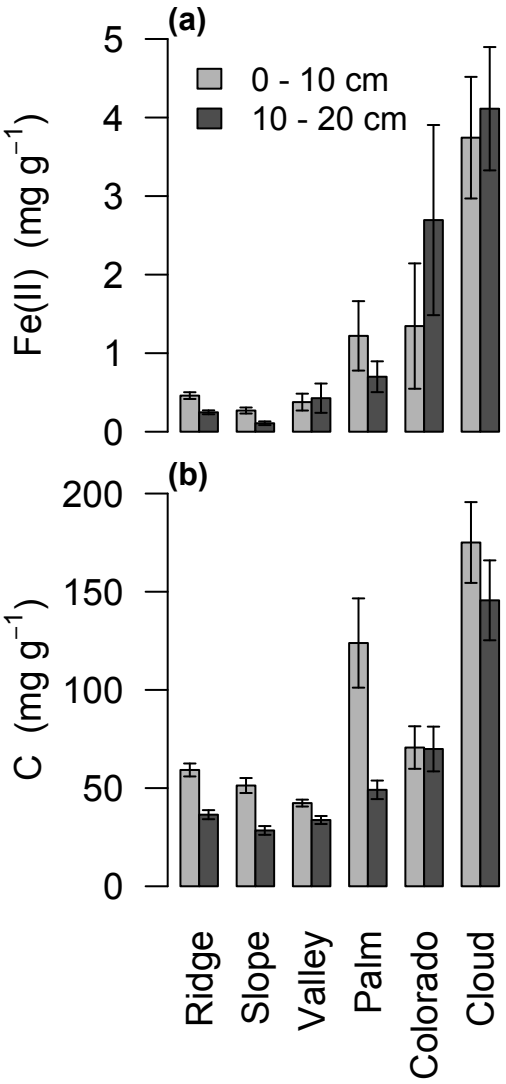
(a)
0 - 10 cm
10 - 20 cm
Fe(II) (mg g^{-1})
0
1
2
3
4
5
(b)
C (mg g^{-1})
0
50
100
150
200
Ridge
Slope
Valley
Palm
Colorado
Cloud

Figure 2

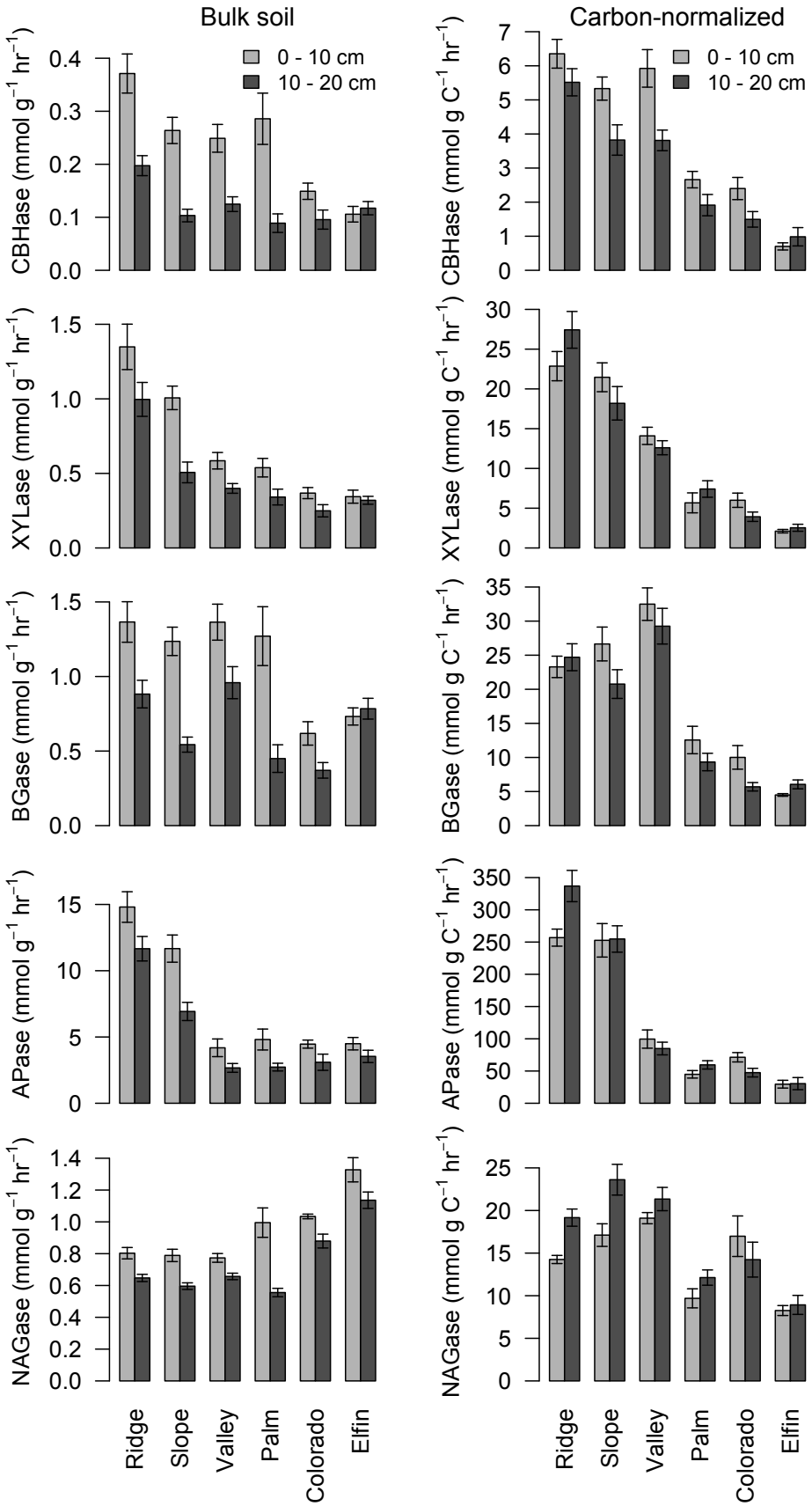
Bulk soil
Carbon-normalized
0 - 10 cm
10 - 20 cm
CBHase (mmol g^{-1} hr^{-1})
XYLase (mmol g^{-1} hr^{-1})
BGase (mmol g^{-1} hr^{-1})
APase (mmol g^{-1} hr^{-1})
NAGase (mmol g^{-1} hr^{-1})
CBHase (mmol g C^{-1} hr^{-1})
XYLase (mmol g C^{-1} hr^{-1})
BGase (mmol g C^{-1} hr^{-1})
APase (mmol g C^{-1} hr^{-1})
NAGase (mmol g C^{-1} hr^{-1})
Ridge
Slope
Valley
Palm
Colorado
Elfin

Figure 3

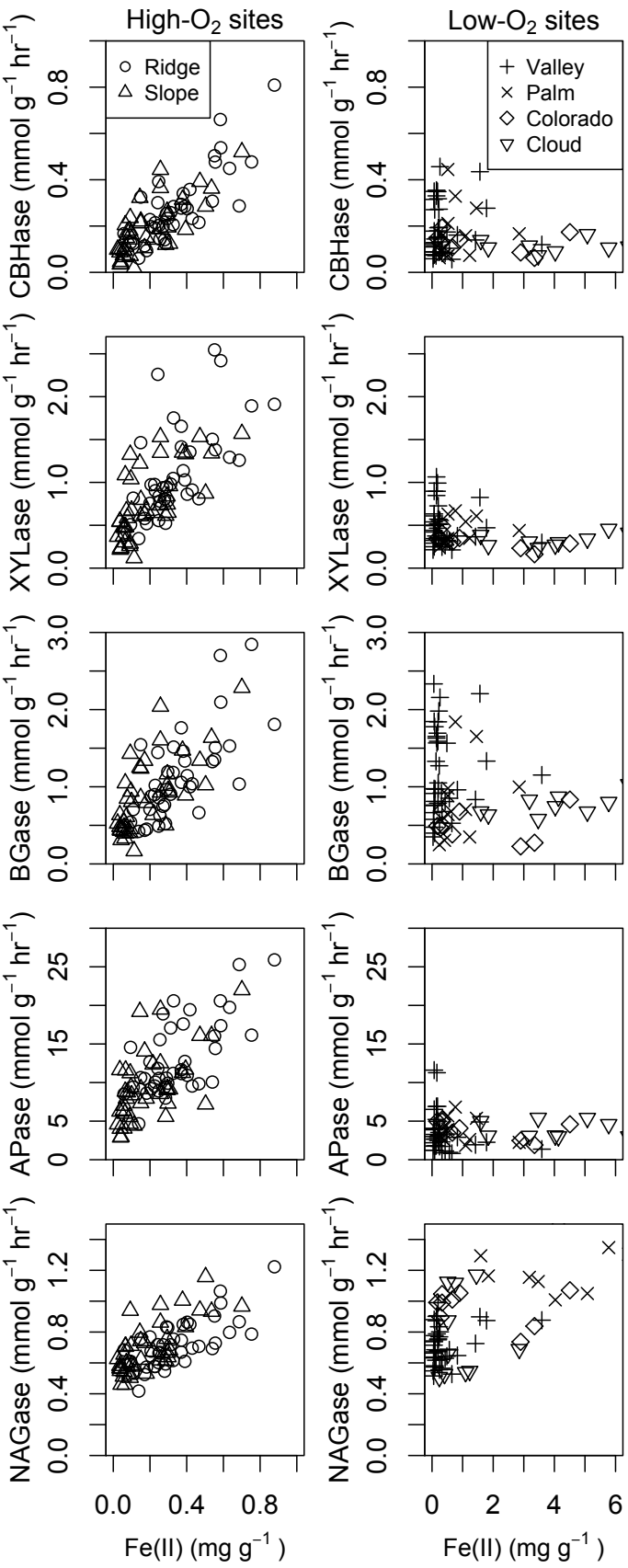
High-O2 sites
Low-O2 sites
Ridge
Slope
Valley
Palm
Colorado
Cloud
CBHase (mmol g−1 hr−1)
XYLase (mmol g−1 hr−1)
BGase (mmol g−1 hr−1)
APase (mmol g−1 hr−1)
NAGase (mmol g−1 hr−1)
Fe(II) (mg g−1)
Fe(II) (mg g−1)

Figure 4

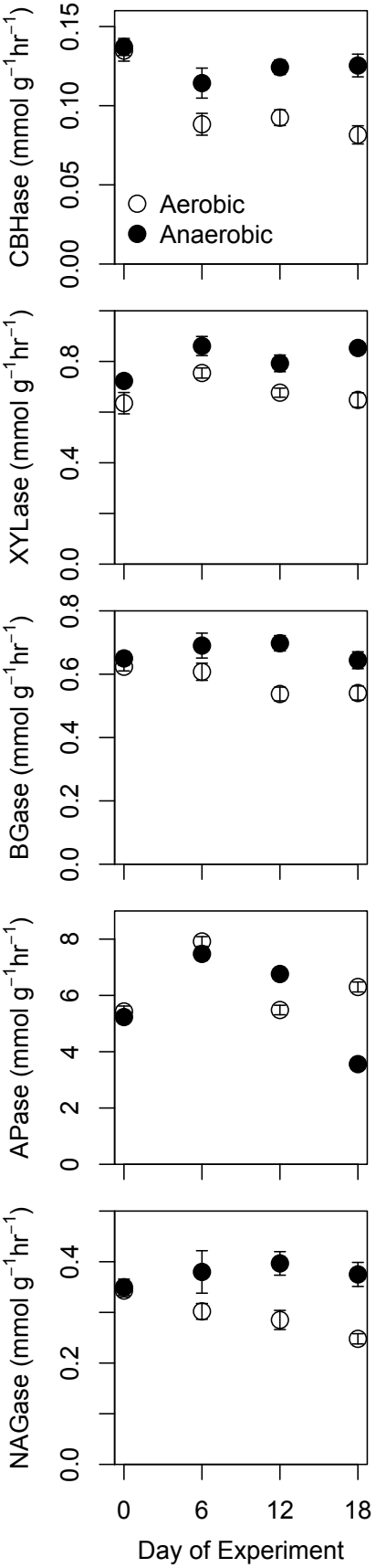
CBHase (mmol g^{-1}hr^{-1})
0.00
0.05
0.10
0.15
Aerobic
Anaerobic
XYLase (mmol g^{-1}hr^{-1})
0.0
0.4
0.8
BGase (mmol g^{-1}hr^{-1})
0.0
0.2
0.4
0.6
0.8
APase (mmol g^{-1}hr^{-1})
0
2
4
6
8
NAGase (mmol g^{-1}hr^{-1})
0.0
0.2
0.4
0
6
12
18
Day of Experiment

Supporting Information

Table S1: Pairwise comparisons (Tukey's honestly significant difference test) of enzyme means among sites expressed on the basis of soil mass (a) or soil C (b). Models were fit using generalized least squares with unequal variances among sites.

a) Soil mass basis

Enzyme	Depth (cm)	Ridge	Slope	Valley	Palm	Colorado	Cloud
CBHase	0 - 10	a	a	a	ab	bc	c
	10 - 20	a	b	b	b	b	b
XYLase	0 - 10	a	a	b	bc	c	c
	10 - 20	a	b	b	bc	c	bc
Bgase	0 - 10	a	a	a	ab	c	bc
	10 - 20	a	bc	a	c	c	ab
Apase	0 - 10	a	a	b	b	b	b
	10 - 20	a	b	c	c	c	c
NAGase	0 - 10	a	a	a	abc	b	c
	10 - 20	ab	ab	a	b	c	d

b) Soil C basis

Enzyme	Depth (cm)	Ridge	Slope	Valley	Palm	Colorado	Cloud
CBHase	0 - 10	a	a	a	b	b	c
	10 - 20	a	ab	b	c	c	c
XYLase	0 - 10	a	a	b	cd	c	d
	10 - 20	a	b	b	c	d	d
Bgase	0 - 10	a	ab	b	c	c	d
	10 - 20	a	a	a	b	b	b
Apase	0 - 10	a	a	b	c	b	c
	10 - 20	a	a	b	bc	c	c
NAGase	0 - 10	a	ab	b	cd	abc	d
	10 - 20	ac	a	a	b	bc	b

Table S2: Optimum mixed effects models for soil hydrolytic enzyme activity normalized by soil C concentration. (a) Models for the lower montane ridge and slope sites (high-O_2 sites), and (b) models for the valley, palm, colorado, and elfin forest sites (low-O_2 sites). Fixed effects represent REML model coefficients and standard errors using data normalized by mean and standard deviation.

a) High-O_2 sites

	Fixed effects			Random effects (variance)			
Enzyme	Fe(II)	Phenolics	Depth	Transect	Depth x transect interaction	Plot	Residual
Cellobiohydrolase	--	--	-0.30 (0.10)	0.39	--	--	0.58
β-xylosidase	--	--	--	0.64	0.06	--	0.38
β-glucosidase	--	--	--	0.33	0.16	--	0.55
Acid phosphatase	-0.38 (0.09)	--	--	0.69	0.06	--	0.41
N-acetyl β-D-glucosaminidase	-0.42 (0.10)	--	0.29 (0.07)	0.23	--	0.17	0.19

b) Low-O_2 sites

	Fixed effects			Random effects (variance)			
Enzyme	Fe(II)	Phenolics	Depth	Transect	Depth x transect interaction	Plot	Residual
Cellobiohydrolase	-0.20 (0.10)	--	-0.24 (0.08)	0.55	0.04	0.08	0.19
β-xylosidase	-0.29 (0.08)	--	-0.58 (0.06)	0.50	0.04	0.12	0.07
β-glucosidase	--	--	--	0.92	0.06	0.07	0.09
Acid phosphatase	-0.52 (0.11)	--	-0.12 (0.05)	0.18	--	0.23	0.18
N-acetyl β-D-glucosaminidase	--	-0.36 (0.09)	--	0.33	0.03	0.21	0.07

Figure S1: Hydrolytic enzyme activities (soil mass basis) and soil C concentrations. CBHase refers to β-cellobiohydrolase, XYLase to β-xylosidase, BGase to β-glucosidase, APase to acid phosphatase, and NAGase to N-acetyl β-D-glucosaminidase, respectively.

Figure S2: Hydrolytic enzyme activities (soil mass basis) and soluble phenolic concentrations for the higher-O_2 sites and the lower-O_2 sites, respectively. Enzyme abbreviations are as above.

Figure S3: Phenolic concentrations and soluble organic C (DOC) concentrations for both sites; these were strongly correlated ($R^2 = 0.72$, $p < 0.0001$).

Figure S1:

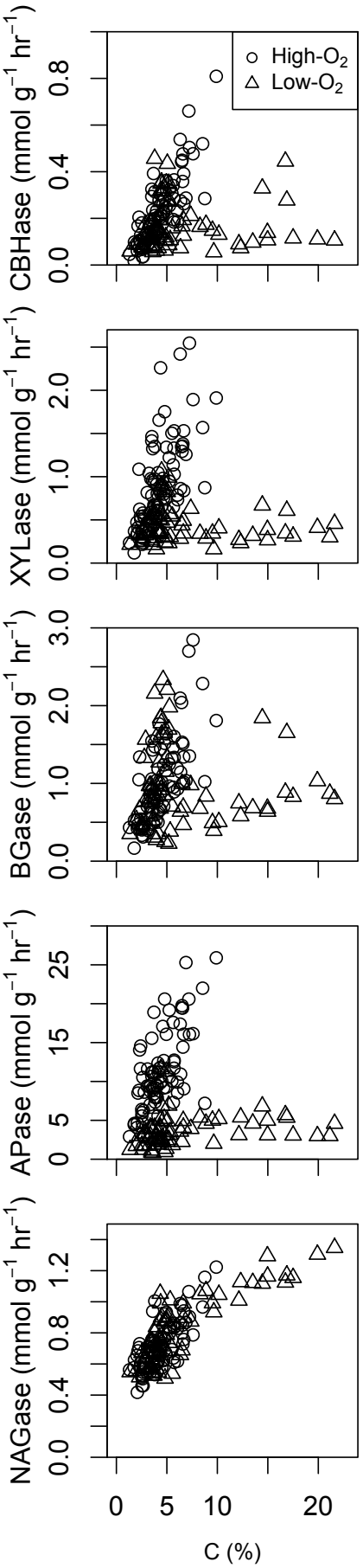
High-O2
Low-O2
CBHase (mmol g−1 hr−1)
XYLase (mmol g−1 hr−1)
BGase (mmol g−1 hr−1)
APase (mmol g−1 hr−1)
NAGase (mmol g−1 hr−1)
0.0
0.4
0.8
1.0
2.0
3.0
0
5
15
25
1.2
10
20
C (%)

Figure S2

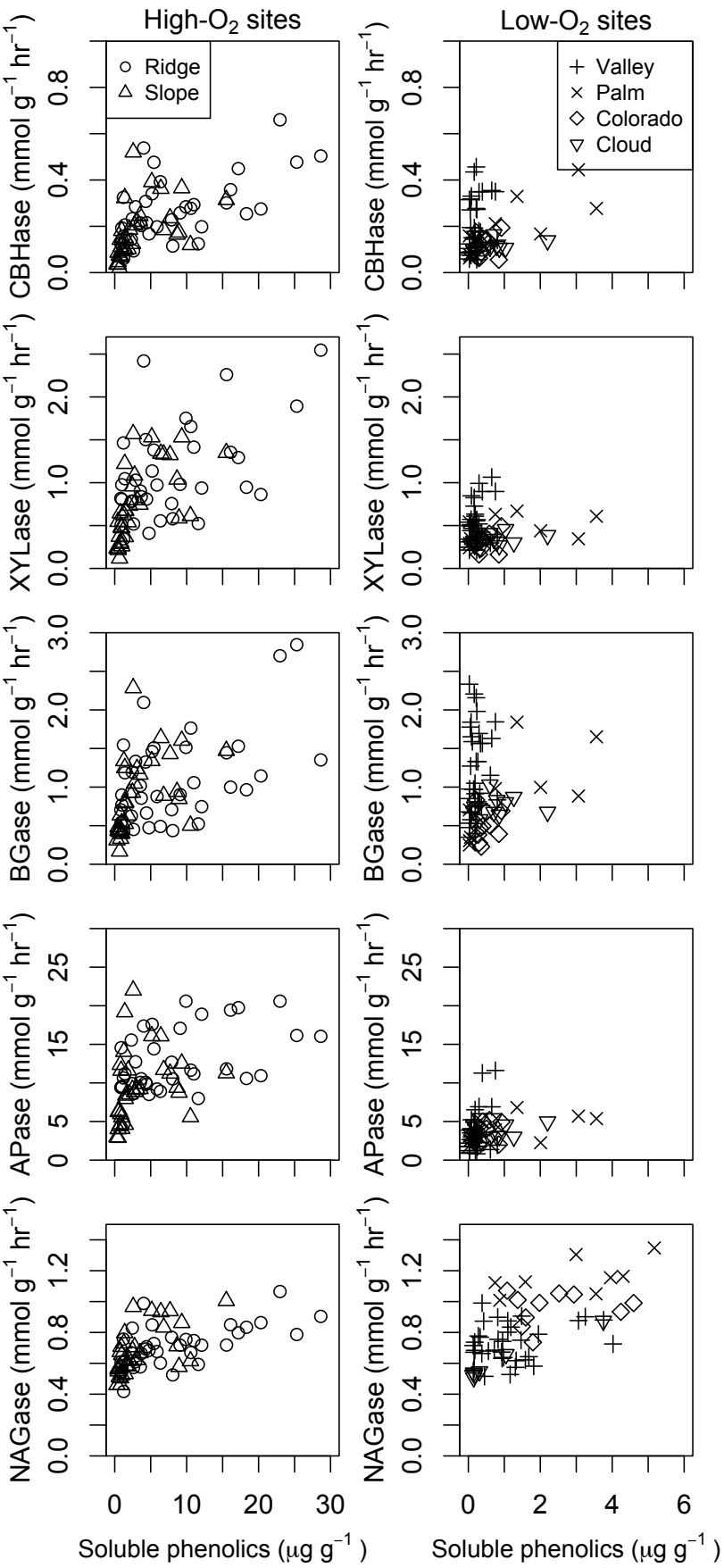
High-O2 sites
Low-O2 sites
Ridge
Slope
Valley
Palm
Colorado
Cloud
CBHase (mmol g−1 hr−1)
XYLase (mmol g−1 hr−1)
BGase (mmol g−1 hr−1)
APase (mmol g−1 hr−1)
NAGase (mmol g−1 hr−1)
Soluble phenolics (μg g−1)
Soluble phenolics (μg g−1)

Figure S3

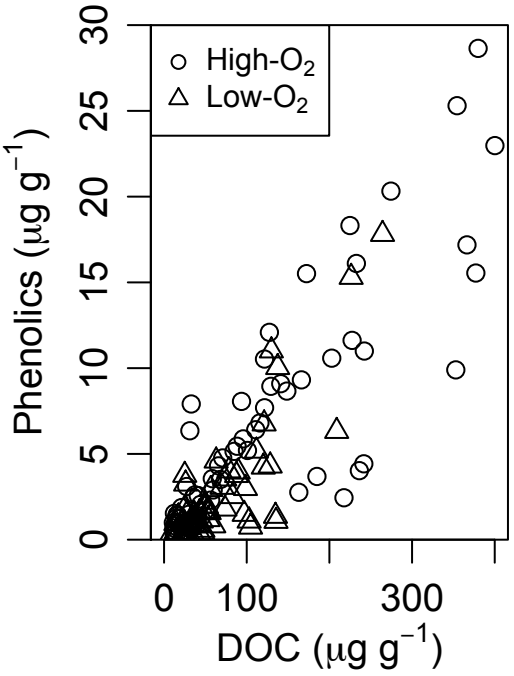
High-O2
Low-O2
Phenolics (μg g−1)
0
5
10
15
20
25
30
0
100
300
DOC (μg g−1)

Chapter Three:

Iron oxidation stimulates organic matter decomposition in humid tropical forest soils

Abstract

Humid tropical forests have the fastest rates of organic matter decomposition globally, which often coincide with fluctuating oxygen (O_2) availability in surface soils. Microbial iron (Fe) reduction generates reduced iron (Fe(II)) under anaerobic conditions, which oxidizes to Fe(III) under subsequent aerobic conditions. We demonstrate that Fe(II) oxidation stimulates organic matter decomposition via two mechanisms: 1) organic matter oxidation, likely driven by reactive oxygen species, and 2) increased dissolved organic carbon (DOC) availability, likely driven by acidification. Phenol oxidative activity increased linearly with Fe(II) concentrations ($p < 0.0001$, pseudo $R^2 = 0.79$) in soils sampled within and among five tropical forest sites. A similar pattern occurred in the absence of soil, suggesting an abiotic driver of this reaction. No phenol oxidative activity occurred in soils under anaerobic conditions, implying the importance of oxidants such as O_2 or hydrogen peroxide (H_2O_2) in addition to Fe(II). Reactions between Fe(II) and H_2O_2 generate hydroxyl radical, a strong non-selective oxidant of organic compounds. We found increasing consumption of H_2O_2 as soil Fe(II) concentrations increased, suggesting that reactive oxygen species produced by Fe(II) oxidation explained variation in phenol oxidative activity among samples. Amending soils with Fe(II) at field concentrations stimulated short-term C mineralization by up to 270 %, likely via a second mechanism. Oxidation of Fe(II) drove a decrease in pH and a monotonic increase in DOC; a decline of two pH units doubled DOC, likely stimulating microbial respiration. We obtained similar results by manipulating soil acidity independently of Fe(II), implying that Fe(II) oxidation affected C substrate availability via pH fluctuations, in addition to producing reactive oxygen species. Iron oxidation coupled to organic matter decomposition contributes to rapid rates of C cycling across humid tropical forests in spite of periodic O_2 limitation, and may help explain the rapid turnover of complex C molecules in these soils.

Introduction

Humid tropical forest soils support the fastest rates of decomposition globally and have the highest soil CO_2 fluxes of any terrestrial biome (Raich and Schlesinger, 1992; Jobbagy and Jackson, 2000). Understanding the factors controlling these high rates of carbon (C) oxidation is critical for predicting feedbacks with the global C cycle (Malhi and Grace, 2000; Parton et al., 2007). Tropical forest soils are typically rich in short-range ordered iron oxide (Fe(III)) minerals, an important but underappreciated biogeochemical catalyst with substantial potential to influence soil C dynamics by undergoing sequential reduction and oxidation. These soils experience fluctuating oxygen (O_2) availability over scales of hours to weeks driven by a combination of abundant rainfall, warm temperatures, finely textured soils, and high soil respiration rates (Silver et al., in press, 1999; Schuur et al., 2001; Cleveland et al., 2010; Liptzin et al., 2011). These O_2 fluctuations drive Fe redox cycling in humid tropical forests, where Fe(III) is reduced to ferrous Fe (Fe(II)) and subsequently reoxidized via biotic or abiotic reactions (Chacon et al., 2006;

Thompson, Chadwick, Rancourt, et al., 2006; Druschel et al., 2008; Dubinsky et al., 2010; Hall et al., 2012). Dissimilatory Fe reducing bacteria are well known to oxidize soil organic matter and can account for the majority of C oxidation under anaerobic conditions (Roden and Wetzel, 1996; Dubinsky et al., 2010).

Here we report on two mechanisms of C oxidation driven by Fe(II) oxidation that have not been previously described in natural terrestrial soils. The first mechanism involves the generation of reactive oxygen species, through reactions such as the following:

(1) $Fe(II) + O_2 + H^+ \rightarrow Fe(III) + HO_2^{\bullet}$

(2) $Fe(II) + H^+ + HO_2^{\bullet} \rightarrow H_2O_2 + Fe(III)$

(3) $Fe(II) + H_2O_2 \rightarrow {}^{\bullet}OH + Fe(III) + OH^-$

Abiotic Fe(II) oxidation by O_2 produces superoxide or hydroperoxyl radical (HO_2) (1). Subsequent abiotic reactions between HO_2 and Fe(II) can produce hydrogen peroxide (H_2O_2) (2), in addition to several other abiotic and enzymatic processes that also produce H_2O_2 (Wood, 1994; McKinzi and DiChristina, 1999; Halliwell and Gutteridge, 2007; Page et al., 2012). Hydrogen peroxide and Fe(II) then react according to the "Fenton reaction" to yield hydroxyl radical (3), a strong and non-selective oxidant of organic compounds including phenolics (Halliwell and Gutteridge, 2007). Recently, other electron donors such as reduced humic substances have also been shown to catalyze the abiotic reduction of H_2O_2 to $^{\bullet}OH$ (Page et al., 2012). In soils and litter, the oxidation of complex organic compounds has typically been ascribed to oxidative enzymes such as laccases and lignin peroxidases, some of which also function by generating reactive oxygen species (Wood, 1994; Hammel et al., 2002; Bodegom et al., 2005; Sinsabaugh, 2010). However, phenolic oxidation could also readily occur in the absence of oxidative enzymes as a result of the abiotic reactions described above. Abiotic reactions between Fe(II) and H_2O_2 have been employed in the context of wastewater treatment and soil toxin remediation, where large quantities of these reagents are typically added to decompose organic compounds (Pignatello et al., 2006). Similar processes may occur in terrestrial soils (Sinsabaugh, 2010), but their importance has not been previously ascertained.

The generation of protons by Fe(II) oxidation provides a separate mechanism that could potentially stimulate decomposition, in this case by releasing soluble or colloidal organic matter (< 0.45 μm) that would otherwise be unavailable for microbial assimilation. Previous research showed that anaerobic conditions associated with Fe reduction can increase dissolved organic C due to increased pH and colloid dispersion (Thompson, Chadwick, Boman, et al., 2006). Here, we test whether strongly acidic conditions (e.g. $pH < 4$) generated by Fe(II) oxidation could also promote the release of DOC and stimulate soil respiration. A pattern of increasing DOC as pH decreases below a point of minimum dissolution been demonstrated in several soils with widely differing mineralogy and organic matter composition (Chorover and Sposito, 1995; Skyllberg and Borggaard, 1998; Chorover et al., 2004). The release of protons accompanying Fe oxidation and hydrolysis of Fe(III) (Ahmad and Nye, 1990) could provide soil microbes with a flush of soluble organic matter immediately following the introduction of O_2. Thus, the anaerobic/aerobic

transitions characteristic of humid tropical forests could stimulate organic matter decomposition via at least two mechanisms that have yet to be investigated in natural terrestrial soils.

We tested whether Fe(II) oxidation could explain trends in multiple indices of soil organic matter decomposition across a range of humid tropical forest soils with differing redox dynamics. First, we assayed soils for phenol oxidative activity using the model humic substance L-dihydroxyphenylalanine (DOPA), and measured net production and loss of added H_2O_2 among similar soils with differing Fe(II) concentrations, as well as in soils amended with Fe(II). We expected increasing consumption of added H_2O_2 and decreasing net H_2O_2 production in soils with greater Fe(II), given that H_2O_2 readily reacts with Fe(II) to produce $^{\bullet}OH$ in the Fenton reaction. Note that we use the term "oxidative activity" as opposed to "oxidase activity" because Fe(II) oxidation could oxidize organic matter in the absence of enzymatic catalysis according to the above mechanism. Secondly, we assessed effects of Fe(II) oxidation on short-term soil CO_2 production in the laboratory by amending replicate soils with Fe(II) at levels similar to field concentrations. Finally, given that Fe(II) oxidation can significantly decrease soil pH, we examined effects of acidity on DOC concentrations and CO_2 production. We also tested effects of Fe(II) oxidation on CO_2 production under constant pH. We hypothesized that increasing soil Fe(II) concentrations and oxidation rates would increase phenol oxidative activity, reactivity to H_2O_2, and CO_2 production over timescales of hours. We also hypothesized that these trends would be at least partially explained by increased DOC solubilization with decreasing pH.

Methods

Site description

Soils were collected from sites differing in topography, rainfall, vegetation, and parent material in the Luquillo Experimental Forest, Puerto Rico, in order to capture a range of redox conditions and soil Fe(II) concentrations. We sampled soils from ridge, slope, and valley topographic zones in a lower montane wet forest site in the Bisley Research Watersheds, an upper montane "colorado" rain forest site in the Rio Icacos watershed (previously described as the "Guaba Ridge" (White et al., 1998)) and an upper elevation cloud forest on Pico del Este (Silver et al., 1999). These soils encompass ultisols, oxisols, and inceptisols in the USDA soil taxonomy (Huffaker, 2002). Site locations and bulk soil O_2 dynamics are summarized in Table 1 and are described in further detail by McDowell et al. (2012). All soils sampled typically exhibit sub-atmospheric O_2 concentrations that fluctuate over timescales of hours to weeks (Silver et al., in press, 1999; Liptzin et al., 2011). The presence of measurable O_2 in the soil matrix, however, does not preclude the occurrence of substantial Fe reduction inside soil aggregates (Liptzin and Silver, 2009; Hall et al., 2012). After O_2, Fe oxides are the most abundant terminal electron acceptor in these soils. Concentrations of nanoscale-ordered Fe oxides (ascorbic acid/citrate extraction), which represent an index of Fe(III) potentially reducible by microbes, average 20 ± 6 mg Fe g soil^{-1} among soils (S. Hall, unpublished data). Aqueous concentrations of Fe(II) fluctuate on the scale of days to weeks in the lower montane forests, indicative of gross Fe reduction and oxidation (Hall et al., 2012). Three replicate soil cores (6 cm diameter) were sampled to a depth of 20 cm at each site, an increment which contains the majority of organic matter and root biomass in these ecosystems (Odum, 1970). The 0 – 20 cm increment typically encompasses an A (enriched organic C) horizon and a B horizon. Cores from each site were

combined into a composite sample and gently homogenized, stored moist at 25°C, and assayed for oxidative activity within four weeks of collection.

Phenol oxidative activity measurements

We measured soil phenol oxidative activity using a standard colorimetric assay with the model humic substance L-dihydroxyphenylalanine (DOPA) (Pind et al., 1994; Sinsabaugh, 2010; German et al., 2011). Here, increasing absorptivity at 460 nm corresponds to increased oxidation of the DOPA substrate. We assayed 3 to 8 subsamples of ~ 10 g soil from each site in order to capture variation in Fe(II) concentrations. Immediately prior to assaying phenol oxidative activity, we homogenized soil subsamples and extracted 3 g (oven dry mass equivalent) in a 1:10 slurry of soil and 0.5 M hydrochloric acid (HCl) for Fe measurements. Soils were extracted on a rotary shaker for 60 min and the supernatant solution was filtered to 0.22 μm on a polyethersulfone membrane. We analyzed these solutions for Fe(II) and Fe(III) using a modified ferrozine method that accounted for Fe(III) interference during Fe(II) measurement (Viollier et al., 2000; Liptzin and Silver, 2009). To determine phenol oxidative activity, we prepared slurries containing 1 g (oven dry mass equivalent) of each soil subsample in 100 ml of 2M sodium acetate buffer using a stainless-steel mixer. This buffer concentration was used because adsorption of DOPA oxidation products to soil colloids (Zimmerman et al., 2004) at low buffer concentrations (e.g. 50 mM) can prevent linear color development over time, a key assumption of this assay (German et al., 2011). Increasing buffer concentrations had no suppressive effect on phenol oxidative activity. To commence the reaction, we combined 0.75 ml of soil slurry with 0.75 ml of 10 mM DOPA in microcentrifuge tubes. Tubes were briefly mixed and incubated in the dark on a rotary shaker. We measured the absorbance of the supernatant solution at 460 nm on a spectrophotometer (Genesys 20, Thermo Scientific, Waltham MA) on four technical replicates for each soil after incubation for 5, 60, and 120 minutes. We report phenol oxidative activity between 5 and 60 minutes for all samples except for the lower montane valley (5 and 180 min) to best meet the assumption of linear color development over time, given that oxidation rates tended to stabilize after 5 minutes. Samples from the lower montane slope site were incubated for 180 minutes because of slow color development. Samples were centrifuged at 15,000 rcf for two minutes prior to measurement (Pind et al., 1994). Measurements were corrected for background absorbance from dissolved humic substances using blank controls that received deionized water instead of DOPA. Trends in color development among samples were similar regardless of when samples were measured. We report phenol oxidative activity in terms of μmol DOPA g $soil^{-1}$ hr^{1} using a mM extinction coefficient of 0.61 generated by reacting DOPA standards with mushroom tyrosinase (Sigma-Aldrich).

We analyzed relationships between phenol oxidative activity and soil Fe(II) concentrations using linear mixed effects models. Given that Fe(III) minerals have also been proposed to oxidize DOPA in soils, we also included HCl-extractable soil Fe(III) concentrations as a potential covariate. Here, we modeled Fe concentrations as fixed effects and sites as random effects (to account for spatial autocorrelation) using the lme4 library (Bates et al., 2012) in R version 2.15. We assessed the significance of fixed effects using likelihood ratio tests of nested models fit using maximum likelihood. We then calculated a pseudo R^2 statistic to estimate the marginal variance in oxidative activity explained by Fe(II) concentrations after accounting for the random effects, using models fit via restricted maximum likelihood (Nakagawa and

Schielzeth, 2013). Experiments that assessed relationships between Fe(II) and H_2O_2 concentrations were conducted using soil from a single site and were thus analyzed using simple linear regression.

To determine whether oxidants such as Fe(III) could oxidize DOPA in the absence of O_2, we conducted the phenol oxidative assay under anaerobic conditions in a glovebox with a N_2, CO_2, and H_2 headspace using de-oxygenated reagents and four soil subsamples from the lower montane ridge and cloud forest sites. Soil Fe(II) and Fe(III) concentrations were measured as above. To determine if Fe(II) could oxidize DOPA in the absence of soil under an *aerobic* atmosphere, we prepared $FeCl_2$ solutions ranging from 0 to 1 mg Fe(II) in 0.75 ml 2M acetate buffer deoxygenated with helium. We combined these solutions with 10 mM L-DOPA under aerobic conditions and measured absorbance after 5 and 60 min as above from three technical replicates. We report data from 5 min given subsequent non-linearity of color development.

We measured net soil H_2O_2 production and consumption using a peroxidase-catalyzed fluorimetric assay based on the Amplex UltraRed reagent (AUR; Invitrogen, Grand Island, NY). Briefly, oxidation of the AUR reagent by horseradish peroxidase enzymes added to soil slurries is proportional to the soil solution concentration of H_2O_2. We conducted H_2O_2 assays over 60-minute incubations to facilitate comparisons with the phenol oxidative activity assays described above. Our H_2O_2 measurements thus represent net production over 60 min. Soil subsamples assayed for H_2O_2 were taken from a single soil core from the lower montane ridge site in order to capture aggregate-scale variation in Fe(II) concentrations while minimizing differences in other soil variables. Soil slurries were generated for soil subsamples as described for the phenol oxidative activity assays above. For each subsample, we added 200 µl of soil slurry to each of eight wells (technical replicates) in a 96-well plate. Solutions of the AUR reagent and horseradish peroxidase were added to achieve final concentrations of 2 µM and 1 kU/l of enzyme activity, respectively, in 250 µl of solution. Additional plate wells received soil and AUR but no peroxidase to account for background AUR oxidation by processes other than the peroxidase enzyme. Relationships between AUR fluorescence and H_2O_2 concentrations were determined for each plate by reacting eight known H_2O_2 standards (0 – 100 nM H_2O_2) with AUR and peroxidase. We also added these H_2O_2 standards to wells containing soil slurry in order to calculate a measure of H_2O_2 consumption, i.e. reaction with soil constituents aside from the AUR substrate. Finally, we added pre-oxidized AUR to wells containing soil to correct for quenching of the fluorescent signal by the soil slurry. We analyzed sample fluorescence (530 nm emission and 590 nm excitation) on a Biotek 96-well plate reader after a 60-min incubation in accordance with the phenol oxidative activity measurements described above. We calculated net soil H_2O_2 production after subtracting background soil AUR oxidation (in the absence of added peroxidase) and accounting for quenching of oxidized AUR by the soil slurry. This measurement provides a conservative estimate of H_2O_2 production because 1) peroxidase enzymes are likely present in the soil solution and contribute to background AUR oxidation measured in the absence of peroxidase addition, and 2) H_2O_2 reacts with soil and catalase enzymes in addition to the AUR target. We then estimated the consumption of H_2O_2 due to reactions with soil by comparing the ratio of regression slopes of the H_2O_2 standards vs. AUR fluorescence in the presence and absence of soil. Recovery of H_2O_2 standards added to soil slurries sometimes exceeded 100%, potentially due to catalytic effects of H_2O_2 addition on H_2O_2 production, or a decline of soil fluorescence quenching at high AUR concentrations. To directly determine effects of Fe(II) on

the net production and consumption of H_2O_2, we amended a single soil slurry with varying concentrations of ferrous chloride ($FeCl_2$) equivalent to 100, 50, 10, 5, 1, 0.5, 0.1, 0.05, and 0 μg Fe(II) g $soil^{-1}$, and measured H_2O_2 as above.

Soil Fe(II) addition experiments

To test the impact of Fe(II) oxidation on short-term C mineralization to CO_2, we conducted a factorial laboratory incubation experiment with soil collected from the lower montane ridge site. We sampled 4 kg of soil from 0 – 20 cm and removed coarse roots and plant debris by hand. Soils were gently homogenized, leaving fine-scale (~1 cm diameter) aggregates intact. Replicates of 10 g soil (dry mass equivalent) were incubated in 240 ml glass jars under anaerobic conditions (glovebox with N_2 headspace) for four days prior to the experiment to simulate conditions typical of anaerobic periods in the field (Liptzin et al., 2011). Soils were then amended with $FeCl_2$ or sodium chloride (NaCl, salt control) in 2 ml of deionized water to increase solute concentrations by 0, 10, 20, 40 or 100 μmol g $soil^{-1}$. After solute addition, jars were exposed to an ambient (aerobic) atmosphere, or alternatively were maintained under anaerobic conditions (n = 6 replicates for each solute concentration/headspace combination). Aerobic replicates were capped with gas-tight lids within ten minutes of exposure to the ambient aerobic atmosphere, and anaerobic replicates were capped inside the N_2 glovebox. Headspace gas was sampled immediately and after 24 hours and measured for CO_2 concentrations on a gas chromatograph with a thermal conductivity detector (Shimadzu; Columbia, MD). Production of CO_2 was calculated on a soil mass (oven dry equivalent) basis as the difference of initial and final headspace CO_2 mass concentration. Soil pH was measured in 1:2 slurries of soil and deionized water on additional replicate samples from the aerobic treatment.

We conducted additional experiments with soil from the same site to investigate effects of Fe(II) oxidation on CO_2 production mediated by pH. We amended soils with $FeCl_2$ or hydrochloric acid (HCl) at concentrations of 0, 10, 25, 50, and 75 μmol g $soil^{-1}$. In an additional experiment, samples were mixed in a 1:2 slurry of soil and buffer (2M sodium acetate or MES) at pH 5 and were amended with $FeCl_2$ at concentrations of 0, 5, 10, 15, 20, and 40 μmol g $soil^{-1}$ to measure effects of Fe(II) oxidation on CO_2 production at constant pH. Production of CO_2 was measured over 24 hours.

We extracted replicate soils from the laboratory incubation experiments in 0.5 M HCl and measured Fe concentrations as above immediately following the 24-hour headspace gas measurement. Soil pH was measured in 1:2 slurries of soil and water from additional samples. Soluble organic C was extracted from a subset of soils in 1:5 slurries of soil and 2 M potassium chloride, which were centrifuged and filtered to 0.45 μm on a nylon membrane for organic C analysis using a Shimadzu TOC-5050A. Effects of treatments on CO_2 fluxes and Fe(II) oxidation were examined using ANOVA.

Results

Phenol oxidative activity and Fe(II) concentrations

Phenol oxidative activity increased linearly with soil HCl-extractable Fe(II) concentrations both within and among the five humid tropical forest sites, where concentrations of extractable Fe(II) varied over two orders of magnitude (0.05 – 7.39 mg Fe g $soil^{-1}$) ($p < 0.0001$) (Fig. 1a). Under aerobic conditions, soil Fe(II) concentrations explained approximately 79 % of the variation (pseudo $R^2 = 0.79$) in phenol oxidative activity after accounting for spatial correlation among samples. In contrast, only 22 % of the variation in phenol oxidative activity was explained by Fe(III) concentrations ($p = 0.02$). Oxidation of DOPA did not significantly differ from zero under anaerobic conditions despite relatively high concentrations of HCl-extractable Fe(II) and Fe(III) (1 – 5 mg Fe g^{-1} soil). Under aerobic conditions, solutions of $FeCl_2$ rapidly oxidized DOPA even in the absence of soil and showed a consistent increase in oxidative activity over the range of Fe(II) concentrations that we employed, which was closely described by a linear regression with a quadratic term ($R^2 = 0.999$, $p < 0.0001$) (Fig. 1b).

Net H_2O_2 production measured in lower montane ridge soils was inversely related to soil Fe(II) concentrations. These variables followed a linear log-log relationship ($R^2 = 0.79$, $p < 0.0001$) (Fig. 2a). Amending soils with $FeCl_2$ generated a similar and even more consistent decline in net H_2O_2 production ($R^2 = 0.95$, $p < 0.0001$, Fig. 2b), suggesting that reaction with $FeCl_2$ provided a significant sink for H_2O_2. The relative recovery of H_2O_2 standards added to soil slurries also declined with increasing soil Fe(II) concentrations, although H_2O_2 recovery appeared to increase at very high Fe(II) concentrations (Fig. 2c). There was a linear log-log relationship between H_2O_2 recovery and Fe(II) below concentrations of 2000 μg g^{-1} ($R^2 = 0.67$, $p < 0.0001$).

Iron oxidation and CO_2 production

Addition of $FeCl_2$ consistently stimulated short-term CO_2 production under aerobic conditions, but had little effect under anaerobic conditions relative to additions of deionized water or sodium chloride (NaCl) solutions (salt control). Total CO_2 production over 24 hours after solute addition differed significantly by headspace treatment (aerobic or anaerobic), solute type ($FeCl_2$, NaCl, or deionized water control), and solute concentration, with significant interactions among all variables ($p < 0.0001$, Fig. 3a,b). In soils exposed to aerobic conditions, CO_2 production increased linearly with initial Fe(II) concentrations up to 270 % of the deionized water and the salt solution controls. In contrast, production of CO_2 responded weakly to NaCl addition. There was little variation in CO_2 production relative to Fe(II) under anaerobic conditions (Fig. 3b). Ferrous chloride stimulated CO_2 production relative to the NaCl controls at low concentrations, but these solutes had equivalent effects at higher concentrations.

Under aerobic conditions, extractable Fe(II) declined over 24 h to 25, 18, 36, and 53 % of initial concentrations in treatments receiving 10, 20, 40, and 100 μmol $FeCl_2$ g $soil^{-1}$, respectively. Declines in extractable Fe(II) were smaller under anaerobic conditions, with decreases of 5, 9, 17, and 24 % among treatments, respectively. A linear increase in HCl-extractable Fe(III) accounted for 41 % of the decline in Fe(II) among the aerobic Fe(II) addition

treatments, while Fe(III) concentrations increased significantly only for the highest Fe(II) concentration added in the anaerobic treatment (Fig. 3c,d). Rates of CO_2 production were strongly linearly correlated with Fe(II) loss under aerobic conditions ($R^2 = 0.92$, $p < 0.0001$), increasing by 0.51 ± 0.02 μg CO_2-C g soil hr^{-1} respired for each mg Fe(II) g $soil^{-1}$ that was lost via oxidation or sorption (Fig. 3e). Changes in Fe(II) concentrations were unrelated to CO_2 production under anaerobic conditions (Fig. 3f). We observed declines in pH from 4.15 in the deionized water control to 3.80, 3.58, 3.41, and 3.28 with increasing Fe(II) addition under aerobic conditions.

To evaluate the relative impacts of Fe(II) oxidation and changes in acidity on CO_2 production, we amended additional replicate soil samples with $FeCl_2$, hydrochloric acid (HCl), or deionized water. Production of CO_2 increased with increasing acidity below pH 4, regardless of which solute was added ($FeCl_2$ or HCl) (Fig. 4a). Concentrations of organic C soluble in 2M KCl increased monotonically with decreasing pH (Fig. 4b). In a separate experiment where we buffered soil slurries at pH 5, Fe(II) oxidation had a inconsistent suppressive effect on CO_2 production (Fig. 4c), as opposed to the stimulatory effects we observed in intact soils where pH decreased with Fe(II) oxidation.

Discussion

Our data provide evidence that Fe(II) oxidation can stimulate soil organic matter decomposition via two separate mechanisms not yet considered in conceptual or mathematical models of soil C dynamics in natural soils. First, the consistent linear increase in phenol oxidative activity with soil Fe(II) concentrations suggests that reactive oxygen species produced via abiotic reactions largely controlled variation in phenol oxidative activity within and among these tropical forest soils. We observed a combination of decreased net H_2O_2 production and increased consumption of H_2O_2 with increasing soil Fe(II) concentrations. These trends suggest that Fe(II) and H_2O_2 reacted according to the Fenton reaction to produce $^{\bullet}OH$, a strong oxidant of organic compounds. Additional reactions likely also contributed to H_2O_2 loss in our souls, such as reduction of H_2O_2 to water by catalase enzymes, although we would not necessarily expect these processes to scale with soil Fe(II). Previous research suggested that the oxidation of organic compounds such as DOPA can also be directly coupled to the reduction of Fe(III) oxide minerals (Mayaudon et al., 1973), but we found little evidence for this mechanism here in comparison to Fe(II) oxidation. Phenol oxidation was negligible under anaerobic conditions despite an abundance of HCl-extractable soil Fe(III), and Fe(III) showed only a weak relationship with phenol oxidation under aerobic conditions.

Oxidative enzymes could also conceivably have contributed to the relationships we observed between Fe(II) and phenol oxidative activity, as proposed by Bodegom et al. (2005) in a study of wetland soils. However, reactions between Fe(II) and H_2O_2 produced by bacteria in laboratory cultures have been shown to oxidize organic compounds in the absence of oxidative enzymes (McKinzi and DiChristina, 1999). Our soils likely represent an analogous situation, where Fe(II) produced via dissimilatory microbial reduction under anaerobic conditions is oxidized abiotically by O_2 and H_2O_2 under aerobic conditions, generating reactive oxygen species that contribute to organic matter oxidation. Biotic (chemolithotrophic) Fe(II) oxidation has also been demonstrated in these humid tropical forest soils (Dubinsky et al., 2010), although

rates of abiotic Fe(II) oxidation likely dwarf biotic oxidation in the presence of near-atmospheric O_2 concentrations (Druschel et al., 2008). The fact that Fe(II) solutions (in the absence of soil) generated a pattern of phenol oxidation similar to what we observed in natural soils demonstrates that abiotic reactions provide a parsimonious explanation for our field data. Conclusively partitioning abiotic vs. biotic catalysis of phenol oxidation in natural soil samples, however, is challenging given that 1) enzymes can remain protected by soil particles during sterilization processes such as autoclaving (Stursova and Sinsabaugh, 2008), and 2) sterilization processes also affect Fe(II) concentrations. Here, autoclaving soils had no consistent effect on phenol oxidation (data not shown). It is likely that a combination of abiotic and biotic processes contributed to our observed rates of phenol oxidation, which fall well within the range of published values after normalizing by soil organic matter content (Sinsabaugh et al., 2008). In fact, previous measurements of phenol oxidative activity in Fe(II)-rich soils may overestimate the contribution of enzymes to the oxidation of phenolic compounds. The generation of reactive oxygen species by reactions between Fe(II) and H_2O_2 have long been appreciated as a potent oxidation mechanism in the fields of chemistry and engineering (Pignatello et al., 2006), as well as a mechanism of fungal lignin degradation (Hammel et al., 2002), but not yet as a widespread mechanism for organic matter oxidation in natural soils that are rich in Fe(II). Abiotic phenol oxidative processes in soils are supported by theory, and our data suggest that they provide an important contribution to rapid rates of organic matter oxidation typical of Fe-rich humid tropical forest soils.

We also found a strong positive relationship between Fe(II) oxidation and short-term CO_2 production, likely driven by a second and separate mechanism: Fe(II) oxidation increased soil acidity and significantly increased concentrations of DOC, potentially stimulating microbial respiration. Dissolved organic C increased monotonically with decreasing pH, and increases in DOC exceeded increases in respiration by at least one order of magnitude, suggesting that only a small fraction of the newly-released DOC was respired during the incubation. The addition of Fe(II) under static anaerobic conditions yielded only a small stimulatory effect on respiration, of similar magnitude to our NaCl controls, showing that the oxidation of added Fe(II) was necessary to consistently stimulate soil respiration. Bodegom *et al*. (2005) similarly measured increasing CO_2 production with increasing Fe(II) concentrations in waterlogged wetland soils, and attributed this relationship to stimulation of enzymatic activity. Microaerophilic conditions could have led to low rates of Fe oxidation and production of reactive oxygen species, contributing to CO_2 production (Bodegom et al., 2005). In our laboratory incubations, however, the majority of Fe(II) rapidly oxidized under aerobic conditions and generated significant acidity due to the hydrolysis of Fe(III). Here, the acidity generated by Fe(II) oxidation appeared primarily responsible for increased short-term CO_2 production, as opposed to reactive oxygen species. Generation of equivalent acidity from Fe(II) oxidation and HCl addition yielded similar increases in CO_2 production, suggesting a primary influence of pH. Separate experiments showed that Fe(II) oxidation had little effect on short-term CO_2 production when pH was held constant in buffered soil slurries. Finally, carbonate dissolution could not have contributed to CO_2 production given the acidic range of soil pH examined here.

The stimulatory effect of Fe(II) oxidation and acidity on soil respiration shown here is surprising given that most previous studies found either no response or a decrease in soil respiration with increasing acidity when comparing similar soils across a pH gradient (Motavalli

et al., 1995; Aciego Pietri and Brookes, 2009; Kemmitt et al., 2009). The discrepancy likely arises from the fact that we examined effects of Fe-induced temporal shifts in pH within a given soil as opposed to comparing across soils with differing pH. The pH-sensitivity of organic C solubility and microbial respiration is also likely to be affected by soil surface charge characteristics, and may be predictable using metrics such as the point of zero charge (i.e. the pH at which a given soil is electrically neutral). Our results highlight the importance of Fe(II) oxidation in stimulating short-term respiration rates by increasing C substrate availability. The dominant effects of pH on respiration over the short time scales (24 hours) shown here, however, do not preclude the importance of Fe(II) oxidation in generating reactive oxygen species (as shown above) on CO_2 production over longer timescales. We expect that oxidative reactions ultimately govern the access of microbes to C associated with biochemically-recalcitrant molecules over longer timescales (Sinsabaugh, 2010).

Implications of Fe redox cycling for organic matter decomposition

Traditional conceptual models of soil C cycling posit that anaerobic conditions limit soil organic matter decomposition, all else being equal, because of energetic and enzymatic constraints on the activity of decomposing microbes (Ponnamperuma, 1972; Linn and Doran, 1984; Freeman et al., 2001). These concepts have been incorporated into the leading mathematical models of soil C cycling, where decomposition rates decline under high soil moisture due to anaerobic conditions (Li et al., 1992; Parton et al., 1993; Davidson et al., 2012). We suggest that these models likely underestimate organic matter decomposition in fluctuating redox environments, characterized by sequential anaerobic and aerobic conditions, because of the stimulatory effects of Fe(II) oxidation on organic matter oxidation and CO_2 production demonstrated here. Although CO_2 production is likely to decline under anaerobic conditions, Fe(II) oxidation and stimulation of decomposition under subsequent aerobic conditions could at least partially compensate for temporary declines under anaerobic conditions. First, Fe(II) oxidation can potentially stimulate the oxidation of organic compounds due to the production of reactive oxygen species. Second, acidity generated by Fe(II) oxidation can potentially increase short-term respiration rates, likely by solubilizing organic C. Frequent transitions between aerobic and anaerobic conditions may contribute to the rapid rates of organic matter decomposition that are frequently observed in wet tropical environments (Parton et al., 2007), in spite of inherent limitations on decomposition imposed by periods of low O_2 availability. Redox fluctuations are closely linked to rainfall dynamics in tropical forests (Liptzin et al., 2011). Thus, changes in the frequency and intensity of precipitation in the humid tropics with global change (Romps, 2011) could have important impacts on redox cycling and associated soil C dynamics.

The oxidizing power of reactions between Fe(II) and O_2 also provide a potential mechanism for the rapid decomposition of chemically recalcitrant organic matter (Schmidt et al., 2011). Oxidative reactions are necessary to decompose lignin and other phenolic compounds, yet relatively few microbial taxa are known to produce oxidative enzymes capable of degrading lignin (Hammel, 1997; Thevenot et al., 2010; DeAngelis et al., 2011). A sequence of bacterial dissimilatory Fe(III) reduction, followed by abiotic Fe(II) oxidation and the production of reactive oxygen species, could promote the non-specific decomposition of chemically recalcitrant C compounds. These reactions could be especially important in environments where oxidative enzyme activity might otherwise be low, such as humid tropical forest soils that

frequently experience anaerobic conditions. In sum, redox cycling may give rise to emergent behavior that could not be predicted under static aerobic or anaerobic conditions. In episodically anaerobic soil environments, even brief periods of O_2 availability could serve to stimulate C decomposition via Fe(II) oxidation.

Acknowledgements

This paper was originally published in Global Change Biology, and we thank Wiley for copyright permission. I thank Whendee L. Silver for her contribution to this manuscript. We thank K. Hammel for stimulating discussion, A. Thompson for insight and critical review, and an anonymous reviewer for their contributions to the paper. J. Treffkorn and A. McDowell provided laboratory assistance. Funding was provided by NSF grant EAR-08199072, an NSF DDIG (1210936), and the NSF-supported Luquillo Critical Zone Observatory (EAR-0722476) with additional support provided by the USGS Luquillo WEBB program and the USDA Forest Service International Institute of Tropical Forestry. This research was also supported by grant DEB 0620910 from NSF to the Institute for Tropical Ecosystem Studies, University of Puerto Rico, and to the International Institute of Tropical Forestry USDA Forest Service, as part of the Luquillo Long-Term Ecological Research Program. SJH was supported by the Department of Energy Office of Science Graduate Fellowship Program, made possible in part by the American Recovery and Reinvestment Act of 2009, administered by ORISE-ORAU under contract no. DE-AC05-06OR23100.

References

Aciego Pietri, J.C., Brookes, P.C., 2009. Substrate inputs and pH as factors controlling microbial biomass, activity and community structure in an arable soil. Soil Biology and Biochemistry 41, 1396–1405.

Ahmad, A., Nye, P., 1990. Coupled diffusion and oxidation of ferrous iron in soils. I. Kinetics of oxygenation of ferrous iron in soil suspension. Soil Science 1990, 395–409.

Bates, D., Maechler, M., Bolker, B., 2012. lme4: Linear mixed-effects models using S4 classes.

Bodegom, P.M.V., Broekman, R., Dijk, J.V., Bakker, C., Aerts, R., 2005. Ferrous iron stimulates phenol oxidase activity and organic matter decomposition in waterlogged wetlands. Biogeochemistry 76, 69–83.

Chacon, N., Silver, W.L., Dubinsky, E.A., Cusack, D.F., 2006. Iron reduction and soil phosphorus solubilization in humid tropical forests soils: The roles of labile carbon pools and an electron shuttle compound. Biogeochemistry 78, 67–84.

Chorover, J., Amistadi, M.K., Chadwick, O.A., 2004. Surface charge evolution of mineral-organic complexes during pedogenesis in Hawaiian basalt. Geochimica et Cosmochimica Acta 68, 4859–4876.

Chorover, J., Sposito, G., 1995. Dissolution behavior of kaolinitic tropical soils. Geochimica et Cosmochimica Acta 59, 3109–3121.

Cleveland, C.C., Wieder, W.R., Reed, S.C., Townsend, A.R., 2010. Experimental drought in a tropical rain forest increases soil carbon dioxide losses to the atmosphere. Ecology 91, 2313–2323.

Davidson, E.A., Samanta, S., Caramori, S.S., Savage, K., 2012. The Dual Arrhenius and Michaelis–Menten kinetics model for decomposition of soil organic matter at hourly to seasonal time scales. Global Change Biology 18, 371–384.

DeAngelis, K.M., Allgaier, M., Chavarria, Y., Fortney, J.L., Hugenholtz, P., Simmons, B., Sublette, K., Silver, W.L., Hazen, T.C., 2011. Characterization of trapped lignin-degrading microbes in tropical forest soil. PLoS ONE 6, e19306.

Druschel, G.K., Emerson, D., Sutka, R., Suchecki, P., Luther III, G.W., 2008. Low-oxygen and chemical kinetic constraints on the geochemical niche of neutrophilic iron(II) oxidizing microorganisms. Geochimica et Cosmochimica Acta 72, 3358–3370.

Dubinsky, E.A., Silver, W.L., Firestone, M.K., 2010. Tropical forest soil microbial communities couple iron and carbon biogeochemistry. Ecology 91, 2604–2612.

Freeman, C., Ostle, N., Kang, H., 2001. An enzymatic "latch" on a global carbon store -- a shortage of oxygen locks up carbon in peatlands by restraining a single enzyme. Nature 409, 149.

German, D.P., Weintraub, M.N., Grandy, A.S., Lauber, C.L., Rinkes, Z.L., Allison, S.D., 2011. Optimization of hydrolytic and oxidative enzyme methods for ecosystem studies. Soil Biology and Biochemistry 43, 1387–1397.

Hall, S., McDowell, W., Silver, W., 2012. When wet gets wetter: decoupling of moisture, redox biogeochemistry, and greenhouse gas fluxes in a humid tropical forest soil. Ecosystems Online Early, DOI 10.1007/s10021–012–9631–2.

Halliwell, B., Gutteridge, J., 2007. Free Radicals in Biology and Medicine, 4th ed. Oxford University Press, Oxford, UK.

Hammel, K., 1997. Fungal degradation of Lignin, in: Cadisch, G., Giller, K. (Eds.), Driven by Nature: Plant Litter Quality and Decomposition. CAB International, Wallingford, UK, pp. 33–35.

Hammel, K., Kapich, A., Jensen, K., Ryan, Z., 2002. Reactive oxygen species as agents of wood decay by fungi. Enzyme and Microbial Technology 30, 445–453.

Huffaker, L., 2002. Soil survey of Caribbean National Forest and Luquillo Experimental Forest, Commonwealth of Puerto Rico. USDA, NRCS.

Jobbagy, E.G., Jackson, R.B., 2000. The vertical distribution of soil organic carbon and its relation to climate and vegetation. Ecological Applications 10, 423–436.

Kemmitt, S.J., Wright, D., Goulding, K.W.T., Jones, D.L., 2009. pH regulation of carbon and nitrogen dynamics in two agricultural soils. Soil Biology and Biochemistry 38, 898–911.

Li, C., Frolking, S., Frolking, T., 1992. A model of nitrous oxide evolution from soil driven by rainfall events: 1. Model structure and sensitivity. Journal of Geophysical Research 97, 9759–9776.

Linn, D.M., Doran, J.W., 1984. Effect of water-filled pore space on carbon dioxide and nitrous oxide production in tilled and non-tilled soils. Soil Science Society of America Journal 48, 1267–1272.

Liptzin, D., Silver, W.L., 2009. Effects of carbon additions on iron reduction and phosphorus availability in a humid tropical forest soil. Soil Biology & Biochemistry 41, 1696–1702.

Liptzin, D., Silver, W.L., Detto, M., 2011. Temporal dynamics in soil oxygen and greenhouse gases in two humid tropical forests. Ecosystems 14, 171–182.

Malhi, Y., Grace, J., 2000. Tropical forests and atmospheric carbon dioxide. Trends in Ecology & Evolution 15, 332–337.

Mayaudon, J., Halfawi, M.E., Batistic, L., 1973. Oxidoreductive degradation of D,L-3(3,4-dihydroxyphenyl) alanine by soil minerals and clays. Soil Science 24, 182–192.
McDowell, W.H., Scatena, F.N., Waide, R.B., Brokaw, N., Camilo, G., Covich, A., Crowl, T., Gonzalez, G., Greathouse, E., Klawinski, P., Lodge, D., Lugo, A., Pringle, C., Richardson, B., Richardson, M., Schaefer, D., Silver, W., Thompson, J., Vogt, D., Vogt, K., Willig, M., Woolbright, L., Zou, X., Zimmerman, J., 2012. Geographic and ecological setting of the Luquillo Mountains, in: Brokaw, N., Crowl, T., Lugo, A., McDowell, W.H., Scatena, F.N., Waide, R.B., Willig, M. (Eds.), A Caribbean Forest Tapestry: The Multidimensional Nature of Disturbance and Response. Oxford University Press, USA, pp. 72–163.
McKinzi, A.M., DiChristina, T.J., 1999. Microbially driven Fenton reaction for transformation of pentachlorophenol. Environ. Sci. Technol. 33, 1886–1891.
Motavalli, P.P., Palm, C.A., Parton, W.J., Elliott, E.T., Frey, S.D., 1995. Soil pH and organic C dynamics in tropical forest soils: Evidence from laboratory and simulation studies. Soil Biology and Biochemistry 27, 1589–1599.
Nakagawa, S., Schielzeth, H., 2013. A general and simple method for obtaining R2 from generalized linear mixed-effects models. Methods in Ecology and Evolution 4, 133–142.
Odum, H.T., 1970. Rain forest structure and mineral-cycling homeostasis, in: Odum, H.T., Pigeon, R.F. (Eds.), A Tropical Rain Forest: a Study of Irradiation and Ecology at El Verde, Puerto Rico. U.S. Atomic Energy Commission, Oak Ridge, TN, pp. H3–H52.
Page, S.E., Sander, M., Arnold, W.A., McNeill, K., 2012. Hydroxyl radical formation upon oxidation of reduced humic acids by oxygen in the dark. Environmental Science & Technology 46, 1590–1597.
Parton, W., Silver, W.L., Burke, I.C., Grassens, L., Harmon, M.E., Currie, W.S., King, J., Adair, E.C., Brandt, L., Hart, S.C., Fasth, B., 2007. Global-scale similarities in nitrogen release patterns during long-term decomposition. Science 315, 361–364.
Parton, W.J., Scurlock, J.M.O., Ojima, D.S., Gilmanov, T.G., Scholes, R.J., Schimel, D.S., Kirchner, T., Menaut, J.-C., Seastedt, T., Moya, E.G., Kamnalrut, A., Kinyamario, J.I., 1993. Observations and modeling of biomass and soil organic matter dynamics for the grassland biome worldwide. Global Biogeochemical Cycles 7, 785–809.
Pignatello, J., Oliveros, E., MacKay, A., 2006. Advanced oxidation processes for organic contaminant destruction based on the Fenton reaction and related chemistry. Critical Reviews in Environmental Science and Technology 36, 1–84.
Pind, A., Freeman, C., Lock, M.A., 1994. Enzymic degradation of phenolic materials in peatlands — measurement of phenol oxidase activity. Plant and Soil 159, 227–231.
Ponnamperuma, F.N., 1972. The chemistry of submerged soils. Advances in Agronomy 24, 29–96.
Raich, J.W., Schlesinger, W.H., 1992. The global carbon dioxide flux in soil respiration and its relationship to vegetation and climate. Tellus B 44, 81–99.
Roden, E., Wetzel, R., 1996. Organic carbon oxidation and suppression of methane production by microbial Fe(III) oxide reduction in vegetated and unvegetated freshwater wetland sediments. Limnology and Oceanography 41, 1733–1748.
Romps, D.M., 2011. Response of tropical precipitation to global warming. Journal of the Atmospheric Sciences 68, 123–138.
Schmidt, M.W.I., Torn, M.S., Abiven, S., Dittmar, T., Guggenberger, G., Janssens, I.A., Kleber, M., Kogel-Knabner, I., Lehmann, J., Manning, D.A.C., Nannipieri, P., Rasse, D.P.,

Weiner, S., Trumbore, S.E., 2011. Persistence of soil organic matter as an ecosystem property. Nature 478, 49–56.
Schuur, E.A.G., Chadwick, O.A., Matson, P.A., 2001. Carbon cycling and soil carbon storage in mesic to wet Hawaiian montane forests. Ecology 82, 3182–3196.
Silver, W., Liptzin, D., Almaraz, M., in press. Soil redox dynamics and biogeochemistry along a tropical elevation gradient, in: Ecological Gradient Analyses in a Tropical Ecosystem, Ecological Bulletins. Oikos.
Silver, W.L., Lugo, A.E., Keller, M., 1999. Soil oxygen availability and biogeochemistry along rainfall and topographic gradients in upland wet tropical forest soils. Biogeochemistry 44, 301–328.
Sinsabaugh, R.L., 2010. Phenol oxidase, peroxidase and organic matter dynamics of soil. Soil Biology & Biochemistry 42, 391–404.
Sinsabaugh, R.L., Lauber, C.L., Weintraub, M.N., Ahmed, B., Allison, S.D., Crenshaw, C., Contosta, A.R., Cusack, D., Frey, S., Gallo, M.E., Gartner, T., Hobbie, S., Holland, K., Keeler, B., Powers, J., Stursova, M., Takacs-Vesbach, C., Waldrop, M., Wallenstein, M., Zak, D., Zeglin, L., 2008. Stoichiometry of soil enzyme activity at global scale. Ecology Letters 11, 1–13.
Skyllberg, U., Borggaard, O.K., 1998. Proton surface charge determination in Spodosol horizons with organically bound aluminum. Geochimica et Cosmochimica Acta 62, 1677–1689.
Stursova, M., Sinsabaugh, R.L., 2008. Stabilization of oxidative enzymes in desert soil may limit organic matter accumulation. Soil Biology and Biochemistry 40, 550–553.
Thevenot, M., Dignac, M.-F., Rumpel, C., 2010. Fate of lignins in soils: A review. Soil Biology and Biochemistry 42, 1200–1211.
Thompson, A., Chadwick, O.A., Boman, S., Chorover, J., 2006. Colloid mobilization during soil iron redox oscillations. Environmental Science & Technology 40, 5743–5749.
Thompson, A., Chadwick, O.A., Rancourt, D.G., Chorover, J., 2006. Iron-oxide crystallinity increases during soil redox oscillations. Geochimica et Cosmochimica Acta 70, 1710–1727.
Viollier, E., Inglett, P., Hunter, K., Roychoudhury, A., van Cappellen, P., 2000. The ferrozine method revisited: Fe(II)/Fe(III) determination in natural waters. Applied Geochemistry 15, 785–790.
White, A.F., Blum, A.E., Schulz, M.S., Vivit, D.V., Stonestrom, D.A., Larsen, M., Murphy, S.F., Eberl, D., 1998. Chemical weathering in a tropical watershed, Luquillo Mountains, Puerto Rico: I. Long-term versus short-term weathering fluxes. Geochimica et Cosmochimica Acta 62, 209–226.
Wood, P., 1994. Pathways for production of Fenton's reagent by wood-rotting fungi. FEMS Microbiology Reviews 13, 313–320.
Zimmerman, A., Chorover, J., Goyne, K., Brantley, S.L., 2004. Protection of mesopore-adsorbed organic matter from enzymatic degradation. Environmental Science and Technology 38, 4542–4548.

Tables

Table 1: Characteristics of soil sampling sites. Soil O_2 concentrations were based on bi-weekly measurements of buried headspace equilibration chambers at 10 cm depth over 2 years from the ridge, slope, valley, and cloud forests. Measurements of O_2 in the colorado forest were made quasi-continuously over 16 months using a buried sensor.

Site	N (°)	W (°)	Elevation (m)	Precipitation (m)	Cumulative $O_2 < 3$ (%)	Cumulative $O_2 < 20$ (%)	Mean O_2 (%)
Ridge	18.316	65.749	240	3500	0.2	0.2	19
Slope	18.316	65.749	230	3500	2.9	18.9	16
Valley	18.316	65.749	220	3500	15.7	48.9	10
Colorado	18.282	65.790	680	4200	0	0	17.5
Cloud	18.294	65.785	936	5000	25.0	68.0	8

Figures

Figure 1**:** Phenol oxidative activity (in terms of μmol DOPA oxidation g soil^{-1} hr^{-1}) and Fe(II) concentrations in soil subsamples from five humid tropical forest sites in the Luquillo Experimental Forest, Puerto Rico (a). Phenol oxidative activity generated by Fe(II) solutions in the absence of soil (b).

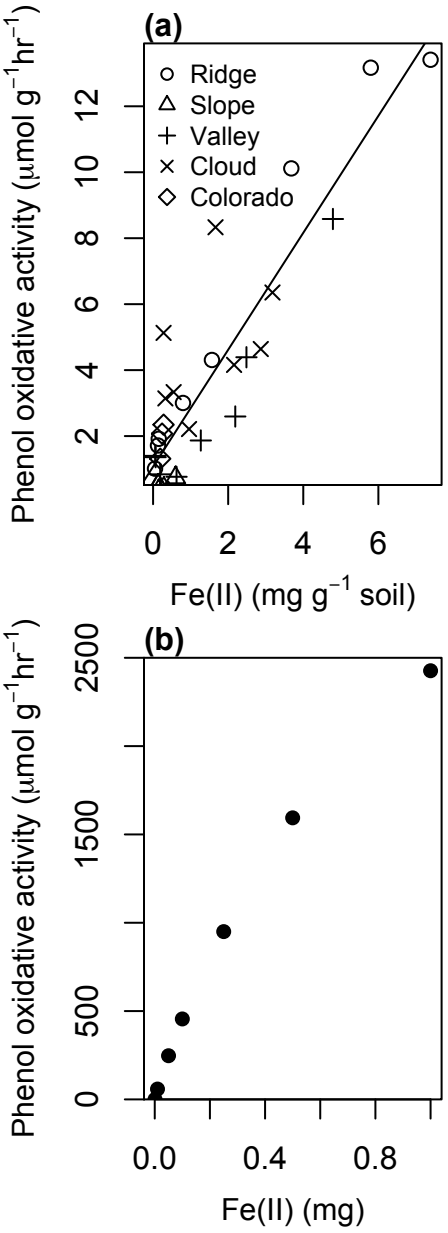

Figure 2: Net H_2O_2 production in lower montane ridge soil subsamples with differing Fe(II) concentrations (a), or amended with aqueous Fe(II) at varying concentrations (b). The relative recovery of H_2O_2 standards added to soil slurries with varying Fe(II) concentrations is shown in panel (c).

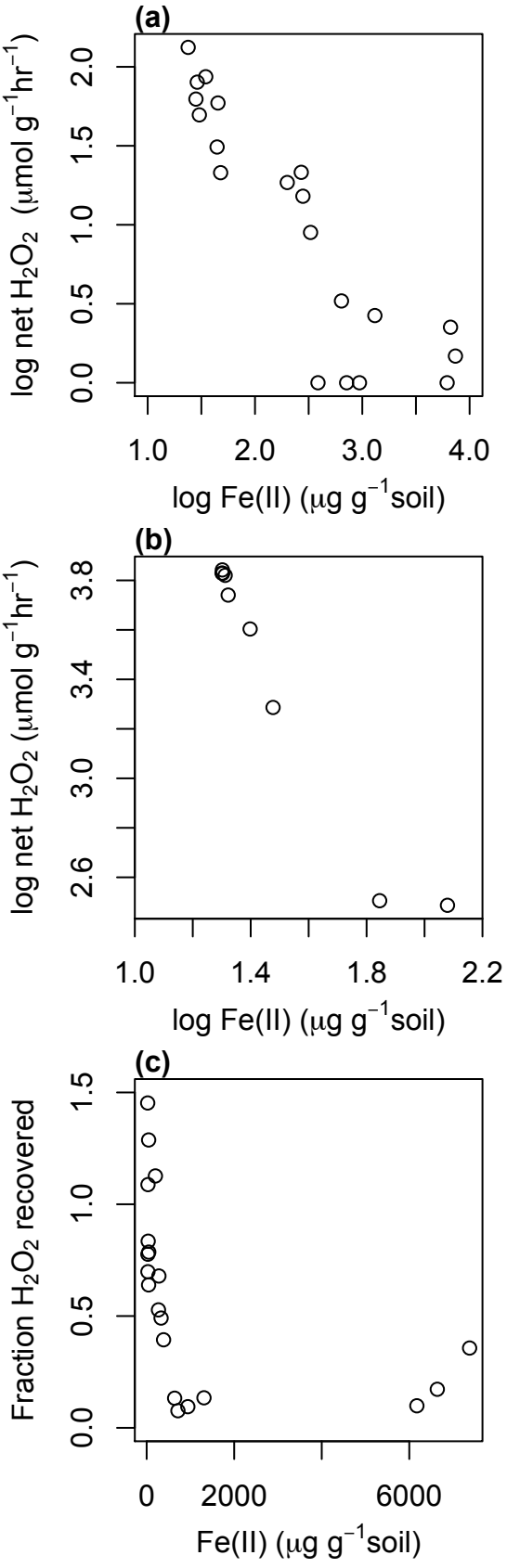

Figure 3: Mean (± SE) CO_2 production from soils amended with $FeCl_2$ and NaCl under aerobic (a) and anaerobic conditions (N_2 headspace) (b). Error bars are smaller than symbols where absent. Relationships between declines in Fe(II) over the 24-hour incubation and increases in HCl-extractable Fe(III) under aerobic (c) and anaerobic conditions (d). Relationships between declines in Fe(II) and CO_2 production under aerobic (e), and anaerobic conditions (f).

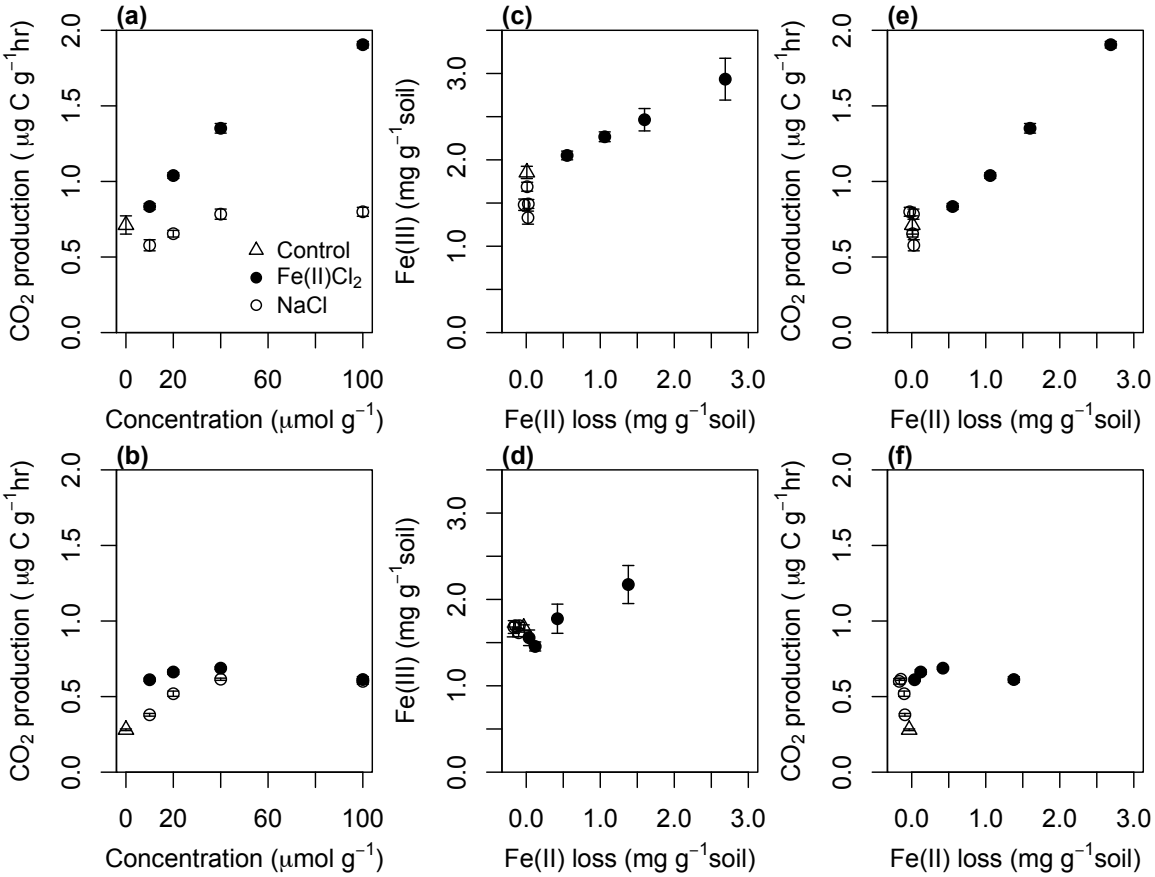

Figure 4: Production of CO_2 in soils amended with $FeCl_2$ or HCl under aerobic conditions plotted against soil pH after 24 hours (a). Relationships between pH and soluble organic C extracted in 2M KCl from control and HCl-amended soils (b). Production of CO_2 from soil slurries buffered at pH 5 in 2M sodium acetate and MES after amendment with $FeCl_2$, plotted against the change in Fe(II) concentrations (c). The controls showed net Fe reduction over the 24-hour incubation.

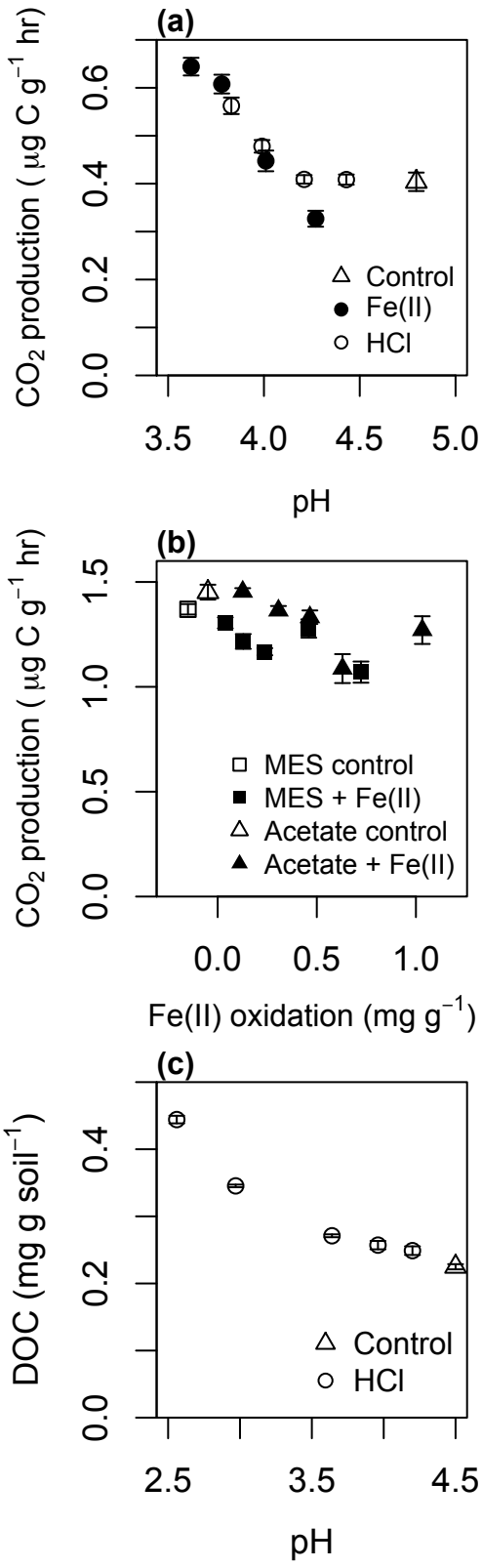

Chapter Four:

Ecosystem drivers of soil C across a humid tropical landscape

Abstract

The stabilization of soil carbon (C) by reactive minerals and an inhibition of decomposition due to oxygen (O_2) limitation (reducing conditions) have been proposed as drivers of the high soil C concentrations characteristic of humid tropical forests, which constitute a major terrestrial C reservoir. Here, we examined relationships between these factors and spatial patterns of C concentrations and C turnover (using radiocarbon modeling) in surface soils of the Luquillo Experimental Forest, Puerto Rico. We used concentrations of reduced iron (Fe(II)) as an index of reducing conditions given the importance of Fe reduction to anaerobic metabolism in these soils. Concentrations of Fe(II), reactive iron and aluminum (Al) minerals, interactions between Fe(II) and Al, and live fine root biomass explained most variation in C concentrations (pseudo $R^2 = 0.84$). Carbon increased with poorly crystalline Fe, in agreement with previous research, but C decreased with citrate/ascorbate extractable Fe, an index of Fe oxides susceptible to microbial reduction. We suggest that availability of Fe oxides to sustain anaerobic respiration partially attenuates soil C accumulation in these ecosystems, despite the role of a subset of reactive Fe in promoting C stabilization. Decomposition rates of mineral-associated C estimated using ^{14}C content increased with Fe(II) in soils with near-atmospheric O_2 concentrations. We propose that Fe redox cycling in soil microsites is associated with increased turnover of mineral-associated C. Our results imply a multifaceted role of reactive minerals in soil C cycling that emphasizes the importance of ecosystem-scale interactions among geochemical, physical, and biological factors.

Introduction

Hans Jenny (1941, 1950) first posed the "organic-matter problem of the tropics" as a matter of explaining how humid tropical forest soils retain high C stocks in spite of the rapid rates of litter decomposition characteristic of this biome. Jenny suggested that a disjunct between fast decomposition of surface litter and slower decomposition of organic matter in mineral soil horizons was responsible for maintaining the large soil C stock in humid tropical ecosystems (ibid). Identifying the factors underlying the distribution of soil C in humid tropical forests, the mechanisms driving C stabilization, and their response to global climate change represent an important research challenge given the large soil C stock that they support (~ 500 Pg), their rapid decomposition rates, and a lack of biogeochemical data relative to temperate soils (Jobbagy and Jackson, 2000; Parton et al., 2007).

Numerous studies have demonstrated the importance of reactive aluminum (Al) and iron (Fe) minerals in protecting organic matter from microbial decomposition via sorption and complexation reactions (Oades, 1988; Baldock and Skjemstad, 2000; Kaiser and Guggenberger, 2000; Wagai and Mayer, 2007). Accordingly, increasing concentrations of "poorly crystalline" or short range-order Al and Fe measured in chemical extractions have often correlated with decreased rates of decomposition and increased C concentrations across a broad spectrum of temperate and tropical ecosystems (Torn et al., 1997; Kleber et al., 2005; Bruun et al., 2010).

Another potentially important mechanism of C stabilization that has received less attention, especially in upland humid tropical forests, concerns the influence of oxygen (O_2) availability on decomposition. Anaerobic conditions have long been identified as an important constraint on organic matter decomposition leading to C accumulation in wetland ecosystems (Ponnamperuma, 1972). Periodic or chronic O_2 limitation can also occur in non-flooded soils in upland humid tropical ecosystems, which are characterized by abundant rainfall, high clay content, and elevated respiration rates (Silver et al., 1999; Cleveland et al., 2010; Liptzin et al., 2011). Soil C stocks increased monotonically as redox potential declined across a precipitation gradient in Hawaii, suggesting that reducing conditions promoted soil C accumulation in these humid tropical forests (Schuur et al., 2001). However, mechanisms driving patterns in soil C concentrations are complex (Schmidt et al., 2011), and include factors that control plant C inputs (Fisher et al., 1994; Alvarez and Lavado, 1998; Powers and Schlesinger, 2002) in addition to those that affect C losses. Few studies have employed a multi-factor approach to determine controls on C storage and loss in humid tropical ecosystems (Schuur et al., 2001; Powers and Schlesinger, 2002; Koning et al., 2003; Tonneijck et al., 2010).

The impact of reducing conditions on soil C storage is likely dependent on a suite of additional variables, especially those involving Fe mineralogy. Although reducing conditions constrain the decomposition of specific compounds such as high molecular-weight lignin (Zeikus et al., 1982), a large proportion of litter can be degraded anaerobically (Kristensen et al., 1995), a process which can be hastened in the presence of thermodynamically favorable electron acceptors such as reactive Fe oxides (Sutton-Grier et al., 2011; DeAngelis et al., 2012). Iron reduction mediated by direct C oxidation or via organic electron shuttling compounds drives high rates of anaerobic microbial respiration in humid tropical soils (Peretyazhko and Sposito, 2005; Chacon et al., 2006; Thompson, Chadwick, Rancourt, et al., 2006; Dubinsky et al., 2010). Furthermore, Fe-reducing bacteria can mediate the complete decomposition of aromatic compounds to CO_2, whereas other anaerobic microbes apparently cannot (Lovley, 1995). Thus, the presence of high concentrations of reactive Fe oxides available to support respiration could increase decomposition rates relative to anaerobic soils that are dependent on terminal electron accepting processes with lower free energy yield, such as methanogenesis. In support of this hypothesis, the addition of ferric Fe (Fe(III)) stimulated anaerobic respiration during long-term incubations of marsh sediments, and in microbial cultures derived from rain forest soils (Sutton-Grier et al., 2011; DeAngelis et al., 2012). The redox cycling (sequential reduction and oxidation) of Fe could also affect decomposition rates indirectly via multiple additional mechanisms. The reduction and oxidation of Fe can both stimulate C solubilization and microbial respiration via changes in pH, and Fe oxidation can produce reactive oxygen species that contribute to organic matter oxidation (Thompson, Chadwick, Boman, et al., 2006; Hall and Silver, 2013). Thus, Fe oxides could play multiple and potentially opposing roles in the soil C cycle given their potential to catalyze anaerobic respiration as well as their potential to sorb and precipitate C. The relative importance of Fe oxides in promoting C stabilization via sorption or precipitation reactions versus their catalytic role in anaerobic decomposition has not yet been examined. These multiple functions could help explain the distinct relationships—positive, negative, and neutral—reported between reactive Fe measured in different soil extractions and C concentrations in different humid tropical ecosystems (Powers and Schlesinger, 2002; Koning et al., 2003; Powers and Veldkamp, 2005; Tonneijck et al., 2010). Ultimately, a prevalence of reducing conditions over pedogenic timescales can lead to a relative depletion of Fe oxides via

reductive dissolution and leaching (Thompson et al., 2011), potentially leading to an overall decline in anaerobic respiration rates and affecting soil C concentrations.

Litter fluxes to soils also potentially influence patterns of C storage, in addition to the abiotic and biotic factors that contribute to soil C stabilization and decomposition. Fine root biomass is thought to provide a dominant input to the soil C pool (Rasse et al., 2005), and thus as a first approximation we might expect soil C concentrations to scale with fine root biomass. Although fine root biomass is not a particularly strong proxy for productivity, it does provide an index of root C inputs at the scale of an individual soil sample, especially within sites containing similar vegetation or plant functional types. Furthermore, fine roots can be assayed at the same fine spatial scales as soil chemical characteristics, a task which is difficult to accomplish for above-ground litter inputs. Nevertheless, few studies of fine roots have been conducted with sufficient replication or at spatial scales appropriate to assess relationships with soil C within ecosystems (Vogt et al., 1996).

Here, we sought to determine the relative importance of multiple proposed drivers of soil C storage and turnover across a humid tropical landscape. We assessed relationships among soil C concentrations and stocks and indices of geochemical, redox, and plant characteristics, using samples collected across topographic zones and forest types that vary in redox dynamics. We sought to address the relative importance of reactive soil minerals and reducing conditions in protecting soil C from decomposition, and the potential dual role of Fe oxides in protecting soil C and sustaining anaerobic respiration. We used a density fractionation procedure on a subset of soil samples and measured the ^{14}C content of mineral-associated organic matter to explore relationships between C residence time and these biogeochemical drivers. Radiocarbon (^{14}C) measurements of soil organic matter provide a promising method to assess the impact of ecosystem variables on C turnover, but relatively few data have been collected in humid tropical forests (Trumbore et al., 1995; Torn et al., 1997; de Camargo et al., 1999; Telles et al., 2003; Marin-Spiotta et al., 2008).

Methods

Site description

We sampled soils from forested sites in the Luquillo Experimental Forest, Puerto Rico, an NSF-funded Long Term Ecological Research and Critical Zone Observatory site. We intensively sampled catenas in a lower montane (200 – 300 masl) tabonuco (*Dacryodes excelsa*) forest in the Bisley watershed. We also sampled higher-elevation montane forests dominated by palm (*Prestoea montana*), colorado (*Cyrilla racemiflora*) and elfin vegetation (*Tabebuia rigida*), at 610, 740, and 940 masl, respectively. Sites are further described by McDowell et al. (2012). The lower montane and palm forest soils are derived from volcanoclastic parent material, whereas the colorado and elfin forest soils were formed from quartz diorite and/or contact metamorphic rocks. These sites represent a gradient in soil O_2 concentrations, which were previously measured in buried equilibration chambers at 10 cm depth over a multi-year study (Silver et al., 1999). Mean soil O_2 concentrations decrease from ridges to slopes to riparian valleys in the lower montane forest (19, 16, and 10 % O_2, respectively), and decrease further from palm to colorado to cloud forests along the montane elevation gradient (10 – 8 % O_2)

(Silver et al., in press, 1999). Soil is not a uniform medium and thus measurable O_2 in the soil atmosphere does not preclude the presence of anaerobic microsites (Sexstone et al., 1985). Given that Fe oxides represent the most abundant anaerobic terminal electron acceptor in these soils, we used measurements of soil Fe redox speciation (described below) to provide an index of reducing conditions. We acknowledge that soil Fe(II) concentrations constitute a one-time measurement in a temporally dynamic redox environment, but indices of redox status among plots differed consistently over time (Hall et al., 2013), and are often strongly correlated with integrative indices of microbial function such as potential extracellular enzyme activity (Hall et al., in review).

Soil sampling and analysis

In the lower montane forest, we sampled four catenas in June 2011 each consisting of a ridge, slope, and riparian valley (sensu *Scatena and Lugo*, (1995)). We established five 0.25-m^2 plots in each topographic zone in each catena, which were randomly situated within 5 – 10-m intervals along a 50 m linear transect. We similarly sampled five plots on transects in each of the three montane forest sites in February 2012, yielding a total of 119 samples from the lower montane forest (rocks prevented collection of one sample) and 30 from the montane forest sites (total n = 149). In each plot, we collected four replicate 6-cm diameter soil cores at depths of 0 – 10 cm and 10 – 20 cm; these increments contain the majority of roots and organic matter in these ecosystems (Odum, 1970; Silver et al., 1994). Soil depth varies significantly among topographic positions and forest types, and often does not exceed 20 cm in riparian valleys. Thus, we sampled common depth intervals that were present in all sites to focus on mechanisms driving surface soil C.

Two cores from each depth were immediately composited and homogenized, and separate subsamples were extracted in solutions of 0.5 M hydrochloric acid (HCl) and 0.2 M sodium citrate/0.05M ascorbic acid solutions in the field within 1 - 2 min of sampling. The HCl extraction solubilizes adsorbed and solid phase Fe(II), including siderite and green rust, but not magnetite (Fredrickson et al., 1998), and also dissolves a reactive fraction of Fe(III) minerals. The low pH of the HCl extraction inhibits oxidation of Fe(II) prior to analysis. Soil subsamples (3 g dry mass equivalent) were immersed in a 1:10 ratio of soil to HCl, vortexed, shaken for 1 hour, and filtered to 0.22 μm. We measured concentrations of Fe(II) and Fe(III) in the HCl extraction colorimetrically using a ferrozine assay that corrected for Fe(III) interference (Viollier et al., 2000). We subsequently used Fe(II) concentrations and the ratio of Fe(II) to total Fe in the HCl extraction ($Fe(II)/Fe_{HCl}$) as indices of reducing conditions, given that Fe reduction represents the dominant anaerobic respiratory process in this system (Dubinsky et al., 2010), and that Fe(II) oxidizes in the presence of O_2. The second index reflects the proportion of the Fe_{HCl} pool that is reduced, thus accounting for differences in the total Fe_{HCl} pool among samples.

We extracted soils with sodium citrate/ascorbate solution following the protocol of Reyes and Torrent (1997) to provide an estimate of reducible Fe oxides (Fe_{ca}) and associated Al (Al_{ca}). This assay reductively dissolves Fe oxides in direct proportion to the pool that is potentially reducible by microbes (Hyacinthe et al., 2006). Soil subsamples (1.5 g dry mass equivalent) were immersed in the field in a 1:30 ratio of soil to citrate/ascorbate solution, vortexed, shaken for 18

hr, and centrifuged for 10 min at 1500 rcf. We also extracted soils with acid ammonium oxalate solution using the method of Loeppert and Inskeep (1996) (omitting the carbonate removal step, as carbonates are negligible in these soils) to provide a separate index of reactive Fe and Al (Fe_{ox} and Al_{ox}), which were defined as "poorly crystalline" pools in previous soil C studies (Torn et al., 1997; Kleber et al., 2005). This extractant likely solubilizes a different Fe pool than the citrate/ascorbate solution given that it involves a different chemical mechanism, chelation, as opposed to reductive dissolution. We used air dried as opposed to moist samples for this extraction for best comparison with previously published results, and because the oxalate solution can extract crystalline Fe in the presence of Fe(II) (Phillips et al., 1993). Roots and coarse organic matter were removed, soils were air dried and ground, and 0.5 g subsamples were extracted for 2 hr in 30 ml of ammonium oxalate solution. Air-dried subsamples were also extracted with sodium citrate/dithionite (CD) solution (Loeppert and Inskeep, 1996) to measure crystalline Fe oxides, calculated as the difference between citrate/dithionite and citrate/ascorbate extractions (Fe_{cd-ca}). Dithionite is a stronger reductant than ascorbate and dissolves crystalline Fe minerals such as goethite and hematite. For all of the above extractions, concentrations of Fe and Al were analyzed in triplicate using an inductively-coupled plasma optical emission spectrometer (ICP-OES; Perkin Elmer Optima 5300 DV, Waltham, Massachusetts) at UC Berkeley. Concentrations of Fe_{HCl} determined separately using the ferrozine method and ICP-OES agreed to within 1%. Additional soil subsamples were analyzed in duplicate for total C and N by combustion on a CE Elantech elemental analyzer (Lakewood, NJ); replicates differed by an average of 2%.

Additional field-moist replicate subsamples were analyzed for texture following the Gee and Bauder (1986) hydrometer method. We analyzed texture on moist soils to avoid artifacts in the particle size distribution generated by drying and rewetting these soils, which form a massive structure under air-dry conditions. Briefly, 50 g samples (dry mass equivalent) were sieved to 2 mm and soaked overnight in sodium hexametaphosphate solution (50 g l^{-1}) to chemically disperse aggregates, which were then physically dispersed in an electric mixer. We measured changes in suspension density over 24 hours to calculate the fractions of clay, sand, and silt.

We assayed the two remaining replicate 6 cm diameter cores from each plot and depth increment for fine root biomass and bulk density, respectively. Fine roots (< 2 mm diameter) were separated from soil by wet sieving and separated into live and dead fractions based on visual observations of turgor, tensile strength, and integrity of the stele tissue [*Silver and Vogt*, 1993]. All roots were thoroughly washed in deionized water and dried at 65°C to constant mass. To determine bulk density from the intact cores, we carefully removed any coarse roots and rocks (which were rare) after cleaning them to retain all soil. We estimated the volume of coarse roots > 5 mm by calculating a cylindrical approximation using their length and diameter, and measured the volumetric water displacement of rocks with diameter > 2 mm; these corrections affected our bulk density calculations by only 2 %, on average. Soils were dried at 105° C to constant mass, and bulk density was calculated as dry soil mass divided by coarse root and rock-corrected sample volume.

Soil density fractionation

For C density fractionation, we collected 30 additional soil samples at 0 – 10 and 10 – 20 cm depths from each of 15 plots along one ridge-slope-valley catena in the lower montane forest,

as described above, in February 2012. Subsamples of these soil cores were extracted in the field with 0.5 M HCl and citrate/ascorbate solution for determination of Fe(II), $Fe(III)_{HCl}$, Fe_{ca}, and Al_{ca} as described above, and air-dried subsamples were extracted with ammonium oxalate. Additional samples from these plots were collected in May 2012 for Fe(II) analysis to further evaluate the consistency of spatial patterns. We separated soil organic matter into three operationally-defined fractions: (1) a free light fraction consisting of low-density (< 1.85 g cm^{-3}) organic matter not contained within aggregates, (2) an occluded light fraction, comprising low-density organic matter released from aggregates following sonication, and (3) a heavy fraction with density > 1.85 g cm^{-3} associated with soil minerals. Samples for density fractionation were stored at field moisture in sealed polyethylene bags at 3° C and analyzed within 6 months of collection. The fractionation assay followed the protocol of Swanston et al. (2005) as modified for tropical soils by Marin-Spiotta et al. (2008). Briefly, we passed moist samples (20 g dry mass equivalent) through a 4.75 mm sieve to remove coarse litter fragments while maintaining aggregate structure. The free light fraction was separated by flotation after immersing soils in sodium polytungstate at a density of 1.85 g cm^{-3}. The occluded light fraction was similarly obtained after mixing and sonicating soils to disrupt aggregates. The heavy fraction consisted of the remaining mineral-associated organic matter. Density fractions were analyzed in duplicate for C concentrations and $\delta^{13}C$ isotopic ratios relative to V-PDB on a Vario Micro elemental analyzer in-line with an Isoprime 100 isotope ratio mass spectrometer (Elementar, Hanau, Germany) at UC Berkeley. Carbon concentrations measured on the Vario instrument were in excellent agreement with additional replicates analyzed on the CE Elantech instrument described earlier (R^2 = 0.996, slope = 1.0006).

Radiocarbon measurements and modeling

We measured the radiocarbon content of heavy fraction samples on the Van de Graaff FN accelerator mass spectrometer at the Center for Accelerator Mass Spectrometry at Lawrence Livermore National Laboratory, Livermore CA. Mineral-associated C fractions were subsampled into 9 mm diameter quartz tubes which were then evacuated, flame-sealed, and combusted in the presence of copper oxide and silver. Resulting CO_2 was reduced to graphite on iron powder in the presence of H_2 at 570 °C (Vogel et al., 1984). Corrections were applied for mass-dependent fractionation using measured $\delta^{13}C$, for sample preparation background using ^{14}C-free coal, and for ^{14}C decay since 1950; final radiocarbon values are reported in $\Delta^{14}C$ notation with an average precision of 3 ‰ (Stuiver and Polach, 1977).

We modeled the residence time of mineral-associated C using a time-dependent steady-state difference equation model of soil ^{14}C dynamics in conjunction with the atmospheric ^{14}C record (Trumbore, 1993; Torn et al., 2009). Under the simplifying assumption that C decomposes according to first order kinetics, the inverse of the modeled decomposition rate constant represents the mean residence time of soil C. We assumed that the ^{14}C content of soil organic matter in a given year is a function of the ^{14}C from the previous year, plus additions from recently-fixed C with an atmospheric ^{14}C signature, minus losses from decomposition and radioactive decay, represented by the following equation (Torn et al., 2009):

$$F'_{soil,t} = kF'_{atm,t} + F'_{soil,t-1}(1 - k - \lambda)$$

Here, F' equals $\Delta^{14}C/1000 + 1$ of the soil or atmospheric pools at time t, k is the decomposition rate constant, and λ is the radioactive decay constant. We used a time series of atmospheric ^{14}C measurements from 1511 – 1950 (Stuiver et al., 1998) and 1950 – 2009 (Hua et al., 2013) for atmospheric zone 2, which includes Puerto Rico, and assumed a 5 per mil annual decline in atmospheric $\Delta^{14}C$ from 2010 – 12 (ibid). We then calculated soil ^{14}C content at an annual timestep using the above difference equation and iteratively adjusted k until the modeled value of soil $\Delta^{14}C$ matched our measured value. Representative temporal trends in soil and atmospheric $\Delta^{14}C$ are given in Supplemental Figure 1. A caveat of this modeling approach is that samples with significant incorporation of bomb ^{14}C yield two potential residence times—a shorter (years to decades) and longer (decades to centuries) solution—as a consequence of the temporal trend in atmospheric $\Delta^{14}C$ over the 20th century. We assumed that the longer residence time was most realistic for all of our samples based on the assumptions of C inputs to the mineral-associated C pool implied by these residence times. A residence time of 10 years, for example, implies an input of approximately 700 g C m^{-3} to the mineral-associated C pool in the 0 – 20 cm depth increment. This annual C input to the mineral-associated C fraction appears unrealistically large in light of the fact that litterfall NPP is approximately 900 g C m^{-3} and root productivity is likely no greater than litterfall NPP. Addition of such a large portion of NPP to the mineral C fraction conflicts with the assumptions of ecosystem models (Parton et al., 1993). Thus, our modeling approach implied a monotonic decreasing relationship between measured $\Delta^{14}C$ and the C residence time (Supplementary Figure 1). The modeled residence time of soil C represents a maximum estimate given that atmospheric C might not enter the soil during the same year that it is fixed via photosynthesis, and represents the residence time of C in the plant/soil system in the case of multiple year lags.

Statistical Analysis

We compared trends in means of soil C concentrations, content and other biogeochemical variables across sites with linear models where variances were allowed to vary among sites, using the gls function in R (Pinheiro et al., 2011). Site means were compared using Tukey's honestly significant difference test. Relationships between soil C concentrations, soil C stocks, and predictor variables were analyzed using linear mixed effects models fit using the lmer function in R (Bates et al., 2012). Models included transects, plots, and depth x transect interactions as potential random effects to account for the spatial structure of our sampling design. We selected the optimal random effect structure by comparing the Akaike information criterion (AIC) of models fit using restricted maximum likelihood that included all potential fixed effects shown in Table 2. Variables were normalized by mean and standard deviation to allow comparison of the relative importance of response variables (a normalized model coefficient of 0.5 implies that varying a predictor variable by one standard deviation yields a change of 0.5 standard deviations in the response variable). We selected the optimum models (fit using maximum likelihood) using backwards selection and AIC with a correction for small sample size (AICc). We also included a potential predictor variable for the possible interaction between Al_{ca} and $Fe(II)/Fe_{HCl}$. We fit models for three datasets: the lower montane soils (n = 119), given that they comprised the majority of our samples and experience a relatively uniform climate, the lower montane and the montane soils together (n = 149), and the mineral-associated C fractions from the lower montane forest (n = 30). Two outliers with extremely high Fe(II) concentrations or fine root biomass, respectively, were excluded from the analysis, as were two

samples with missing values for root biomass. We used an analogous approach to model relationships between C turnover times and predictor variables. We present marginal pseudo-R^2 values, which reflect the model variance explained by fixed effects relative to the total model variance (Nakagawa and Schielzeth, 2013).

Results

Landscape patterns in soil C and covariates

Soil C concentrations were heterogeneous across the landscape, varying between 1.3 – 9.9 and 3.7 – 21.6 % in the lower montane and montane soils, respectively, while C stocks varied between 11 – 45.5 and 13.5 – 107 mg cm^{-3}, respectively. Mean C concentrations differed among sites and topographic positions, but did not directly scale with differences in long-term bulk soil O_2 among sites (Fig. 1a). Surface (0 – 10 cm) C concentrations significantly decreased from ridges to valleys in the lower montane forest soils, were greatest in the palm and elfin forests, and intermediate in the colorado forest; pairwise statistical comparisons are given in Table S1. Subsurface (10 – 20 cm) C concentrations were similar among ridges, slopes, and valleys in the lower montane forest and significantly greater in the palm, colorado, and elfin forests (Fig. 1b). Soil C stocks from 0 – 10 cm, in contrast, were similar among all sites with the exception of the elfin forest, but showed an increasing trend from the lower montane, to the palm, colorado, and elfin forest in 10 – 20 cm soil. Bulk density in 0 – 10 cm soil differed by a factor of three among sites, and was greatest in the lower montane valleys and lowest in the palm forest (Fig. 1c). Bulk density of the 10 – 20 cm depth, in contrast, was much less variable and did not differ significantly among sites. Live fine root biomass significantly declined by a factor of two from ridges to valleys in 0 – 10 cm soil, was greatest in the palm and elfin forests, and was generally similar among sites in 10 – 20 cm soil (Fig. 1d). Dead fine root biomass was more than four-fold greater in the elfin forest than the other sites. The C/N ratio of live fine root biomass was lowest in the valley and palm sites but showed no consistent trend across the site O_2 gradient (Fig. 1e).

Soil Fe pools differed greatly among sites (Fig. 2a,b). Concentrations of Fe(II) increased by more than five-fold between the lower montane sites and the elfin forest, while the palm and colorado sites had intermediate and highly variable Fe(II) concentrations. Trends in the $Fe(II)/Fe_{HCl}$ ratio across sites were similar to those of Fe(II), with fewer significant differences among sites (Supplemental Table 1). Crystalline Fe oxides ($Fe_{cd\text{-}ca}$) decreased more than two-fold from lower montane slopes to ridges to valleys, which were similar to the palm and colorado sites, and $Fe_{cd\text{-}ca}$ was essentially absent in the elfin site. Microbially-reducible Fe (Fe_{ca}) was greatest in the lower montane ridges and smallest in the colorado site. Trends across sites in Fe_{ox}, in contrast, bore little resemblance to those of Fe_{ca} (Fig. 2c). Concentrations of Fe_{ox} and Fe_{ca} were similar in the palm and elfin forests, but Fe_{ox} was 30 – 60 % lower than Fe_{ca} in the other sites. Trends in Al_{ca} among sites were distinct from those of Fe_{ca} and concentrations were more variable within sites, with significantly lower concentrations in the lower montane valleys relative to the other sites (Fig. 2d).

Topographic variation in C density fractions and modeled turnover times

Mineral-associated C comprised the dominant fraction in the lower montane forest, representing 88, 87, and 78 % of total soil C in the ridge, slope, and valley soils, respectively (Table 3, Figure 3). Ridge soils had significantly greater mineral-associated C concentrations than valleys in 0 – 10 cm soil, whereas C stocks were similar among landscape positions due to differences in bulk density. Valley soils had significantly greater C concentrations and stocks in the occluded light fraction than did the ridge and slope soils in 10 – 20 cm soil. Free light C did not differ among positions. Modeled residence times based on the $\Delta^{14}C$ content of mineral-associated C varied between 67 – 298 years for individual soil samples. Mean residence times were similar among topographic positions in 0 – 10 cm soil, but differed between the valley 10 – 20 cm soil (94 ± 4 yr) and the 10 – 20 slope soil (195 ± 35 yr, $p < 0.05$, Table 3).

Statistical models of soil C and residence times

The optimum statistical models describing patterns in soil C concentrations were fairly similar for the lower montane forest soils and for the entire data set; model fixed effects could account for most of the variation in soil C (pseudo $R^2 = 0.75$ and 0.84, respectively). Carbon concentrations in the lower montane forest increased with Al_{ca}, live fine roots, Fe_{ox}, the redox indicator $Fe(II)/Fe_{HCl}$, $Fe(III)_{HCl}$, and the interaction between $Fe(II)/Fe_{HCl}$ and Al_{ca}, and decreased with Fe_{ca} and $Fe_{cd\text{-}ca}$ (Table 4, Figure 4). Estimated correlations between fixed effect coefficients were all < 0.5. The model for lower montane and montane soils together also included a relationship between C and depth, but did not include crystalline Fe oxides ($Fe_{cd\text{-}ca}$). Including the C/N ratio of live fine root biomass as a predictor variable improved model fit (live root C/N showed a weak negative relationship with soil C), but as live fine roots were not present in 10 samples we omitted this variable from the final model to maximize use of all collected data. Including clay or sand content did not improve the fit of any model.

The model for mineral-associated C concentrations in the lower montane soils showed similar relationships to the model for bulk soil C. Mineral-associated C increased with Al_{ca}, live fine root biomass, and $Fe(III)_{HCl}$, and declined with Fe_{ca}. The optimum model for the residence time of mineral-associated C, however, included only one fixed effect predictor and no random effects. Residence times decreased with the log-transformed concentrations of soil Fe(II) (standardized regression coefficient = -0.57, $R^2 = 0.30$). Soil Fe(II) concentrations were similar in ridge and valley 0 – 10 cm soils over three different sampling events, but were significantly lower in slope 10 – 20 cm soil (Supplemental Figure 2).

Models of soil C stocks

Soil bulk density and C concentrations showed a strong negative correlation at the samples ($r = -0.73$, Figure 4) and catena scale in the lower montane forest soils. Thus, surface C stocks in ridge and valley soils were similar despite their differences in C concentrations, and the optimum model of soil C stocks for the lower montane soils contained fewer fixed effects and had much lower explanatory power (pseudo $R^2 = 0.18$) than the model for C concentrations (Table 5). Carbon stocks increased with Fe_{ox} and Al_{ca}, and decreased with Fe_{ca} and depth. The model of C stocks for the overall dataset, in contrast, had a much greater contribution from fixed effect predictors (pseudo $R^2 = 0.60$). Here, C stocks increased with $Fe(II)/Fe_{HCl}$, Fe_{ox}, an interaction between $Fe(II)/Fe_{HCl}$ and Al_{ca}, and decreased with Fe_{ca}.

Discussion

Landscape patterns in C and biogeochemical factors

Trends in mean soil C concentrations among sites did not directly parallel either our index of reducing conditions, concentrations of reactive Fe and Al, or root biomass, whereas our statistical models suggested the importance of additive and interactive relationships among these biogeochemical factors in controlling patterns of soil C. The Fe(II) concentrations that we measured, especially in the montane palm, colorado, and cloud forest sites, were similar to those measured in flooded wetland sediments and rice paddy soils under anaerobic conditions (Roden and Wetzel, 1996; Frenzel et al., 1999), confirming the prevalence of reducing conditions in soil microsites concomitant with the presence of measureable gas-phase O_2 in soil macropores (Silver et al., 1999). Reactive Fe and Al minerals were also abundant in our soils: concentrations of Fe_{ca} and Al_{ca} typically exceeded those reported by Reyes and Torrent [*1997*] and concentrations of Fe_{ox} were similar to those measured by Kleber et al. [*2005*] across a wide range of soils. Concentrations of reactive Al, however, were significantly lower than those measured in allophanic soils by Torn et al. [*1997*]. In these previous studies, either citrate/ascorbate or ammonium oxalate extractions have been used as indices of "poorly-crystalline" or nano-scale order Fe and Al (Reyes and Torrent, 1997; Kleber et al., 2005; Thompson et al., 2011). Differences in the concentrations of Fe and Al isolated by these extractions in our soils, their trends among sites, and their relationships with soil C suggest that they likely represent pools with qualitatively different characteristics and impacts on C cycling. Concentrations of Fe_{ca} exceeded Fe_{ox} by approximately a factor of two in the lower montane and palm soils, implying the presence of additional Fe vulnerable to microbe-catalyzed reductive dissolution that exceeded oxalate-extractable Fe. In the colorado and elfin forest soils, however, we found that Fe_{ca} and Fe_{ox} pools were approximately equivalent, suggesting they were extracting a similar pool of Fe. Crystalline Fe oxides ($Fe_{cd\text{-}ca}$) declined steeply across the site O_2 gradient and were essentially absent in the elfin forest, the site with the greatest prevalence of reducing conditions. This trend is consistent with the overall depletion of Fe due to reductive dissolution and leaching concomitant with an increased prevalence of reducing conditions, and a relative retention of increasingly reactive Fe pools (extractable with ammonium oxalate and 0.5 M HCl). These findings agree with landscape patterns in Fe across a rainfall gradient in Hawaii, where increased rainfall drove Fe loss concomitant with retention of metastable phases (Schuur et al., 2001; Thompson et al., 2011). Importantly, however, we did not find a similar trend in Al_{ca} with reducing conditions across our sites. Concentrations of Al_{ca} were the single best predictor of soil C concentrations, but these varied idiosyncratically across the O_2 gradient.

Our data suggest that an overall depletion of Fe oxides over pedogenic timescales coupled with the retention of reactive Fe and Al phases involved in C complexation may provide two important mechanisms for promoting C accumulation, especially in soils characterized by reducing conditions. Positive relationships between C and Fe_{ox} agree with previous research documenting correlations between oxalate-extractable minerals and C concentrations within and among ecosystems (Powers and Schlesinger, 2002; Kleber et al., 2005). However, we also found a negative relationship between C and microbially-reducible Fe (Fe_{ca}) that was consistent regardless of whether Fe_{ox} was included in the model. We propose that the role of reducible, short range-order Fe oxides in fueling anaerobic microbial respiration in humid tropical

ecosystems (Peretyazhko and Sposito, 2005; Thompson, Chadwick, Rancourt, et al., 2006; Dubinsky et al., 2010) can attenuate soil C accumulation where these minerals are abundant, despite the fact that a portion of short range-order Fe is demonstrably associated with C accumulation due to protective interactions (Kaiser and Guggenberger, 2000; Kleber et al., 2005). This "protective" Fe fraction has been defined operationally using ammonium oxalate extractions, and research in Hawaiian soils linked Fe_{ox} to nanoscale-ordered Fe oxides using Mössbauer spectroscopy (Thompson et al., 2011). Further work is needed to characterize the Fe minerals involved in C protection, and additional Fe fractions susceptible to reductive dissolution. We speculate that if the physical structure of Fe-organic complexes implicated in C protection (Wagai and Mayer, 2007) serves as a barrier to electron transfer, the Fe_{ox} pool might not be as readily accessible to Fe reducers or electron shuttles as the Fe_{ca} pool. Consistent with this hypothesis, Varela and Tien (2003) showed that high concentrations of organic ligands (oxalate) can inhibit Fe reduction.

A multivariate perspective on soil C

Earlier work focused separately on the importance of organo-mineral interactions (Torn et al., 1997; Powers and Schlesinger, 2002) and reducing conditions (Torn et al., 1997; Schuur et al., 2001) as controls on soil C concentrations in humid tropical forests. We found evidence for the combined and synergistic importance of both factors, in addition to fine root biomass. A mechanistic interpretation of the coefficients yielded by our statistical mixed-effects models implies that each of these variables had a similar effect on C concentrations. Our model also suggested a synergistic relationship between concentrations of reactive Al and reducing conditions, especially when considering samples from the lower montane and montane soils as a whole. This interaction might reflect enhanced protection of C due to sorption/complexation reactions with Al oxides in soils that experience an increasing prevalence of reducing conditions. This finding also might illustrate the importance of O_2 in disrupting these mineral/organic complexes, given that oxidative enzymes and reactive oxygen species are suppressed in the absence of O_2. Our measured variables were able to account for most variation in soil C in both the lower montane forest soils and for the lower montane and montane soils combined, with relatively small variation in model structure and coefficients between the two datasets. Thus, despite considerable diversity in soil forming factors within and among these sites (vegetation, topography, precipitation, parent material), the same biogeochemical factors appeared broadly relevant for controlling C concentrations. Our model poorly predicted C stocks on a soil volume basis in the lower montane forest, however, likely as a result of a strong inverse relationship between C concentrations and bulk density. This relationship is commonly observed in soils given that organic matter stimulates aggregate formation, generating an increasingly porous soil structure with lower bulk density (Saini, 1966). Increased bulk density in valley soils compensated for their decreased C concentrations relative to ridges, resulting in equivalent surface C stocks. Ridge soils are significantly deeper than valley soils in this ecosystem, however (Johnson et al., 2011), so our surface soil measurements did not capture C translocated to deeper horizons. Our overall model including all soils accounted for much more variation in C stocks, however, and was similar to the model of C concentrations. Thus, when considering our sites as a whole, the same biogeochemical mechanisms appeared broadly important for controlling surface soil C concentrations and stocks. A notable difference was the absence of fine root

biomass from the C stock model, suggesting the primacy of geochemical and physical factors in controlling C stocks as opposed to C concentrations.

Numerous studies have examined patterns of fine root biomass in humid tropical forests (Vogt et al., 1996; Espeleta and Clark, 2007), but few have examined relationships with soil C over small spatial scales. Our data confirms previous reports of positive pairwise relationships between fine root biomass and soil C concentrations within ecosystems (Alvarez and Lavado, 1998; Leff et al., 2012). It is notable that dead fine root biomass and total fine root biomass (live + dead) displayed weaker relationships with soil C than live fine root biomass. In the lower montane forest, variation in live fine root biomass could provide an index of C inputs from root production among soil samples, given their similar vegetation and climate. Interpretation of relationships with live fine root biomass becomes more complicated when comparing the montane sites with the lower montane sites. The upper elevation sites have significantly lower litterfall NPP, but higher live fine root biomass. High standing stocks of fine roots may reflect stresses such as nutrient limitation and do not necessarily indicate increased root production (Ostertag, 2001; Espeleta and Clark, 2007). A large stock of fine roots, however, could ultimately increase soil C by mechanisms irrespective of net productivity. Increasing the proportion of soil in close proximity to the rhizosphere, for example, facilitates the spatial association between C inputs, microbes, and mineral surfaces that are likely ultimately involved in C stabilization. We interpret positive relationships between live fine root biomass and C concentrations across our samples as an overall consequence of rhizosphere processes.

Distribution and residence times of mineral-associated C

A high proportion of soil C in the lower montane forest was contained in the mineral-associated soil fraction, consistent with previous studies in humid tropical forests (Marin-Spiotta et al., 2009; Cusack et al., 2011), and exceeded the proportion of mineral-associated C measured in a Brazilian forest soil (Trumbore, 1993). Intriguingly, mineral-associated C concentrations and bulk soil C were greatest on ridges, despite the fact that riparian valley soils experience significantly lower bulk soil O_2 concentrations (Silver et al., 1999). These data confirm topographic trends in bulk soil C documented in 1988 (Silver et al., 1994). Our statistical model implies that an increase in soil C on ridges could be explained by a combination of high concentrations of reactive Al, fine roots, and reducing conditions in soil microsites, which were all equivalent or greater in ridges than slopes or riparian valleys. Ridges are also dominated by *Dacryodes excelsa*, a species that forms dense root mats and tissue rich in secondary chemical defenses. Previous research in this ecosystem documented greater above-ground plant biomass and resistance to hurricane disturbance on ridges as opposed to slopes or valleys, which experience greater erosion rates and landslides (Scatena and Lugo, 1995), and thus may experience greater rates of C loss due to erosion.

The topographic distribution of mineral-associated C documented here contrasts with the traditional catena model of soil C, which predicts C accumulation in valleys as a consequence of erosion, clay accumulation, and an increased prevalence of reducing conditions (Berhe et al., 2007; Johnson et al., 2011). Our Fe(II) data, however, demonstrate that the prevalence of reducing microsites may in fact be equivalent in the ridge and valley soils despite their differences in bulk soil O_2—a pattern that was broadly consistent over three separate sampling

events. Equivalent Fe(II) concentrations in ridges and valleys were not likely explained by increased cation leaching in valley soils, given that other divalent cations such as calcium and magnesium accumulate in this landscape position (Hall et al. unpublished data) and infiltration rates are very low in valley soils relative to ridges and slopes (Harden and Scruggs, 2003). Possible relationships between bulk soil O_2 and C pool sizes were only evident in the occluded light fraction in 10 – 20 cm soil, where valley soils showed significant C accumulation relative to the ridge and slope. The topographic distribution of soil texture across this catena suggests that removal of clay-sized particles and associated organic matter from valley soils appear to exceed rates of clay deposition in this hydrologically open system (Hall et al., unpublished data). An increase in sand-sized particles in valleys could also reflect deposition during flood events (F. Scatena, personal communication). Thus, the presence of disturbance-resistant vegetation with dense root biomass could play an important role in the retention of clays and mineral-associated C on ridges in this ecosystem.

High concentrations of mineral-associated C, nevertheless, did not imply increased C residence times modeled using ^{14}C content. Mean residence times of mineral-associated C were equivalent across topographic positions in 0 – 10 cm soil and were similar to those measured in other humid tropical forest soils (Trumbore et al., 1995; de Camargo et al., 1999; Marin-Spiotta et al., 2008). Surprisingly, reactive Al and Fe concentrations were not positively correlated with decreased decomposition rates despite their apparent role in explaining increased C concentrations, suggesting that their impact on C stabilization might be ephemeral in these soils. This finding contrasts with data from Hawaii, where soil $\Delta^{14}C$ declined with non-crystalline mineral content, implying decreased decomposition rates (Torn et al., 1997). The discrepancy between these findings could be explained by differences in mineralogy between Hawaii and Puerto Rico (i.e. the lack of allophanic minerals derived from volcanic activity in the current study), or by climatic differences and the importance of dissimilatory Fe reduction as a metabolic process in our ecosystem. Here, the best predictor of mineral-associated C turnover time was a negative relationship with soil Fe(II) concentrations, an index of reducing conditions. Thus, reducing conditions were unexpectedly associated with increasing C turnover rates, despite the fact that they also correlated with increased C concentrations.

Complex relationships between C and reducing conditions are consistent with the importance of labile C as a driver of reducing conditions in relatively well-drained upland soils. Previous work in this ecosystem documented strong positive relationships between extracellular hydrolytic decomposition enzymes and Fe(II) concentrations, implicating patterns of microbial decomposition activity as an important driver of reducing conditions in addition to microsite differences in soil moisture (Hall et al., in review; Chapter 2). We propose that high rates of NPP lead to high C concentrations, promoting high rates of microbial respiration, O_2 depletion, Fe reduction, explaining an overall increase in mineral-associated C turnover associated with Fe reduction. The Fe(II) thus generated, however, is vulnerable to oxidation given that soil macropores often contain high O_2 concentrations in the lower montane forests (Silver et al., 1999). The high concentrations of Fe oxides vulnerable to reductive dissolution in these soils suggest that a substantial fraction of Fe(II) is re-oxidized before it can be leached. Thus, additional mechanisms could also contribute to explaining increased C turnover concomitant with Fe redox cycling. Reduction and oxidation of Fe affect soil pH and C solubility, and can stimulate short-term decomposition rates (Thompson, Chadwick, Boman, et al., 2006; Hall and

Silver, 2013). These mechanisms could explain why a prevalence of reducing conditions in soil microsites, in a system characterized by O_2 fluctuations, were not associated with decreased decomposition rates of mineral-associated C in the lower montane ecosystem.

Notably, subsurface soils from the lower montane slope site showed significantly increased C residence times relative to the other topographic positions. This pattern could reflect the importance of erosion and landslides in removing surface soil horizons dominated by more recent C inputs (Scatena and Lugo, 1995), exposing deeper soil horizons with lower C concentrations, older C inputs, and higher concentrations of crystalline Fe oxides. We found spatially heterogeneous patterns of soil depth horizonation consistent with this hypothesis. On the ridge site, soils contained a brown surface horizon, followed by yellow and then orange/red subsurface horizons consistent with a depth transition from goethite to hematite mineralogy [*S. Hall, personal observation*]. Some slope plots, in contrast, lacked the yellow subsurface horizons, consistent with their removal by geomorphic processes.

Conclusions

In the current conceptual framework of soil C stabilization, sorption of organic matter by reactive minerals and an attenuation of decomposition due to O_2 limitation are thought to contribute to C accumulation (Kleber, 2010; Schmidt et al., 2011). Previous studies of soil C in humid tropical forests largely focused on relationships between C and soil mineralogy and geochemistry. We found that a suite of variables, including Al and Fe in chemical extractions, fine root biomass, and a proxy for reducing conditions explained most of the variation in C concentrations across a humid tropical forest landscape. Our models also suggested the importance of synergies between reducing conditions and Al-organic interactions in promoting C accumulation. We also found, however, that C concentrations declined with the availability of Fe minerals that can sustain anaerobic microbial respiration (citrate/ascorbate extraction), which typically exceeded concentrations of oxalate-extractable Fe. Furthermore, residence times of mineral-associated C implied by models of soil $\Delta^{14}C$ content showed negative relationships with Fe(II) concentrations, an index of reducing conditions, in Fe oxide-rich lower montane soils. High concentrations of reducible Fe oxides and fluctuations in O_2 availability may account for relatively rapid *turnover* of mineral-associated C in the lower-montane forest, irrespective of the fact that Fe(II) is also associated with increasing C *concentrations*. Our findings suggest a mechanistic framework for understanding the distribution and persistence of soil C in humid tropical forests, a major reservoir with important couplings to the global climate system.

Acknowledgements

Whendee Silver and Gavin McNicol contributed to the text of this chapter. We thank H. Dang, J. Treffkorn, T. Natake, J. Cosgrove, R. Ryals, O. Gutierrez, A. McDowell, and C. Torrens for crucial help in the field and lab. G. Sposito, M. Firestone, and R. Rhew provided valuable discussion and comments. SJH was supported by the DOE Office of Science Graduate Fellowship Program supported by the American Recovery and Reinvestment Act of 2009, administered by ORISE-ORAU under contract no. DE-AC05-06OR23100. Funding was provided by NSF grant EAR-08199072 to WLS, the NSF Luquillo Critical Zone Observatory (EAR-0722476) with additional support provided by the USGS Luquillo WEBB program, and

grant DEB 0620910 from NSF to the Institute for Tropical Ecosystem Studies, University of Puerto Rico, and to the International Institute of Tropical Forestry USDA Forest Service, as part of the Luquillo Long-Term Ecological Research Program.

References

Alvarez, R., Lavado, R.S., 1998. Climate, organic matter and clay content relationships in the Pampa and Chaco soils, Argentina. Geoderma 83, 127–141.

Baldock, J.A., Skjemstad, J.O., 2000. Role of the soil matrix and minerals in protecting natural organic materials against biological attack. Organic Geochemistry 31, 697–710.

Bates, D., Maechler, M., Bolker, B., 2012. lme4: Linear mixed-effects models using S4 classes.

Berhe, A.A., Harte, J., Harden, J.W., Torn, M.S., 2007. The significance of the erosion-induced terrestrial carbon sink. BioScience 57, 337–346.

Bruun, T.B., Elberling, B., Christensen, B.T., 2010. Lability of soil organic carbon in tropical soils with different clay minerals. Soil Biology and Biochemistry 42, 888–895.

Chacon, N., Silver, W.L., Dubinsky, E.A., Cusack, D.F., 2006. Iron reduction and soil phosphorus solubilization in humid tropical forest soils: The roles of labile carbon pools and an electron shuttle compound. Biogeochemistry 78, 67–84.

Cleveland, C.C., Wieder, W.R., Reed, S.C., Townsend, A.R., 2010. Experimental drought in a tropical rain forest increases soil carbon dioxide losses to the atmosphere. Ecology 91, 2313–2323.

Cusack, D.F., Silver, W.L., Torn, M.S., McDowell, W.H., 2011. Effects of nitrogen additions on above- and belowground carbon dynamics in two tropical forests. Biogeochemistry 104, 203–225.

De Camargo, P.B., Trumbore, S.E., Martinelli, L.A., Davidson, E.A., Nepstad, D.C., Victoria, R.L., 1999. Soil carbon dynamics in regrowing forest of eastern Amazonia. Global Change Biology 5, 693–702.

DeAngelis, K.M., Fortney, J.L., Borglin, S., Silver, W.L., Simmons, B.A., Hazen, T.C., 2012. Anaerobic decomposition of switchgrass by tropical soil-derived feedstock-adapted consortia. mBio 3.

Dubinsky, E.A., Silver, W.L., Firestone, M.K., 2010. Tropical forest soil microbial communities couple iron and carbon biogeochemistry. Ecology 91, 2604–2612.

Espeleta, J.F., Clark, D.A., 2007. Multi-scale variation in fine-root biomass in a tropical rain forest: a seven-year study. Ecological Monographs 77, 377–404.

Fisher, M.J., Rao, I.M., Ayarza, M.A., Lascano, C.E., Sanz, J.I., Thomas, R.J., Vera, R.R., 1994. Carbon storage by introduced deep-rooted grasses in the South American savannas. Nature 371, 236–238.

Fredrickson, J.K., Zachara, J.M., Kennedy, D.W., Dong, H., Onstott, T.C., Hinman, N.W., Li, S., 1998. Biogenic iron mineralization accompanying the dissimilatory reduction of hydrous ferric oxide by a groundwater bacterium. Geochimica et Cosmochimica Acta 62, 3239–3257.

Frenzel, P., Bosse, U., Janssen, P.H., 1999. Rice roots and methanogenesis in a paddy soil: ferric iron as an alternative electron acceptor in the rooted soil. Soil Biology and Biochemistry 31, 421–430.

Gee, G., Bauder, J., 1986. Particle size analysis, in: Klute, A. (Ed.), Methods of Soil Analysis, Part 1, Physical and Mineralogical Methods, Agronomy Monograph. American Society of Agronomy, Madison, WI, USA, pp. 383–411.

Hall, S.J., McDowell, W.H., Silver, W.L., 2013. When wet gets wetter: Decoupling of moisture, redox biogeochemistry, and greenhouse gas fluxes in a humid tropical forest soil. Ecosystems 16, 576–589.
Hall, S.J., Silver, W.L., 2013. Iron oxidation stimulates organic matter decomposition in humid tropical forest soils. Global change biology 19.
Harden, C.P., Scruggs, P.D., 2003. Infiltration on mountain slopes: a comparison of three environments. Geomorphology 55, 5–24.
Hua, Q., Barbetti, M., Rakowski, A.Z., 2013. Atmospheric Radiocarbon for the Period 1950–2010. Radiocarbon 55, in press.
Hyacinthe, C., Bonneville, S., Van Cappellen, P., 2006. Reactive iron(III) in sediments: Chemical versus microbial extractions. Geochimica et Cosmochimica Acta 70, 4166–4180.
Jenny, H., 1941. Factors of Soil Formation: A System of Quantitative Pedology. Courier Dover Publications, Mineola, New York, USA.
Jenny, H., 1950. Causes of the high nitrogen and organic matter content of certain tropical forest soils. Soil Science 69, 63–70.
Jobbagy, E.G., Jackson, R.B., 2000. The vertical distribution of soil organic carbon and its relation to climate and vegetation. Ecological Applications 10, 423–436.
Johnson, K.D., Scatena, F.N., Silver, W.L., 2011. Atypical soil carbon distribution across a tropical steepland forest catena. Catena 87, 391–397.
Kaiser, K., Guggenberger, G., 2000. The role of DOM sorption to mineral surfaces in the preservation of organic matter in soils. Organic Geochemistry 31, 711–725.
Kleber, M., 2010. What is recalcitrant soil organic matter? Environmental Chemistry 7, 320–332.
Kleber, M., Mikutta, R., Torn, M.S., Jahn, R., 2005. Poorly crystalline mineral phases protect organic matter in acid subsoil horizons. European Journal of Soil Science 56, 717–725.
Koning, G.H.J. de, Veldkamp, E., López-Ulloa, M., 2003. Quantification of carbon sequestration in soils following pasture to forest conversion in northwestern Ecuador. Global Biogeochemical Cycles 17, 12 PP.
Kristensen, E., Ahmed, S., Devol, A., 1995. Aerobic and anaerobic decomposition of organic matter in marine sediment: which is fastest? Limnology and Oceanography 40, 1430–1437.
Leff, J.W., Wieder, W.R., Taylor, P.G., Townsend, A.R., Nemergut, D.R., Grandy, A.S., Cleveland, C.C., 2012. Experimental litterfall manipulation drives large and rapid changes in soil carbon cycling in a wet tropical forest. Global Change Biol 18, 2969–2979.
Liptzin, D., Silver, W.L., Detto, M., 2011. Temporal dynamics in soil oxygen and greenhouse gases in two humid tropical forests. Ecosystems 14, 171–182.
Loeppert, R., Inskeep, W., 1996. Iron, in: Sparks, D. (Ed.), Methods of Soil Analysis, Part 3--Chemical Methods. Soil Science Society of America, Madison, WI, USA, pp. 639–664.
Lovley, D.R., 1995. Microbial Reduction of Iron, Manganese, and Other Metals, in: Donald L. Sparks (Ed.), Advances in Agronomy. Academic Press, Waltham, MA, USA, pp. 175–231.
Marin-Spiotta, E., Silver, W.L., Swanston, C.W., Ostertag, R., 2009. Soil organic matter dynamics during 80 years of reforestation of tropical pastures. Global Change Biology 15, 1584–1597.

Marin-Spiotta, E., Swanston, C.W., Torn, M.S., Silver, W.L., Burton, S.D., 2008. Chemical and mineral control of soil carbon turnover in abandoned tropical pastures. Geoderma 143, 49–62.

McDowell, W.H., Scatena, F.N., Waide, R.B., Brokaw, N., Camilo, G., Covich, A., Crowl, T., Gonzalez, G., Greathouse, E., Klawinski, P., Lodge, D., Lugo, A., Pringle, C., Richardson, B., Richardson, M., Schaefer, D., Silver, W., Thompson, J., Vogt, D., Vogt, K., Willig, M., Woolbright, L., Zou, X., Zimmerman, J., 2012. Geographic and ecological setting of the Luquillo Mountains, in: Brokaw, N., Crowl, T., Lugo, A., McDowell, W.H., Scatena, F.N., Waide, R.B., Willig, M. (Eds.), A Caribbean Forest Tapestry: The Multidimensional Nature of Disturbance and Response. Oxford University Press, New York, USA, pp. 72–163.

Nakagawa, S., Schielzeth, H., 2013. A general and simple method for obtaining R2 from generalized linear mixed-effects models. Methods in Ecology and Evolution 4, 133–142.

Oades, J.M., 1988. The retention of organic matter in soils. Biogeochemistry 5, 35–70.

Odum, H.T., 1970. Rain forest structure and mineral-cycling homeostasis, in: Odum, H.T., Pigeon, R.F. (Eds.), A Tropical Rain Forest: a Study of Irradiation and Ecology at El Verde, Puerto Rico. U.S. Atomic Energy Commission, Oak Ridge, TN, USA, pp. H3–H52.

Ostertag, R., 2001. Effects of nitrogen and phosphorus availability on fine-root dynamics in Hawaiian montane forests. Ecology 82, 485–499.

Parton, W., Silver, W.L., Burke, I.C., Grassens, L., Harmon, M.E., Currie, W.S., King, J., Adair, E.C., Brandt, L., Hart, S.C., Fasth, B., 2007. Global-scale similarities in nitrogen release patterns during long-term decomposition. Science 315, 361–364.

Parton, W.J., Scurlock, J.M.O., Ojima, D.S., Gilmanov, T.G., Scholes, R.J., Schimel, D.S., Kirchner, T., Menaut, J.-C., Seastedt, T., Moya, E.G., Kamnalrut, A., Kinyamario, J.I., 1993. Observations and modeling of biomass and soil organic matter dynamics for the grassland biome worldwide. Global Biogeochemical Cycles 7, 785–809.

Peretyazhko, T., Sposito, G., 2005. Iron(III) reduction and phosphorous solubilization in humid tropical forest soils. Geochimica et Cosmochimica Acta 69, 3643–3652.

Phillips, E.J.P., Lovley, D.R., Roden, E.E., 1993. Composition of Non-Microbially Reducible Fe(III) in Aquatic Sediments. Applied and Environmental Microbiology 59, 2727–2729.

Pinheiro, J., Bates, D., DebRoy, S., Sarkar, D., R Core Development Team, 2011. nlme: Linear and Nonlinear Mixed Effects Models.

Ponnamperuma, F.N., 1972. The chemistry of submerged soils. Advances in Agronomy 24, 29–96.

Powers, J.S., Schlesinger, W.H., 2002. Relationships among soil carbon distributions and biophysical factors at nested spatial scales in rain forests of northeastern Costa Rica. Geoderma 109, 165–190.

Powers, J.S., Veldkamp, E., 2005. Regional variation in soil carbon and δ13C in forests and pastures of northeastern Costa Rica. Biogeochemistry 72, 315–336.

Rasse, D.P., Rumpel, C., Dignac, M.-F., 2005. Is soil carbon mostly root carbon? Mechanisms for a specific stabilisation. Plant and Soil 269, 341–356.

Reyes, I., Torrent, J., 1997. Citrate-ascorbate as a highly selective extractant for poorly crystalline iron oxides. Soil Science Society of America Journal 61, 1647–1654.

Roden, E., Wetzel, R., 1996. Organic carbon oxidation and suppression of methane production by microbial Fe(III) oxide reduction in vegetated and unvegetated freshwater wetland sediments. Limnology and Oceanography 41, 1733–1748.
Saini, G.R., 1966. Organic matter as a measure of bulk density of soil. Nature 210, 1295–1296.
Scatena, F.N., Lugo, A.E., 1995. Geomorphology, disturbance, and the soil and vegetation of two subtropical wet steepland watersheds of Puerto Rico. Geomorphology 13, 199–213.
Scatena, F.N., Moya, S., Estrada, C., Chinea, J.D., 1996. The first five years in the reorganization of aboveground biomass and nutrient use following Hurricane Hugo in the Bisley Experimental Watersheds, Luquillo Experimental Forest, Puerto Rico. Biotropica 28, 424–440.
Schmidt, M.W.I., Torn, M.S., Abiven, S., Dittmar, T., Guggenberger, G., Janssens, I.A., Kleber, M., Kogel-Knabner, I., Lehmann, J., Manning, D.A.C., Nannipieri, P., Rasse, D.P., Weiner, S., Trumbore, S.E., 2011. Persistence of soil organic matter as an ecosystem property. Nature 478, 49–56.
Schuur, E.A.G., Chadwick, O.A., Matson, P.A., 2001. Carbon cycling and soil carbon storage in mesic to wet Hawaiian montane forests. Ecology 82, 3182–3196.
Sexstone, A., Revsbech, N., Parkin, T., Tiedje, J., 1985. Direct measurement of oxygen profiles and denitrification rates in soil aggregates. Soil Science Society of America Journal 49, 645–651.
Silver, W., Liptzin, D., Almaraz, M., in press. Soil redox dynamics and biogeochemistry along a tropical elevation gradient, in: Ecological Gradient Analyses in a Tropical Ecosystem, Ecological Bulletins. Oikos.
Silver, W.L., Lugo, A.E., Keller, M., 1999. Soil oxygen availability and biogeochemistry along rainfall and topographic gradients in upland wet tropical forest soils. Biogeochemistry 44, 301–328.
Silver, W.L., Scatena, F.N., Johnson, A.H., Siccama, T.G., Sanchez, M.J., 1994. Nutrient availability in a montane wet tropical forest - Spatial patterns and methodological considerations. Plant and Soil 164, 129–145.
Stuiver, M., Polach, H.A., 1977. Discussion: reporting of 14C data. Radiocarbon 19, 355–63.
Stuiver, M., Reimer, P.J., Braziunas, T.F., 1998. High-precision radiocarbon age calibration for terrestrial and marine samples. Radiocarbon 40, 1127–1151.
Sutton-Grier, A.E., Keller, J.K., Koch, R., Gilmour, C., Megonigal, J.P., 2011. Electron donors and acceptors influence anaerobic soil organic matter mineralization in tidal marshes. Soil Biology and Biochemistry 43, 1576–1583.
Swanston, C.W., Torn, M.S., Hanson, P.J., Southon, J.R., Garten, C.T., Hanlon, E.M., Ganio, L., 2005. Initial characterization of processes of soil carbon stabilization using forest stand-level radiocarbon enrichment. Geoderma 128, 52–62.
Telles, E. de C.C., Camargo, P.B. de, Martinelli, L.A., Trumbore, S.E., Costa, E.S. da, Santos, J., Higuchi, N., Jr, R.C.O., 2003. Influence of soil texture on carbon dynamics and storage potential in tropical forest soils of Amazonia. Global Biogeochemical Cycles 17.
Thompson, A., Chadwick, O.A., Boman, S., Chorover, J., 2006. Colloid mobilization during soil iron redox oscillations. Environmental Science & Technology 40, 5743–5749.
Thompson, A., Chadwick, O.A., Rancourt, D.G., Chorover, J., 2006. Iron-oxide crystallinity increases during soil redox oscillations. Geochimica et Cosmochimica Acta 70, 1710–1727.

Thompson, A., Rancourt, D., Chadwick, O., Chorover, J., 2011. Iron solid-phase differentiation along a redox gradient in basaltic soils. Geochimica et Cosmochimica Acta 75, 119–133.
Tonneijck, F.H., Jansen, B., Nierop, K.G.J., Verstraten, J.M., Sevink, J., De Lange, L., 2010. Towards understanding of carbon stocks and stabilization in volcanic ash soils in natural Andean ecosystems of northern Ecuador. European Journal of Soil Science 61, 392–405.
Torn, M., Trumbore, S., Chadwick, O., Vitousek, P., Hendricks, D., 1997. Mineral control of soil organic carbon storage and turnover. Nature 389, 170–173.
Torn, M.S., Swanston, C.W., Castanha, C., Trumbore, S.E., 2009. Storage and turnover of organic matter in soil, in: Senesi, N., Xing, B., Huang, P.M. (Eds.), Biophysico-Chemical Processes Involving Natural Nonliving Organic Matter in Environmental Systems. John Wiley & Sons, Inc., Hoboken, NJ, USA, pp. 219–272.
Trumbore, S.E., 1993. Comparison of carbon dynamics in tropical and temperate soils using radiocarbon measurements. Global Biogeochemical Cycles 7, 275–290.
Trumbore, S.E., Davidson, E.A., Camargo, P.B. de, Nepstad, D.C., Martinelli, L.A., 1995. Belowground cycling of carbon in forests and pastures of eastern Amazonia. Global Biogeochemical Cycles 9, 515–528.
Varela, E., Tien, M., 2003. Effect of pH and oxalate on hydroquinone-derived hydroxyl radical formation during brown rot wood degradation. Applied and Environmental Microbiology 69, 6025–6031.
Viollier, E., Inglett, P., Hunter, K., Roychoudhury, A., van Cappellen, P., 2000. The ferrozine method revisited: Fe(II)/Fe(III) determination in natural waters. Applied Geochemistry 15, 785–790.
Vogel, J.S., Southon, J.R., Nelson, D.E., Brown, T.A., 1984. Performance of catalytically condensed carbon for use in accelerator mass spectrometry. Nuclear Instruments and Methods in Physics Research Section B: Beam Interactions with Materials and Atoms 5, 289–293.
Vogt, K.A., Vogt, D.J., Palmiotto, P.A., Boon, P., O'Hara, J., Asbjornsen, H., 1996. Review of root dynamics in forest ecosystems grouped by climate, climatic forest type and species. Plant and Soil 187, 159–219.
Wagai, E., Mayer, L., 2007. Sorptive stabilization of organic matter in soils by hydrous iron oxides. Geochimica et Cosmochimica Acta 71, 25–35.
Zeikus, J.G., Wellstein, A. l., Kirk, T.K., 1982. Molecular basis for the biodegradative recalcitrance of lignin in anaerobic environments. FEMS Microbiology Letters 15, 193–197.

Tables

Table 1: Site characteristics. Above-ground litterfall represents annual means (SE) from 1994 – 2002 from the palm, colorado, and elfin sites, based on monthly litter collection from five replicate baskets per site (W. Silver, unpublished data). Bisley data represent bi-weekly litter collections from 60 baskets for 18 months in 1988-89 (Scatena et al., 1996).

Site	Elevation (m)	N (°)	W (°)	Total aboveground litterfall (g m^{-2} yr^{-1})
Bisley ridges	240 - 300	18.3157	65.7487	870 (70)
Bisley slopes	220 - 280			
Bisley valleys	210 - 240			
Palm	614	18.2988	65.7803	470 (107)
Colorado	736	18.2942	65.7852	560 (90)
Elfin	936	18.2702	65.761	366 (55)

Table 2: Potential predictors of soil C concentrations and stocks in mixed effects models. See the methods for details of soil analyses.

Category	Variable	Description
Soil chemistry	$Fe(III)_{HCl}$	0.5 M HCl-extractable Fe(III)
	Fe_{ca}	Citrate/ascorbate extractable Fe
	Fe_{ox}	Ammonium oxalate extractable Fe
	Fe_{cd-ca}	Citrate/dithionite – citrate/ascorbate Fe
	Al_{HCl}	0.5 M HCl-extractable Al
	Al_{ox}	Ammonium oxalate extractable Al
	Al_{ca}	Citrate/ascorbate extractable Al
	Clay	
	Sand	
Redox	Fe(II)	0.5 M HCl-extractable Fe(II)
	$Fe(II)/Fe(III)_{HCl}$	Ratio of Fe(II)/Fe(III)in 0.5 M HCl
	Live fine roots	Live roots < 2 mm diameter
Roots	Dead fine roots	Dead roots < 2 mm diameter
	Live fine root C/N	

Table 3: Mean (SE) concentrations and isotope ratios of soil C in density fractions summarized by topographic position in the lower montane forest; n = 5 per position/depth combination. Residence times with different letters are significantly different ($p < 0.05$).

Position	Depth	Free light C (mg g^{-1})	Occluded light C (mg g^{-1})	Mineral-associated C (mg g^{-1})	Mineral-associated $\delta^{13}C$ (‰)	Mineral-associated $\Delta^{14}C$ (‰)	Mineral-associated C residence time (yr)
Ridge	0 - 10 cm	3.69 (0.81)	2.72 (0.25)	47.74 (1.87)	-28.15 (0.05)	80.7 (3.9)	102 (5) a
	10 - 20 cm	1.31 (0.38)	1.26 (0.27)	31.57 (2.6)	-27.63 (0.09)	63.6 (11.2)	136 (22) ab
Slope	0 - 10 cm	2.35 (0.5)	2.61 (0.95)	32.89 (3.28)	-28.21 (0.18)	74.3 (13.7)	120 (25) a
	10 - 20 cm	1.52 (0.91)	0.85 (0.3)	21.83 (5.07)	-27.45 (0.18)	40.1 (14.3)	195 (35) b
Valley	0 - 10 cm	4.37 (2.04)	4.71 (1.78)	32.72 (2.44)	-28.62 (0.19)	81.3 (5.0)	101 (7) a
	10 - 20 cm	2.56 (0.68)	3.79 (0.81)	26.1 (2.13)	-28.36 (0.23)	86.2 (3.0)	94 (4) a

Table 4: Linear mixed effects models of soil C concentrations incorporating predictors listed in Table 1. Model parameters (SE) were estimated using REML for the optimum models of soil C concentrations selected by AICc. Separate models were fit for the lower montane and overall datasets. The marginal pseudo-R^2 is the proportion of the total model variance (fixed effects, random effects, and residuals) explained by the fixed effects. The lower montane model included random effects for transects and plots, and the lower montane + montane model also included a random effect for transect by depth interactions.

Variable	Parameter estimate (SE)	Variable	Parameter estimate (SE)
Lower montane		**Lower montane + montane**	
Alca	0.49 (0.09)	Alca	0.34 (0.05)
live fine roots	0.40 (0.05)	Fe(II)/FeHCl	0.31 (0.05)
Feox	0.36 (0.08)	Al_{ca} x Fe(II)/FeHCl	0.27 (0.04)
Feca	-0.35 (0.09)	depth	-0.25 (0.07)
Fe(II)/FeHCl	0.29 (0.06)	live fine roots	0.21 (0.05)
Fe(III)HCl	0.15 (0.07)	Feox	0.20 (0.04)
Fecd-ca	-0.12 (0.07)	Feca	-0.18 (0.05)
Alca x Fe(II)/FeHCl	0.12 (0.06)		
Marginal pseudo-R^2	0.75	*Marginal pseudo-R^2*	*0.84*

Table 5: Model parameters (SE) estimated using REML for the optimum models of soil C stocks selected by AICc. See Table 1 for an explanation of parameter abbreviations. Separate models were fit for the lower montane and overall datasets.

Variable	Parameter estimate (SE)	Variable	Parameter estimate (SE)
Lower montane		**Lower montane + montane**	
Fe_{ox}	0.50 (0.11)	$Fe(II)/Fe_{HCl}$	0.36 (0.06)
depth	-0.39 (0.12)	Fe_{ox}	0.24 (0.06)
Fe_{ca}	-0.34 (0.12)	$Fe(II)/Fe_{HCl}$ x Al_{ca}	0.23 (0.05)
Al_{ca}	0.31 (0.12)	Al_{ca}	0.22 (0.06)
		Fe_{ca}	-0.19 (0.07)
Marginal pseudo-R^2	*0.22*	*Marginal pseudo-R^2*	*0.60*

Figure Captions

Figure 1: Means (SE) of soil attributes by depth increment across the site gradient; mean bulk soil O_2 concentrations decrease by site from left to right. For the ridge, slope, and valley sites, n = 20 for each bar, and for the palm, colorado, and cloud sites, n = 5 per bar.

Figure 2: Means (SE) of soil attributes by depth increment across the site gradient; mean bulk soil O_2 concentrations decrease by site from left to right. (a) Concentrations of Fe(II) and Fe(III) in 0.5 M HCl extractions, (b) Fe in citrate/dithionite and citrate/ascorbate extractions, (c) Fe in ammonium oxalate extractions, (d) Al in citrate/ascorbate extractions. For the ridge, slope, and valley sites, n = 20 for each bar, and for the palm, colorado, and cloud sites, n = 5 for each bar.

Figure 3: Mean (SE) C concentrations for (a) 0 – 10 cm and (b) 10 – 20 cm soil, and C stocks for (c) 0 – 10 cm and (d) 10 – 20 cm soil in the lower montane forest, with n = 5 for each bar. Means with different letters are significantly different ($p < 0.05$).

Figure 4: Pairwise relationships between soil C concentrations and biogeochemical variables included in the optimum statistical model, total n = 149. Variable descriptions are given in Table 1.

Figures

Figure 1

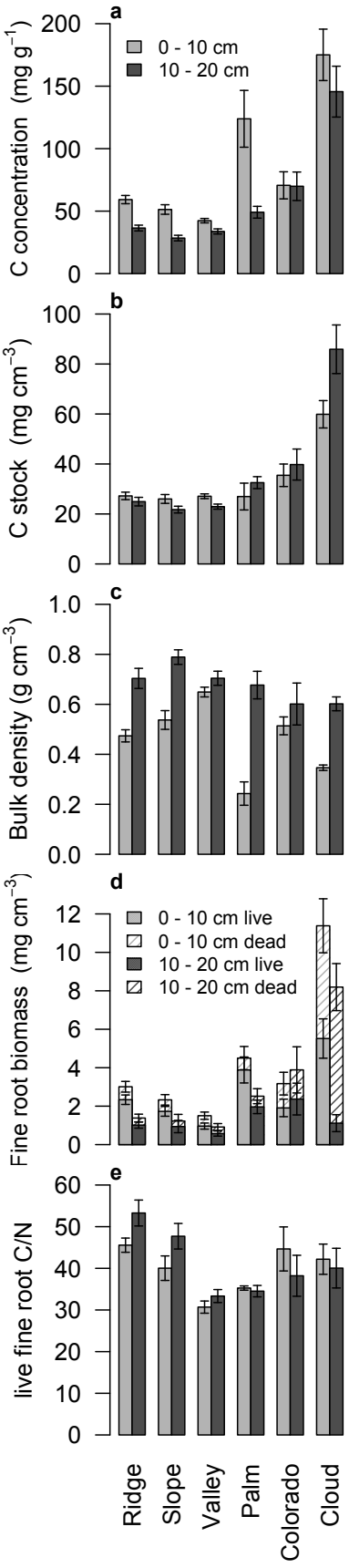

Figure 2

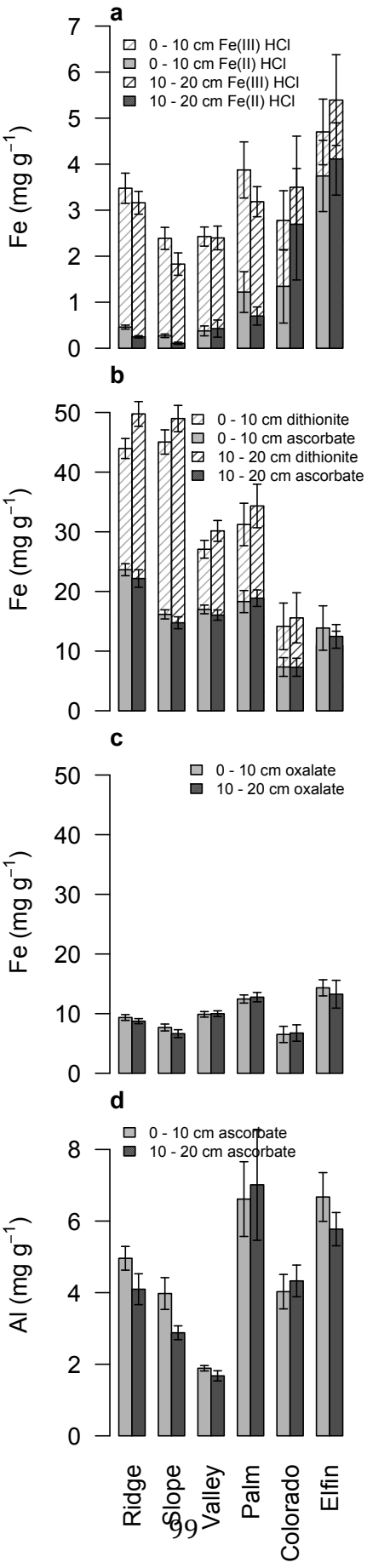
a
0 - 10 cm Fe(III) HCl
0 - 10 cm Fe(II) HCl
10 - 20 cm Fe(III) HCl
10 - 20 cm Fe(II) HCl
Fe (mg g^{-1})
b
0 - 10 cm dithionite
0 - 10 cm ascorbate
10 - 20 cm dithionite
10 - 20 cm ascorbate
Fe (mg g^{-1})
c
0 - 10 cm oxalate
10 - 20 cm oxalate
Fe (mg g^{-1})
d
0 - 10 cm ascorbate
10 - 20 cm ascorbate
Al (mg g^{-1})
Ridge
Slope
Valley
Palm
Colorado
Elfin

Figure 3

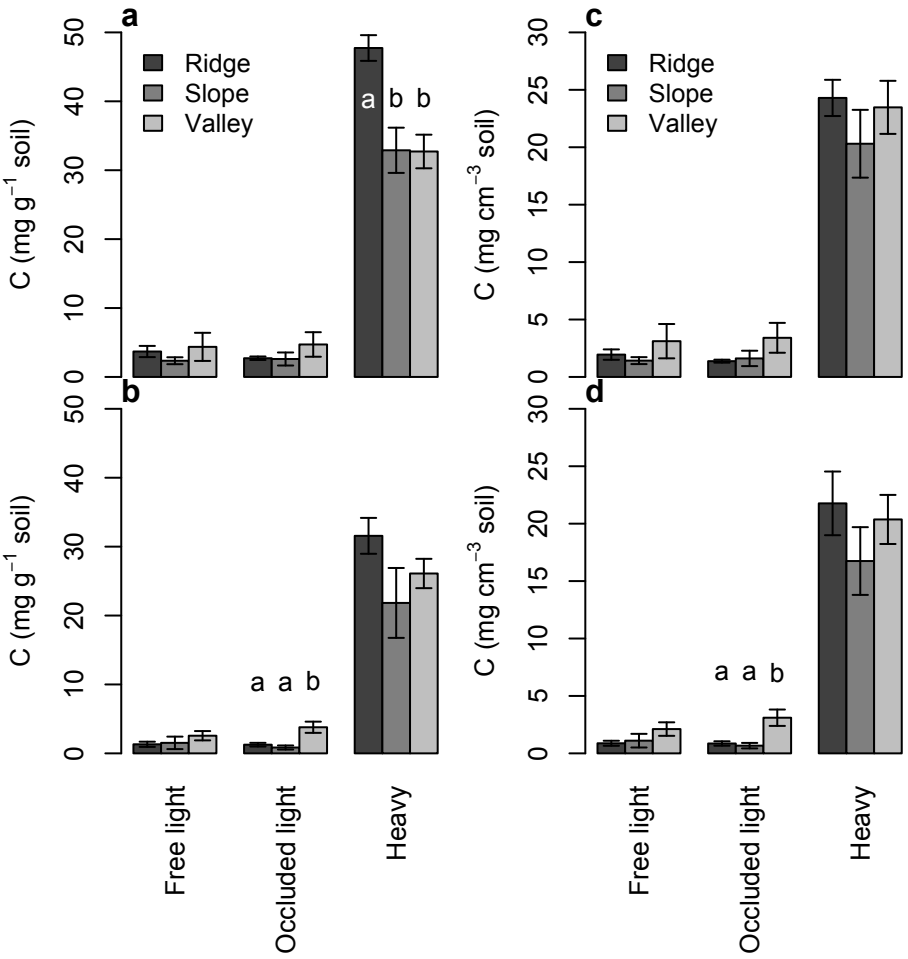
a
b
c
d
Ridge
Slope
Valley
C (mg g^{-1} soil)
C (mg cm^{-3} soil)
a b b
a a b
Free light
Occluded light
Heavy

Figure 4

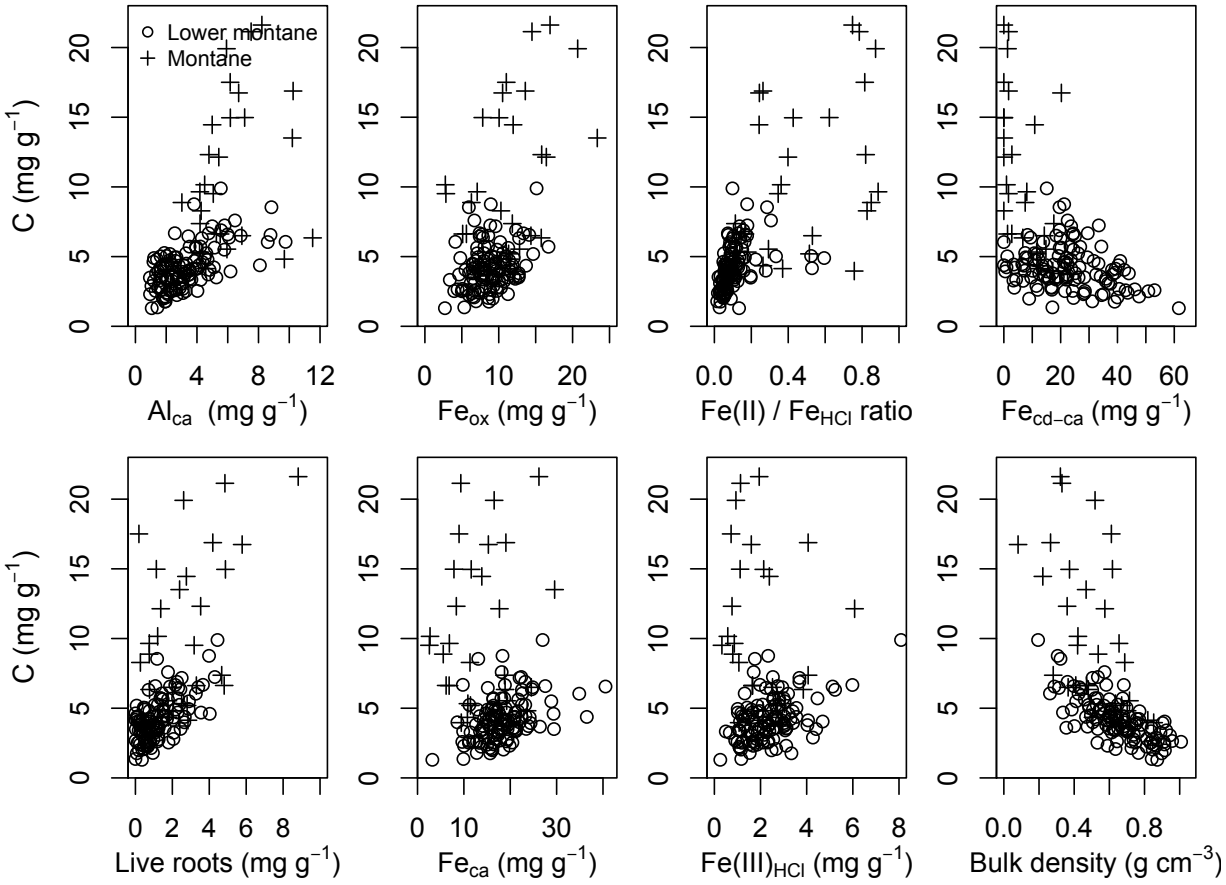
Lower montane
Montane
C (mg g^{-1})
Al$_{ca}$ (mg g^{-1})
Fe$_{ox}$ (mg g^{-1})
Fe(II) / Fe$_{HCl}$ ratio
Fe$_{cd-ca}$ (mg g^{-1})
Live roots (mg g^{-1})
Fe$_{ca}$ (mg g^{-1})
Fe(III)$_{HCl}$ (mg g^{-1})
Bulk density (g cm^{-3})

Supplemental Information

Supplemental Table 1: Multiple comparisons among site means of soil C and other covariates stratified by depth interval. Sites with different letters significantly differ according to Tukey's honestly significant difference test. Differences were only assessed within a given depth interval for each variable.

Variable	Depth	Ridge	Slope	Valley	Palm	Colorado	Cloud
Soil C concentration	0 - 10 cm	a	ab	b	cd	abc	d
	10 -20 cm	ab	a	a	bc	c	d
Soil C stock	0 - 10 cm	a	a	a	a	a	b
	10 -20 cm	a	a	a	ab	b	c
Bulk density	0 - 10 cm	a	a	b	c	ab	ac
	10 -20 cm	a	a	a	a	a	a
Live fine roots	0 - 10 cm	ad	ab	b	cd	bd	c
	10 -20 cm	ab	ab	a	ab	b	ab
Dead fine roots	0 - 10 cm	a	a	a	a	a	b
	10 -20 cm	a	a	a	ab	b	c
Live fine root C/N	0 - 10 cm	a	ab	c	b	abc	ab
	10 -20 cm	a	a	b	b	ab	ab
$Fe(II)_{HCl}$	0 - 10 cm	b	a	ab	abc	abc	c
	10 -20 cm	b	a	ab	b	abc	c
$Fe(III)_{HCl}$	0 - 10 cm	a	a	a	a	a	a
	10 -20 cm	b	a	ab	ab	a	ab
$Fe(II)/Fe_{HCl}$	0 - 10 cm	a	a	a	a	ab	b
	10 -20 cm	a	a	a	ab	bc	c
Fe_{cd-ca}	0 - 10 cm	c	a	b	bc	bd	d
	10 -20 cm	a	a	b	b	bc	c
Fe_{ca}	0 - 10 cm	b	a	a	ab	c	a
	10 -20 cm	b	a	a	ab	c	ac
Fe_{ox}	0 - 10 cm	ab	a	b	c	ab	c
	10 -20 cm	ab	a	b	c	ab	abc
Al_{ca}	0 - 10 cm	ac	a	b	ac	a	c
	10 -20 cm	ac	a	b	ac	c	c

Supplemental Figure 1: (a) The measured temporal trend in atmospheric $\Delta^{14}C$ of CO_2, and modeled trends in $\Delta^{14}C$ of mineral-associated organic matter based on the mean ^{14}C content of 0 – 10 cm and 10 – 20 cm soil sampled in 2012. (b) The relationship between measured $\Delta^{14}C$ of mineral-associated organic matter and modeled C turnover time, assuming the slower of two possible modeled turnover times suggested by the atmospheric ^{14}C-CO_2 curve. (c) Modeled C turnover times plotted against soil Fe(II) concentrations on a log scale.

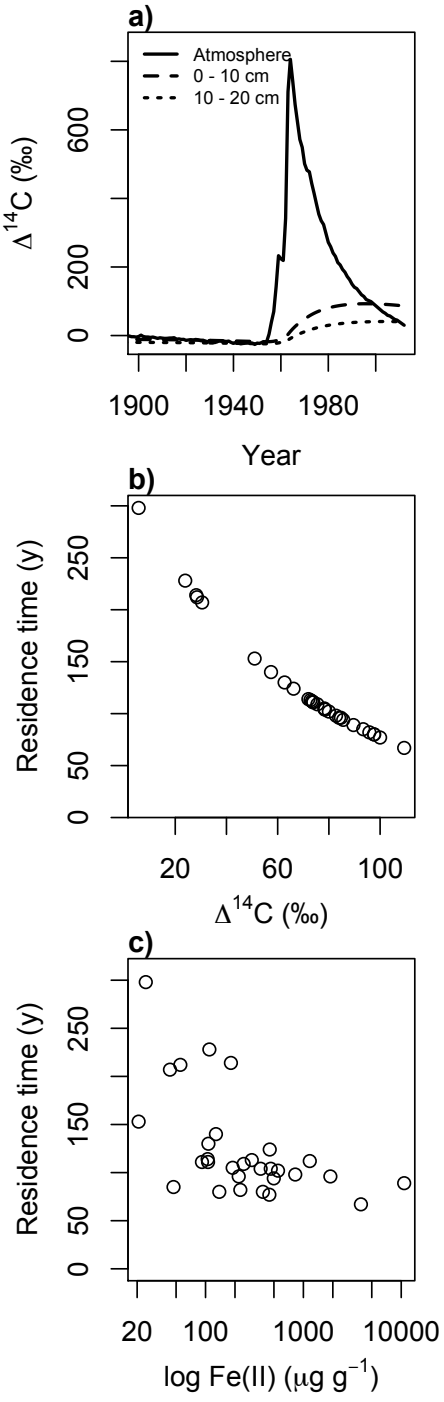

Supplemental Figure 2:

Soil Fe(II) concentrations in the lower montane forest soils by topographic position and depth. Data from three different sampling events (June 2011, Feb 2012, May 2012) are combined here. (a) box and whisker plots with outliers shown as dots. (b) data with outliers removed; means with different letters are significantly different.